

ORIGIN OF THE MARSDEN AND KRACHT GROUPS OF SUNSKIRTING COMETS. I. ASSOCIATION WITH COMET 96P/MACHHOLZ AND ITS INTERPLANETARY COMPLEX

ZDENEK SEKANINA AND PAUL W. CHODAS

Jet Propulsion Laboratory, California Institute of Technology, 4800 Oak Grove Drive, Pasadena, CA 91109;

zs@sek.jpl.nasa.gov, paul.w.chodas@jpl.nasa.gov

Received 2005 February 23; accepted 2005 August 19

ABSTRACT

Of the three major groups of comets approaching the Sun to between 6 and 12 solar radii and discovered with the coronagraphs on board *SOHO*, we investigate the Marsden and Kracht groups. We call these comets “sunskirters” to distinguish them from the Kreutz system sungrazers. Our objective is to understand the origin, history, and orbital evolution of the two groups. The tendency for their members to arrive at perihelion in pairs or clusters is a result of their recent fragmentation. As fragments of more massive precursor objects, the Marsden- and Kracht-group comets are mostly less than 10 yr old. Although the two groups and several meteoroid swarms, such as the Daytime Arietids and Southern δ Aquarids, appear as separate populations of a complex associated with comet 96P/Machholz, our orbit integrations suggest that we deal with a single, essentially continuous population that extends from the comet’s orbit for more than 160° in the longitude of the node. First-generation fragments of their common progenitor with comet 96P, which were the initial direct ancestors of this population, are called the first precursors. Nearly 60,000 orbit integration runs are made in our search for their birth scenarios. We find that these objects separated from the progenitor comet before AD 950 and, as sources of continuing activity, pursued an orbital evolution very different from that of 96P. All first precursors of this low-inclination population experienced a sequence of encounters with Jupiter within 0.5 AU, starting in AD 1059 or earlier and continuing for centuries. In the process, they split into smaller pieces in a fashion reminiscent of “cascading” fragmentation of the Kreutz system. The secular planetary (mainly Jovian) perturbations control the motions of both 96P and the low-inclination population, but the dynamical evolution of the latter has been markedly accelerated by Jupiter during close encounters, so that the population’s present-day orbital changes are similar to those the comet will undergo centuries from now. Precursors to the Southern δ Aquarids of the 1950s passed through the Marsden-group stage around 1700 and through the Kracht-group stage in the 1780s. The Daytime Arietids appear to be related most directly to the Marsden-group comets, which can closely approach Earth around June 12, the time of the stream’s peak activity.

Subject headings: celestial mechanics — comets: general — comets: individual (96P/Machholz, 8P/Tuttle, C/1490 Y1, C/1882 R1, C/1965 S1, C/1992 F2, C/1996 V2, C/1997 L2, C/1998 A2, C/1998 A3, C/1998 A4, C/1999 J6, C/1999 M3, C/1999 N5, C/1999 N6, C/1999 P6, C/1999 P8, C/1999 P9, C/1999 U2, C/2000 C2, C/2000 C3, C/2000 C4, C/2000 C5, C/2000 C7, C/2000 O3, C/2001 E1, C/2001 Q7, C/2001 Q8, C/2001 R8, C/2001 R9, C/2001 X8, C/2002 N2, C/2002 Q8, C/2002 Q10, C/2002 R1, C/2002 R4, C/2002 S4, C/2002 S5, C/2002 S7, C/2002 S11, C/2002 V5, C/2003 Q1, C/2003 Q6, C/2004 A3, C/2004 B3, C/2004 J4, C/2004 J12, C/2004 J13, C/2004 J15, C/2004 J16, C/2004 J17, C/2004 J18, C/2004 L10, C/2004 V9, C/2004 V10, C/2004 W10, C/2005 E4, C/2005 G2) — meteors, meteoroids — methods: data analysis — methods: n -body simulations — methods: statistical — minor planets, asteroids

1. INTRODUCTION

The Kreutz sungrazer system had for a long time been the only known group of comets in similar orbits that closely approach the Sun. Thanks to recent astonishingly successful comet searches in images taken with two coronagraphs on board the *Solar and Heliospheric Observatory* (*SOHO*), the number of the Kreutz system’s known members passed the 850 mark by mid-2005.

An important by-product of this effort was the discovery of three major new comet groups, whose members approach the Sun to 6–12 R_\odot ($1 R_\odot = 0.0046524$ AU)—compared to the Kreutz system’s upper limit of $\sim 2 R_\odot$. We show in this study that there are other fundamental differences between the Kreutz system and at least two of the newly discovered groups, including the role of tidally driven fragmentation, which is profound for the Kreutz system but essentially nonexistent for the other groups. We feel that it is inaccurate to refer to the members of the new groups as “sungrazers” and we prefer to call them the “sunskirting” comets or “sunskirters.”

Even though a possible orbital relationship between the non-Kreutz *SOHO* comets C/2000 C2 and C/2000 C5 (Marsden 2000a; Green 2000) had been suggested shortly after their discovery, it was 2 yr later that three *SOHO* comets—C/1997 L2, C/2001 X8, and C/2001 E1—were shown by M. Meyer to move in similar orbits (Marsden 2002a; Green 2002). Subsequently, Meyer (Green 2002) suggested that the orbits of C/2001 T1, C/2000 C2, and C/2000 C5 also fitted this group, when their initially published retrograde orbital solutions were replaced with the alternative prograde solutions. These six comets have made up the core of the Meyer group of sunskirting comets, whose perihelion distance is near $8 R_\odot$ and inclination close to 72° .

At the same time, it was noticed by Marsden (2002a) that two earlier *SOHO* comets, C/1999 J6 and C/1999 U2, were also moving in similar orbits, having a perihelion distance of 0.049 AU, or $10.5 R_\odot$, and an inclination of 27° . He also concluded that when the retrograde solutions for C/2000 C3 and C/2000 C4 (Marsden 2000b) were replaced with alternative prograde solutions, the orbits of these last two comets were also nearly identical with those

TABLE 1
DISCOVERY STATISTICS FOR GROUPS OF *SOHO* SUNSKIRTING
COMETS BY MID-2005

YEAR	ANNUAL RATE OF DETECTED MEMBERS		
	Meyer Group	Marsden Group	Kracht Group
1996.....	1	1	0
1997.....	7	0	0
1998.....	2	3	0
1999.....	4	6	2
2000.....	6	3	1
2001.....	9	0	4
2002.....	9	3	7
2003.....	7	(2) ^a	0
2004.....	7	3	10
2005 ^b	6	2	0
Totals.....	58	21 (23)	24

^a Group membership of these two objects is questionable.

^b From January 1 through June 30.

of C/1999 J6 and C/1999 U2 (Marsden 2002a; Green 2002). These comets were the first four of the Marsden group, whose members can pass rather close to Earth's orbit. D. A. J. Seargent reported a pronounced orbital similarity between the Marsden group and the Daytime Arietid meteor stream (Marsden 2002b), which is detected annually by radar mostly in early to mid-June (e.g., Sekanina 1970, 1973, 1976; Cook 1973) but has a perihelion distance about twice that of the Marsden group. Marsden (2002b) then remarked on similar perihelion directions between comet 96P/Machholz (known originally as P/Machholz 1986e = 1986 VIII and, after 1994, as P/Machholz 1) and the Marsden group. Similarities between the orbital evolutions of the Quadrantid, δ Aquarid, and Daytime Arietid meteor streams and this comet have been known from McIntosh's (1990) integrations of the comet's motion (§ 3). When combined, the relationships between the Arietids and 96P and between the Arietids and the Marsden group obviously imply a relationship between 96P and the Marsden group.

Next, R. Kracht suggested a loose association between two other *SOHO* comets, C/1999 M3 and C/2000 O3, whose lines of

apsides agree to within $\sim 3^\circ$ (Marsden 2002c), even though their nodal lines differ by nearly 20° . Kracht also argued that there is a relationship between the Marsden group and the pair of C/1999 M3 and C/2000 O3. Then, Marsden (2002d) remarked on a possible association of C/1999 N6 with C/1999 M3 and Kracht pointed out that C/2001 Q7 may be a yet another member of the Marsden population (Marsden 2002e). At that time, in 2002 March, Marsden suggested that C/1999 M3, C/1999 N6, C/2000 O3, and C/2001 Q7 belong to the Kracht group (Marsden 2002e), three more members of which were reported some four months later (Marsden 2002f).

2. PROPERTIES OF COMETS IN NEW GROUPS

A fairly large number of additional members of the three new comet groups were detected in *SOHO* images more recently, both in near-real time and in archival frames, bringing the totals by mid-2005 to 58 for the Meyer group, 21 (or 23) for the Marsden group, and 24 for the Kracht group. Their temporal distributions are summarized in Table 1.

Contrary to *SOHO* sungrazers, comets of the new groups generally appear stellar. Many Meyer-group members and nearly all Marsden- and Kracht-group members were observed after perihelion, at least for a fraction of 1 day. The apparent ability of many sunskirters to survive may be the result of their larger perihelion distance: the Meyer-group comets have perihelia between 6.6 and 8.7 R_\odot , the definite members of the Marsden group from 8.8 to 11.2 R_\odot (from 6.9 R_\odot when the uncertain members are included), and the Kracht-group comets from 6.7 to 11.6 R_\odot . For comparison, the perihelion distance of comet 96P is currently about 27 R_\odot (see Table 2 and § 5.2 for more information).

The greater perihelion distance of the sunskirters implies that they are less affected by solar tidal forces than are the sungrazers. Since the tidal stress varies inversely as the cube of distance, a sunskirter at 10 R_\odot is subjected to a tidal stress that is only ~ 0.005 times the stress on a sungrazer of the same dimensions in the orbits of comets C/1882 R1 and C/1965 S1 (Ikeya-Seki), both of which are known to have split very near perihelion. Thus, the greater chance of survival for the sunskirters makes sense dynamically.

Also unlike the *SOHO* sungrazers, the Meyer comets do not show a strong tendency toward clustering or closely spaced

TABLE 2
ORBITAL ELEMENTS BY M. S. W. KEESEY FOR COMET 96P/MACHHOLZ AT ITS FOUR APPARITIONS 1986–2002 (EQUINOX J2000.0)

Orbital Element	Apparition 2002	Apparition 1996	Apparition 1991	Apparition 1986
Perihelion time T (ET).....	2002 Jan 8.62539 \pm 0.00014	1996 Oct 15.06790	1991 Jul 21.98557	1986 Apr 23.52258
Argument of perihelion ω (deg).....	14.58069 \pm 0.00006	14.58614	14.53641	14.53370
Longitude of ascending node Ω (deg).....	94.60846 \pm 0.00003	94.53201	94.51754	94.50057
Orbital inclination i (deg).....	60.18673 \pm 0.00007	60.07432	60.14624	59.98837
Perihelion distance q (AU).....	0.12410553 \pm 0.00000029	0.12471874	0.12554718	0.12677369
Orbital eccentricity e	0.95880961 \pm 0.00000010	0.95863579	0.95836868	0.95801169
Orbital period P (yr).....	5.23	5.24	5.24	5.25
Longitude of perihelion L_π (deg).....	101.97736	101.92870	101.87229	101.88878
Latitude of perihelion B_π (deg).....	+12.61655	+12.60679	+12.57326	+12.55068
Osculation epoch (ET).....	2002 Jan 6.0	1996 Oct 4.0	1991 Jul 3.0	1986 May 10.0
Nongravitational parameters:				
A_1 (10^{-8} AU day $^{-2}$).....	+0.0264 \pm 0.0063			
A_2 (10^{-8} AU day $^{-2}$).....	-0.0001500 \pm 0.0000037			
Observations used:				
Number of ground-based.....	139			
Number of <i>SOHO</i> -based.....	5			
Period of time covered.....	1986 May 13–2002 Jun 16			
Time interval (days).....	5878			
Weighted rms residual.....	$\pm 0''.89$			

pairing, the tightest temporal separation between two consecutive members being about 3 days. On the other hand, nine Marsden-group comets appeared in triplets that spanned, respectively, 0.7, 7, and 10 days. In three cases the temporal separation between two members was only ~ 0.1 day or less. Clumping is also clearly apparent for the Kracht-group comets: a six-pack and a triplet each reached perihelion in less than 3 days, whereas four pairs arrived, respectively, 0.7, 1.6, 2.1, and 3 days apart. The spatial distribution of the Meyer group is rather compact, while the Marsden group and especially the Kracht group are spread out more loosely.

The high-inclination Meyer group, while by far the most populous of the three, is the most difficult to explore, because no potential parent object is known and the group's orbital period remains indeterminate, a major drawback for any study of its dynamical evolution. The absence of clusters or closely spaced pairs suggests an orbit with a fairly large aphelion distance.

The history of the Marsden and Kracht groups is less difficult to decipher, especially if their association with the major comet-meteor complex is confirmed. Although some avenues of analysis are impeded by very limited photometric data available in the literature (§ 4.5), the presumed short lifetimes of the Marsden and Kracht-group comets on their sunskirting orbits make a comprehensive exploration of their birth and evolution—the objective of this investigation—highly desirable.

3. THE MACHHOLZ INTERPLANETARY COMPLEX

Bailey et al. (1992) used 96P as one of several periodic comets for which they demonstrated that objects initially with inclinations near 90° and perihelion distances of up to about 2 AU can evolve into sungrazing objects due to secular perturbations by the planets. Cyclic orbital changes triggered by these perturbations display distinct correlations between the individual elements over a period of time, which is ~ 4000 yr in the case of 96P, as first shown by Rickman & Froeschlé (1988). The nature of these orbital variations is such that the perihelion distance systematically decreases with increasing deviation of the inclination from the initial value near 90° . This slow process can, however, change dramatically if fragmentation, tidal or nontidal (Sekanina 1997), becomes important. The effects on the long-term dynamical evolution have never been systematically explored, in part because the number of sungrazing comets known until recently had been very limited.

The calculations of Bailey et al. (1992) represent a numerical experiment, which indicates (as do the earlier results by Rickman & Froeschlé 1988 and by McIntosh 1990) that the perihelion distance and the inclination of comet 96P have recently been decreasing with time. However, one should not conclude from Figure 2 of Bailey et al. that this comet will collide with the Sun in $\sim 13,000$ yr from now. The comet is unlikely to survive intact over this extended period of time (more than 2000 revolutions about the Sun) and is expected to disintegrate before then. If the association with 96P is confirmed, the existence of the Marsden and Kracht groups offers indirect evidence in favor of the comet's inevitable demise over a limited period of time. In addition, nongravitational effects varying on shorter timescales might affect the comet's dynamical evolution over periods of many thousands of years. Overextended extrapolations are notoriously unreliable and have a dubious predictive value.

The nature of the relationship between comet 96P and several potentially related meteor streams—the Quadrantids in particular—has been a subject of considerable interest ever since 1986, when the comet was discovered. In the mid-1990s, the number of objects associated with comet 96P/Machholz began to grow rap-

idly, including, among others, the Marsden and Kracht groups of sunskirting comets. While the extent and envelope of the assemblage of apparently related bodies are not yet known very well, the existence of this association in the inner solar system cannot be questioned. We will refer to it hereafter as the *Machholz interplanetary complex*. The orbital elements (whose variables are defined by letters in Table 2) for all candidate contributors are listed in Table 3.

The first to consider the relationship between comet 96P and some of the meteor streams was McIntosh (1990), who found that 96P was unlikely to be the parent of the Quadrantid stream because of a 2000 yr shift (a half the cycle) in the perturbed orbital elements, implying too high an age for the stream. Following Hasegawa (1979), he instead preferred comet C/1490 Y1 (old designation 1491 I), but its orbit is poorly known. Jenniskens et al. (1997) concurred with McIntosh that 96P is not associated with the stream and proposed that the most likely parent is an as yet undetected inactive asteroid-like object. Williams & Collander-Brown (1998) suggested that 96P, C/1490 Y1, and an Apollo-type asteroid 5496 (1973 NA) are all fragments of one comet and related to the present-day Quadrantids through an unknown fragment. Very recently, the parent was identified with asteroid 2003 EH₁ by Jenniskens (2004), who added that the stream's estimated mass of 10^{13} kg could be explained if the origin dates back to a breakup ~ 500 yr ago. Williams et al. (2004), while upbeat, expressed some caution about this parentage.

On the other hand, McBride & Hughes (1990) regarded 96P as a candidate for the stream's parent, and Jones & Jones (1993) found that if 96P was captured by Jupiter during its last close approach 2200 yr ago, the resulting stream had time enough to produce most of the observed features of the meteoroid complex made up by the Quadrantids, Daytime Arietids, and the Southern δ Aquarids. Gonczi et al. (1992) favored a hypothesis according to which the present-day Quadrantids had been released from 96P about 4000 yr ago, when the comet had a very small perihelion distance. Although the last authors suggested that the most likely meteoroids to survive as part of the stream were those with semimajor axes just inside the 2:1 resonance with Jupiter, they cautioned that close encounters with the planet should lead to numerous instances of chaotic behavior, making the dynamical evolution of the stream very complex. Green et al. (1990) showed that the comet's motion has been under the strong influence of the 2:1 resonance, which has kept the comet orbiting on the inner side of the resonance boundary for at least 4000 yr, with its mean motion oscillating around the value corresponding to a weak 9:4 resonance. Babadzhanov & Obruchov (1992) listed a total of eight meteor streams they believed to be associated with 96P (four with perihelia below 0.15 AU and four with perihelia between 0.9 and 1 AU) and argued that the Quadrantids were released from the comet 6500 yr ago. Besides the Quadrantids, the streams attributed to the comet by these authors are the Daytime Arietids and the Southern and Northern δ Aquarids, all of which were also considered by McIntosh (1990), but also the Ursids (usually associated with comet 8P/Tuttle), the α Cetids, and two weak southern-hemisphere showers, the κ Velids and the Carinids.

Of particular interest is a recent conclusion by Ohtsuka et al. (2003) that the present-day orbits of the Marsden group and the Daytime Arietids coincide with the orbit of 96P in AD 2319 and, similarly, the orbits of the Kracht group coincide with the comet's orbit in AD 2408. According to Ohtsuka et al., this is evidence for time lags in the orbital evolution of the two groups and the comet.

The evolution of the Marsden and the Kracht groups of sunskirting comets and their basic relationship to the other contributors

TABLE 3
MEAN ORBITAL ELEMENTS OF COMET GROUPS, TWO OBJECTS, AND METEOR STREAMS THAT MAY BELONG
TO THE MACHHOLZ INTERPLANETARY COMPLEX (EQUINOX J2000.0)

Object(s)/Stream	Year (s) ^a	ω (deg)	Ω (deg)	i (deg)	q (AU)	e	P (yr)	L_{π} (deg)	B_{π} (deg)	Reference
Marsden Group ^b	1996–2005	22.7	81.8	27.0	0.048	(1.0)	...	102.2	+10.1	<i>SOHO</i> comet Web site ^c
Kracht Group.....	1996–2005	59.4	42.8	13.3	0.045	(1.0)	...	101.5	+11.4	<i>SOHO</i> comet Web site ^c
Daytime Arietids.....	*1951	29	78	21	0.09	0.94	2.0	105	+10	Cook (1973)
	*1961–1965	29.5	78.7	27.9	0.094	0.946	2.3	105.3	+13.3	Sekanina (1973)
	*1968–1969	25.9	77.6	25.0	0.085	0.938	1.6	101.4	+10.6	Sekanina (1976)
Southern δ Aquarids.....	†1950s	152.8	305.7	27.2	0.069	0.976	4.8	101.1	+12.1	Cook (1973)
	†1952–1953	151.0	307.6	26.6	0.078	0.972	4.7	101.2	+12.5	Jacchia & Whipple (1961)
	†1936–1989 ^{d,e}	148.8	310.6	26.3	0.09	0.97	5.2	102.1	+13.3	Welch (2001)
	*1961–1965	151.9	308.0	29.9	0.083	0.955	2.5	103.2	+13.6	Sekanina (1970)
	*1968–1969	155.4	306.4	28.2	0.069	0.958	2.1	104.4	+11.3	Sekanina (1976)
	*1990/7/21–23	156.0	299.7	29.5	0.060	0.95	1.3	98.5	+11.6	Baggaley & Taylor (1992)
	*1990/8/3–5	152.0	319.7	24.6	0.117	0.96	5.0	113.9	+11.3	Baggaley & Taylor (1992)
Northern δ Aquarids.....	†1950s	332	140	20	0.07	0.97	4.2	113	–9	Cook (1973)
	*1961–1965	324.5	140.5	16.0	0.132	0.927	2.4	106.1	–9.2	Sekanina (1970)
	*1968–1969	323.2	142.4	19.2	0.169	0.866	1.4	107.2	–11.4	Sekanina (1976)
α Cetids.....	*1960s	202	259	20	0.06	0.95	1.3	100	–7	Babadzhanov & Oubrov (1992)
Asteroid 2003 EH ₁	2003–2004	171.4	282.9	70.8	1.193	0.618	5.5	100.1	+8.1	Marsden (2004a)
Comet C/1490 Y1.....	1491	164.9	280.2	73.4	0.761	(1.0)	...	95.8	+14.5	Hasegawa (1979)
Quadrantids.....	†1950s	170.0	283.4	72.5	0.977	0.683	5.4	100.4	+9.5	Cook (1973)
	†1954	170.7	283.3	71.9	0.977	0.682	5.4	100.4	+8.8	Jacchia & Whipple (1961)
	†1936–1989 ^d	170.2	283.3	72.0	0.98	0.67	5.1	100.2	+9.3	Welch (2001)
	*1961–1965 ^f	168.1	283.0	70.3	0.974	0.682	5.4	98.9	+11.2	Sekanina (1970)
	*1964–1971	170.4	283.2	71.4	0.979	0.681	5.4	100.1	+9.1	Poole et al. (1972)
Ursids ^g	†1950s	205.8	271.4	53.6	0.939	0.85	13.6	107.4	–20.5	Cook (1973)
	*1961–1965 ^h	194.7	281.6	63.0	0.968	0.761	8.1	108.4	–13.1	Sekanina (1970)
Carinids.....	*1968–1970	354	109	79	0.98	0.61	4.0	108	–6	Babadzhanov & Oubrov (1993)
κ Velids.....	*1968–1970	18	103	77	0.97	0.51	2.8	107	+18	Babadzhanov & Oubrov (1993)

^a For meteor streams, results from photographic surveys are marked by a dagger (†); from radar surveys, by an asterisk (*).

^b Average of 21 entries, excluding the two questionable members.

^c Through 2005 June 30; see <http://ares.nrl.navy.mil/sungrazer>.

^d Based on stream search in the photographic meteor archive of the IAU Meteor Data Center (Lindblad & Steel 1994).

^e Average of two possible stream branches.

^f During the Synoptic Year 1968–1969, the radar system was not in operation near the peak period of the Quadrantids.

^g This stream is usually associated with comet 8P/Tuttle; relation to 96P was proposed by Babadzhanov & Oubrov (1992).

^h Relationship to photographic Ursids questionable; earliest radar Ursids detected 5 days after last photographic ones.

to the Machholz complex is the main subject of this first part of our investigation. We note that the orbital similarity between the Daytime Arietid stream and the Marsden group is pronounced enough that they are likely to be more closely related to one another than either of them is to comet 96P. In practice, this could indicate that the Arietids derived not from comet 96P but from a related object or even from some members of the Marsden group relatively recently. On the other hand, inspection of the orientation of the line of apsides (via L_{π} and B_{π} ; cf. Table 2) in Table 3 raises doubts about a close association with the Machholz complex of some of the candidate streams, in particular the Northern δ Aquarids, α Cetids, Ursids, and Carinids.

The second part of our investigation, to appear in the near future, will focus more closely on the nature of the fragmentation process that led to the formation of the Marsden and Kracht groups. We will also examine their expected future evolution and the problems of their population size, long-term replenishment, and steady-state conditions.

4. LIFETIMES OF MARS DEN-GROUP AND KRACHT-GROUP COMETS

No viable approach to the problem of evolution of the Machholz complex can ignore the critical problem of fragment lifetime and survival. One of the most important factors that constrain the life

span of comets, their fragments, or meteoroids in interplanetary space is the number of approaches to the Sun that they can withstand essentially intact. The number of “safe” revolutions about the Sun is shown below to be rather severely limited for objects in sunskirting orbits.

4.1. Orbital Period

The orbital period for comet 96P is known with very high accuracy (Table 2), amounting currently to slightly more than 5.2 yr. The orbital periods of the other members of the Machholz complex have been less well determined, as is apparent from Table 3. Among the listed meteor streams, the best values—near or slightly exceeding 5 yr—have been derived for the Southern δ Aquarids and the Quadrantids from a variety of photographic surveys. A high-quality determination of the orbital period of meteoroids requires painstakingly accurate measurements of the atmospheric velocity (on the order of 0.1%) and deceleration, which are needed in the calculation of the preatmospheric velocity. Bright meteors and fireballs with long atmospheric trails, detected photographically by multistation monitoring networks, provide the most satisfactory results (e.g., Whipple 1938, 1955; Jacchia & Whipple 1956, 1961). Fainter meteors are observed by radar techniques (e.g., McKinley 1961, p. 309), which are known for providing less accurate decelerations and preatmospheric

TABLE 4
ORBITAL CHARACTERISTICS OF THE MARSDEN GROUP COMETS (MARSDEN'S PARABOLIC SOLUTIONS; EQUINOX J2000.0)

Comet	T (ET)	q (R_{\odot})	i (deg)	L_{π} (deg)	B_{π} (deg)	Observed Arc ^a (hr)	Span ^b (hr)	Instrument ^c
C/1996 V2.....	1996 Nov 11.78	10.49	33.41	99.29	+9.47	+4.9 → +13.4	8.5	C3
C/1998 A2.....	1998 Jan 3.74	8.81	27.93	104.38	+11.98	+3.4 → +5.8	2.4	C2
C/1998 A3.....	1998 Jan 9.30	9.01	27.35	101.36	+10.33	+3.9 → +7.3	3.4	C2
C/1998 A4.....	1998 Jan 10.79	9.26	26.87	100.25	+9.47	+4.5 → +7.0	2.5	C2
C/1999 J6 ^d	1999 May 11.59	10.58	26.53	102.00	+9.83	-20.7 → +19.2	39.9	C2, C3
C/1999 N5 ^e	1999 Jul 11.24	10.66	27.08	107.08	+12.01	-7.2 → +12.9	20.1	C2, C3
C/1999 P6.....	1999 Aug 5.11	10.62	26.57	101.41	+9.43	-1.2 → +4.8	6.0	C2
C/1999 P8.....	1999 Aug 14.99	10.62	26.56	101.06	+9.34	+0.3 → +5.7	5.4	C2
C/1999 P9.....	1999 Aug 15.04	10.60	26.55	101.16	+9.43	+4.5 → +13.2	8.7	C2
C/1999 U2.....	1999 Oct 25.23	10.58	27.05	102.04	+9.90	-0.2 → +12.2	12.4	C2, C3
C/2000 C7.....	2000 Feb 4.48	10.34	24.89	101.50	+9.21	0.0 → +2.6	2.6	C2
C/2000 C3.....	2000 Feb 4.59	10.47	24.97	103.33	+9.68	-0.6 → +12.4	13.0	C2
C/2000 C4.....	2000 Feb 5.17	10.47	24.97	103.04	+9.51	-0.2 → +11.9	12.1	C2, C3
C/2002 R1.....	2002 Sep 2.54	10.58	22.19	102.10	+12.09	+3.4 → +7.6	4.2	C2
C/2002 R4.....	2002 Sep 3.30	11.18	28.31	103.60	+9.41	+4.4 → +10.0	5.6	C2
C/2002 V5.....	2002 Nov 12.42	10.88	34.24	102.61	+10.63	-13.6 → +8.6	22.2	C2, C3
C/2003 Q1 ^f	2003 Aug 20.97	6.88	29.33	91.95	+22.83	-1.4 → +2.3	3.7	C2
C/2003 Q6 ^f	2003 Aug 26.51	7.87	25.43	86.85	+13.59	+1.2 → +4.2	3.0	C2
C/2004 V10 ^d	2004 Nov 8.45	10.49	26.40	102.48	+9.92	-7.7 → -4.9	2.8	C2
C/2004 V9 ^d	2004 Nov 8.56	10.58	26.52	101.86	+9.84	-19.3 → +19.3	38.6	C2, C3
C/2004 W10.....	2004 Nov 29.26	10.04	25.97	105.12	+10.78	-3.8 → -0.1	3.7	C2
C/2005 E4 ^e	2005 Mar 10.54	10.47	26.43	100.71	+9.70	-6.0 → +12.0	18.0	C2, C3
C/2005 G2 ^e	2005 Apr 14.26	10.58	26.84	101.92	+10.38	-13.8 → +11.5	25.3	C2, C3

^a Times of first and last observations, reckoned from perihelion time (negative = before, positive = after).

^b Time interval between first and last observations.

^c Instrument detection: C2 coronagraph images field up to $\sim 6 R_{\odot}$ from Sun's center, whereas C3 coronagraph up to $\sim 30 R_{\odot}$; C2 detects fainter objects than C3.

^d C/2004 V9 is apparently a major fragment and C/2004 V10 a minor fragment of C/1999 J6 at next return to Sun.

^e C/2005 E4 and C/2005 G2 are apparently fragments of C/1999 N5 at next return to Sun.

^f Group membership questionable.

velocities (e.g., Southworth 1962); a major improvement was introduced only relatively recently (e.g., Baggaley et al. 1993). The orbital periods for most radar-based meteor stream entries in Table 3 are believed to be significantly underestimated.

The discrepancy between the preatmospheric velocities (and the orbital periods) of the Southern δ Aquarid stream determined by photographic and radar techniques had been commented on by Wright et al. (1954) more than 30 yr before comet 96P was discovered. They noticed that the difference of 2.5 km s^{-1} was greater than the scatter among the individual meteors in the photographic sample and offered several possible explanations, including high decelerations of the radar meteors that were unaccounted for. They also suggested that meteoroids in this stream must be very young and had arisen from a recently disrupted comet.

The parabolic orbits derived by Marsden (e.g., Marsden & Williams 2003, p. 169) are described in Table 4 for the Marsden group and in Table 5 for the Kracht group. The column headings use the parametric symbols introduced in Table 2. The last two columns present information, respectively, on the time span of the observed orbital arc, which can serve as a crude proxy parameter for the brightness, and on the *SOHO* coronagraphs used. The orbital arcs appear to be too short to successfully solve, in addition to the other elements, for the orbital period. Yet we attempted such a solution for C/1999 J6, a member of the Marsden group, whose observed arc is nearly 40 hr (Table 4), longer than for any other object of either group. Based on a total of 70 astrometric observations, the optimum osculating value of the orbital period came out to be $3.0^{+2.0}_{-1.0}$ yr, which is consistent with the comet's value within 1.1σ , but—in the absence of corroborating evidence at the time—it was judged too uncertain to offer a convincing argument for the short-period nature of the orbit. Our additional

runs, which forced the orbital periods between 5.22 and 5.34 yr, fitted the data nearly equally well, with the rms residual increasing from $\pm 4''.81$ to $\pm 4''.83$.

With no bright comet observed in the Marsden and Kracht groups, it has become increasingly evident that a more attractive approach to determining the period is to find an object at two consecutive returns to the Sun and link its astrometric observations, even though a potential pitfall of this technique is obvious: the short orbital arcs available allow one to consider a variety of linkages and therefore different orbital periods, depending on the choice of objects. It appears that this ambiguity can ultimately be removed only using a third return.

Recent developments suggest, however, that on a few occasions at least the situation is more promising than for the rest of the comets. Marsden (2004b, 2005a, 2005b) was able to link the observations of C/1999 J6 with C/2004 V9 and also those of C/1999 N5 with both C/2005 E4 and C/2005 G2 (§ 4.4). These orbital solutions show no systematic residuals and imply orbital periods of 5.49 yr for C/1999 J6 = C/2004 V9, 5.66 yr for C/1999 N5 = C/2005 E4, and 5.76 yr for C/1999 N5 = C/2005 G2. Marsden's result for C/1999 J6 and our above single-appearance value (which is within 1.25σ of 5.49 yr) reinforce each other, and together they make the identity C/1999 J6 \equiv C/2004 V9 virtually certain.

In his orbital runs, Marsden used only astrometric positions obtained with the C2 coronagraph. The run for C/1999 J6 versus C/2004 V9 was based on 58 such positions, which left residuals of up to $9''.7$ in right ascension and up to $8''.9$ in declination. The run for C/1999 N5 versus C/2005 E4 was based on 33 positions, with residuals of up to $11''.4$ in right ascension and up to $9''.3$ in declination, whereas the run for C/1999 N5 versus C/2005 G2

TABLE 5
ORBITAL CHARACTERISTICS OF THE KRACHT GROUP COMETS (MARSDEN'S PARABOLIC SOLUTIONS; EQUINOX J2000.0)

Comet	T (ET)	q (R_{\odot})	i (deg)	L_{π} (deg)	B_{π} (deg)	Observed Arc ^a (hr)	Span ^b (hr)	Instrument ^c
C/1999 M3.....	1999 Jun 30.70	9.48	12.35	103.89	+11.44	-7.3 → +5.7	13.0	C2
C/1999 N6.....	1999 Jul 12.30	9.35	12.15	95.95	+10.90	-4.3 → +8.7	13.0	C2
C/2000 O3.....	2000 Jul 30.94	11.61	14.58	100.65	+10.80	-17.3 → +13.5	30.8	C2, C3
C/2001 Q7.....	2001 Aug 21.80	9.56	13.28	97.98	+10.81	+1.2 → +4.6	3.4	C2
C/2001 Q8.....	2001 Aug 24.81	9.69	13.07	100.28	+10.83	+1.4 → +5.4	4.0	C2
C/2001 R8.....	2001 Sep 6.67	9.39	13.58	101.11	+11.69	+3.5 → +7.8	4.3	C2
C/2001 R9.....	2001 Sep 7.32	10.15	12.47	101.55	+9.97	+4.4 → +6.2	1.8	C2
C/2002 N2.....	2002 Jul 11.92	10.53	13.80	106.92	+11.24	-6.6 → +7.4	14.0	C2
C/2002 Q8.....	2002 Aug 25.92	9.93	13.84	98.01	+10.15	+2.4 → +8.8	6.4	C2
C/2002 Q10.....	2002 Aug 27.50	10.40	13.54	101.22	+10.49	+2.4 → +6.4	4.0	C2
C/2002 S4.....	2002 Sep 18.22	10.40	13.51	101.04	+10.46	-14.6 → +14.8	29.4	C2, C3
C/2002 S5.....	2002 Sep 19.33	10.04	14.03	100.18	+11.01	+7.6 → +12.2	4.6	C2
C/2002 S7.....	2002 Sep 21.06	10.38	13.53	101.16	+10.53	-8.1 → +10.7	18.8	C2, C3
C/2002 S11.....	2002 Sep 30.34	10.36	13.68	101.74	+10.72	-6.5 → +23.4	29.9	C2, C3
C/2004 A3.....	2004 Jan 16.16	9.31	14.75	102.43	+12.54	-3.9 → -1.9	2.0	C2
C/2004 B3.....	2004 Jan 18.27	11.07	13.28	98.13	+10.71	-2.6 → +10.0	12.6	C2
C/2004 J4.....	2004 May 5.33	8.96	12.35	103.07	+11.54	-5.1 → -2.1	3.0	C2
C/2004 J12.....	2004 May 12.91	8.55	12.68	105.11	+12.04	-4.0 → -1.0	3.0	C2
C/2004 J13.....	2004 May 13.85	9.48	12.47	100.06	+11.24	-4.0 → -0.6	3.4	C2
C/2004 J15.....	2004 May 14.75	9.41	12.28	101.32	+11.31	-3.6 → -0.9	2.7	C2
C/2004 J16.....	2004 May 14.97	6.75	14.63	103.00	+13.66	-1.1 → +1.6	2.7	C2
C/2004 J17.....	2004 May 15.55	7.65	13.79	107.19	+13.11	-2.8 → -0.4	2.4	C2
C/2004 J18.....	2004 May 15.69	9.91	11.89	99.03	+10.79	-3.1 → -1.1	2.0	C2
C/2004 L10.....	2004 Jun 14.10	9.26	12.54	105.03	+11.75	-10.3 → +2.7	13.0	C2

^a Times of first and last observations, reckoned from perihelion time (negative=before, positive=after).

^b Time interval between first and last observations.

^c Instrument detection: C2 coronagraph images field up to $\sim 6 R_{\odot}$ from Sun's center, whereas C3 coronagraph up to $\sim 30 R_{\odot}$; C2 detects fainter objects than C3.

was based on 34 positions, with residuals of up to $4''.9$ in right ascension and up to $14''.0$ in declination. Before addressing, in § 4.3, the ambiguity of the linkage of C/1999 N5 with the two 2005 comets, we needed to examine the accuracy of the orbital solutions. We recalculated the runs for C/1999 J6 versus C/2004 V9 and for C/1999 N5 versus C/2005 E4, but we rejected all C2 coronagraphic positions that left residuals greater than 0.75 pixel or $8''.5$ in one or both coordinates. The resulting elements for C/1999 J6=C/2004 V9 are listed and compared with Marsden's

(2004b) elements in Table 6, while the residuals are presented in Table 7. For C/1999 N5=C/2005 E4 the elements are in Table 8 and the residuals in Table 9. We find that the differences between our and Marsden's orbital sets are up to about 2σ in both the angular elements, the perihelion distance, and the eccentricity in the first case, but much better, up to at most $\sim 1 \sigma$ in the second case.

Next, we used the opportunity provided by Kracht's recent discovery of a Marsden-group comet C/1996 V2, and we tried to

TABLE 6
ORBITAL ELEMENTS FOR MARSDEN COMET C/1999 J6 = C/2004 V9 (EQUINOX J2000.0)

ORBITAL ELEMENT	APPARITION 1999	APPARITION 2004	DIFFERENCES: OUR SOLUTION MINUS MARSDEN (2004b)	
			1999	2004
Perihelion time T (ET).....	1999 May 11.58386 ± 0.00054	2004 Nov 8.56127	+0.00030	+0.00052
Argument of perihelion ω (deg).....	22.187 ± 0.032	22.295	-0.023	-0.021
Longitude of ascending node Ω (deg).....	81.724 ± 0.040	81.604	-0.076	-0.076
Orbital inclination i (deg).....	26.615 ± 0.008	26°587	+0.021	+0.005
Perihelion distance q (AU).....	0.049227 ± 0.000057	0.049167	+0.000095	+0.000105
Orbital eccentricity e	0.984176 ± 0.000018	0.984208	-0.000037	-0.000034
Orbital period P (yr).....	5.49	5.49	0.00	0.00
Longitude of perihelion L_{π} (deg).....	101.757	101.740	-0.101	-0.097
Latitude of perihelion B_{π} (deg).....	+9.740	+9.776	-0.003	-0.007
Osculation epoch (ET).....	1999 May 22.0	2004 Nov 11.0		
Observations used:				
Number from C2 images.....		54		
Number from C3 images.....		0		
Period of time covered.....	1999 May 10–2004 Nov 8			
Time interval (days).....	2009			
Weighted rms residual (arcsec).....		±3.26		

TABLE 7

POSITIONAL RESIDUALS FROM ORBITAL SOLUTION FOR C/1999 J6 = C/2004 V9
(CORONAGRAPH C2 ONLY; EQUINOX J2000.0)

TIME OF OBSERVATION (UT)	RESIDUALS: OBSERVED MINUS COMPUTED	
	R.A. ^a (arcsec)	Decl. (arcsec)
1999 May:		
10.72646.....	(-6.0)	(-15.8)
10.74958.....	(-8.7)	(-15.4)
10.76273.....	+1.3	-6.1
10.78075.....	-8.4	-1.9
10.83252.....	-7.2	-6.2
10.85080.....	(+0.4)	(-9.0)
10.90979.....	(+19.2)	(-28.6)
10.93479.....	+1.4	-1.4
10.97645.....	(-3.9)	(+10.3)
10.99312.....	+4.9	-0.8
11.00423.....	-0.4	+5.5
11.01812.....	(+10.9)	(-9.0)
11.03479.....	+0.1	+4.1
11.06030.....	(+7.1)	(-10.8)
11.07647.....	(-3.6)	(-24.0)
11.08758.....	(-9.7)	(-23.2)
11.10145.....	(-23.3)	(+11.0)
11.11812.....	-0.4	+3.9
11.12923.....	-2.2	+6.0
11.14312.....	(+9.8)	(-4.0)
11.15979.....	(-7.1)	(+9.5)
11.18480.....	-3.3	-1.9
11.20145.....	+2.5	-3.1
11.21257.....	(-8.5)	(-16.0)
11.22765.....	-0.3	+4.6
11.24431.....	(-0.3)	(+10.4)
11.25423.....	(+5.7)	(-11.4)
11.26929.....	(-12.6)	(+3.2)
11.28598.....	+0.8	+1.2
11.31166.....	+4.8	+3.9
11.33757.....	+3.0	+3.9
11.35264.....	-6.5	-4.9
11.36931.....	(-11.2)	(+13.5)
11.37924.....	-0.6	-0.4
11.39429.....	(+10.2)	(+5.3)
11.43596.....	+0.3	+1.2
11.45262.....	-1.3	+2.7
11.46257.....	+0.5	-1.1
2004 Nov:		
7.75423.....	(+9.9)	(-59.1)
7.77091.....	+0.3	-1.3
7.78758.....	-3.6	+5.5
7.81376.....	+2.3	+3.4
7.82924.....	-6.4	-7.2
7.83757.....	-4.2	+3.8
7.85424.....	+4.5	+0.8
7.89593.....	+0.7	-1.9
7.91256.....	-6.1	-0.4
7.92090.....	+1.3	+2.6
7.93756.....	+1.3	+2.1
7.96307.....	-1.7	+3.7
7.99590.....	+2.9	-2.1
8.00423.....	+0.1	+1.5
8.02090.....	-0.2	+1.0
8.03757.....	+1.3	+2.6
8.06373.....	-4.4	+0.4
8.07925.....	-0.9	+2.3
8.08757.....	+6.4	+2.1
8.10423.....	-1.2	-2.9
8.12111.....	+3.1	-5.4

TABLE 7—Continued

TIME OF OBSERVATION (UT)	RESIDUALS: OBSERVED MINUS COMPUTED	
	R.A. ^a (arcsec)	Decl. (arcsec)
8.12924.....	(-10.4)	(-8.7)
8.14590.....	-2.0	-1.9
8.16257.....	+1.8	-4.5
8.17090.....	-3.6	-6.9
8.18757.....	0.0	-3.8
8.20423.....	-4.5	+1.3
8.21256.....	+1.7	-3.1
8.22923.....	+3.7	-2.9
8.24591.....	+0.4	+1.4
8.25423.....	+1.8	+0.5
8.27090.....	+1.2	+0.5
8.28758.....	(+2.0)	(-13.0)
8.31379.....	-2.7	-0.4
8.32923.....	-2.5	-0.4
8.33757.....	-0.5	+0.4
8.35423.....	-2.5	-0.8

^a Including factor cos (decl.).

link its astrometric positions with those of the 2002 Marsden-group comets. Unfortunately, the C2 coronagraph was not in use at the time of appearance of C/1996 V2, so it was necessary to employ the comet's low-accuracy C3 coronagraphic data. We tried in vain to link C/1996 V2 with either C/2002 R1 or C/2002 R4. However, we were successful in linking C/1996 V2 with C/2002 V5. The resulting elements, listed in Table 10, imply an orbital period of almost exactly 6 yr. Table 11 indicates that the orbital solution is based on only three consistent astrometric positions from 1996, but the scatter in the remaining positions shows no systematic trends. All but three available C2 positions from 2002 are fitted quite satisfactorily, while the residuals from the eight C3 positions, although systematic, remain smaller than the pixel size of 56". In addition, the 2002 elements are in good agreement with Marsden's (2003) parabolic orbit for C/2002 V5 (generally within 6 σ , but 12 σ in the perihelion distance) and the 1996 elements are reasonably close to Marsden's (2005c) very approximate parabola for C/1996 V2, especially in the inclination.

We also attempted to link astrometric positions of a few Kracht-group comets: C/1999 M3 with C/2004 L10, yielding an orbital period of 4.95 yr and C/1999 N6 with C/2004 J4 (4.81 yr), with C/2004 J13 (4.84 yr), and with C/2004 J18 (4.84 yr). The linkage of C/1999 M3 with C/2004 L10 is based on the longest orbital arcs, 13 hr in both 1999 and 2004, whereas the arcs for C/2004 J4, C/2004 J13, and C/2004 J18 are in the range of only 2–3 hr (Table 5). Although the linked orbital arcs are fitted quite satisfactorily, we believe that the identity of C/1999 M3 with C/2004 L10—not to mention the other Kracht-group members—is much less likely than the above identities of the Marsden-group comets. We were unable to link C/1999 N6 with C/2004 L10.

Based on this limited evidence, the orbital-period range for the Marsden-group comets appears to be between 5.5 and 6.0 yr in the least. Although no results are available for the Kracht group, its orbital-period range is expected to be similar. We tentatively conclude that (1) the linkage of C/1999 M3 with C/2004 L10 is spurious and (2) both the three Marsden-group comets from early 1998 (Table 4), which should have reappeared by early 2004, and the two Kracht-group comets from mid-1999 (Table 5), which should have returned most probably before 2005 August, seem to have become too faint to be detected again (see § 4.4).

TABLE 8
ORBITAL ELEMENTS FOR MARSDEN COMET C/1999 N5 = C/2005 E4 (EQUINOX J2000.0)

ORBITAL ELEMENT	APPARITION 1999	APPARITION 2005	DIFFERENCES: OUR SOLUTION MINUS MARSDEN (2005a)	
			1999	2005
Perihelion time T (ET).....	1999 July 11.19513 \pm 0.00036	2005 Mar 10.54660	-0.00008	+0.00029
Argument of perihelion ω (deg).....	22.163 \pm 0.046	22.271	-0.005	-0.005
Longitude of ascending node Ω (deg).....	81.768 \pm 0.018	81.618	-0.007	-0.008
Orbital inclination i (deg).....	26.617 \pm 0.010	26.497	+0.006	+0.006
Perihelion distance q (AU).....	0.049178 \pm 0.000014	0.049155	-0.000016	-0.000016
Orbital eccentricity e	0.984517 \pm 0.000004	0.984526	+0.000005	+0.000004
Orbital period P (yr).....	5.66	5.66	0.00	0.00
Longitude of perihelion L_{π} (deg).....	101.778	101.747	-0.013	-0.013
Latitude of perihelion B_{π} (deg).....	+9.730	+9.735	-0.001	0.000
Osculation epoch (ET).....	1999 July 1.0	2005 Mar 11.0		
Observations used:				
Number from C2 images.....		31		
Number from C3 images.....		0		
Period of time covered.....	1999 July 10–2005 Mar 11			
Time interval (days).....		2070		
Weighted rms residual (arcsec).....		\pm 2.76		

The two Marsden-group comets observed in 2003 August could not be the returns of the 1998 objects because of their orbital incompatibility. A currently undecided issue is whether orbital periods of some Marsden- and Kracht-group comets can significantly exceed 6 yr.

The premise of an orbital-period distribution confined to a range of 5.5–6.0 yr can further be tested by searching the pre-1999 *SOHO* coronagraphic images for previous returns of the 2001–2005 members of the two groups, that is, the cases similar to the apparent identity of C/1996 V2 with C/2002 V5. The difficulty is that the LASCO coronagraphic operations were rather incomplete in the early times of the *SOHO* mission, with occasional gaps especially in the first half of 1996. The operations were suspended when contact with the *SOHO* spacecraft was lost in 1998 July–September and again during the gyroscope failure in 1998 December–1999 January. Also, at times when one could rely only on the less sensitive C3 coronagraph must it be most difficult to detect previous appearances of the Marsden-group comets C/2002 R1, C/2002 R4, and C/2004 W10 (comet C/2004 V10 is discussed in § 4.2) and most of the Kracht-group comets from the years 2001, 2002, and 2004. The best chances are probably offered by C/2002 S4, C/2002 S7, and C/2002 S11, which were detected with both coronagraphs and should have previously been at perihelion in late 1996 or early 1997.

4.2. Fragmentation Modeling of Marsden-Group Pairs

The apparent identity of comets C/1999 J6 and C/2004 V9 offered a new insight into the source of clustering in the Marsden group. The fairly bright object C/2004 V9 was preceded by a fainter companion, C/2004 V10, which moved in a nearly identical orbit, passing through perihelion only 0.11 day before C/2004 V9. No such companion was reported to move with C/1999 J6, and a new search in the archival frames conducted by K. Battams¹ in 2004 December confirmed its absence. While there is no doubt that C/2004 V9 and C/2004 V10 are fragments of their common parent object, the question is, when did the splitting occur?

Fortunately, the relatively small separation between C/2004 V9 and C/2004 V10, about 0°.6, rendered it possible to measure

their simultaneous astrometric positions on nine images taken with the C2 coronagraph on board the *SOHO* spacecraft during a 2.8 hr long period of time on 2004 November 8, just before their perihelion passage. The offsets in right ascension and declination, listed in Table 12 after their conversion to the geocentric coordinate system, allow us to examine in detail the process of separation from their common parent.

The fragmentation model that we employ was developed long ago (Sekanina 1978, 1982). Linked with an orbit-determination code based on a simple Keplerian motion, which is more than adequate for scenarios involving not-too-long intervals of time between fragmentation and observation, the model was successfully tested on many occasions since its inception. The full-scale version describes a fragmentation event by up to five parameters: (1) the time of fragmentation t_{fig} ; (2) the components of the separation velocity V_{sep} in three cardinal directions; and (3) the differential deceleration γ due to outgassing asymmetry. The directions defined by the heliocentric orbit of the parent comet are the radial (away from the Sun), transverse, and normal directions of the right-handed RTN coordinate system at time t_{fig} . The respective components of the separation velocity are V_R , V_T , and V_N .

More recently, the software for the fragmentation model was linked with an elaborate orbit-integration code, and in this configuration it was employed for the first time in our investigation of the fragmentation sequence and hierarchy of comet D/1993 F2 (Shoemaker-Levy 9; see Sekanina et al. 1998). The code's equations of motion account for the differential planetary perturbations affecting the fragments and include the relativistic effect and the nongravitational terms in Style II of Marsden et al. (1973), characterized by parameters A_1 and A_2 . The code allows the user to integrate the motion numerically forward or backward in time with a variable step that automatically prevents the accumulation of error from exceeding a prescribed tolerance limit.

The integration of motion starts from an osculation epoch at which the orbit of the primary fragment is known. An iterative least-squares differential-correction procedure, which makes use of software that solves the normal equations for an arbitrary number of unknowns, is applied to determine the parameters of the fragmentation model from available astrometric offsets, as described above. An important feature of the software is the option to solve for any combination of fewer than the five parameters,

¹ See <http://groups.yahoo.com/group/sohohunter/message/1442>.

TABLE 9

POSITIONAL RESIDUALS FROM ORBITAL SOLUTION FOR C/1999 N5 = C/2005 E4
(CORONAGRAPH C2 ONLY; EQUINOX J2000.0)

TIME OF OBSERVATION (UT)	RESIDUALS: OBSERVED MINUS COMPUTED	
	R.A. ^a (arcsec)	Decl. (arcsec)
1999 July:		
10.93756.....	+3.3	+3.1
10.97923.....	+5.3	-3.6
10.99590.....	-2.9	+0.7
11.00423.....	(+14.4)	(+6.0)
11.02090.....	+2.2	-0.8
11.03756.....	+5.8	-0.9
11.06349.....	-1.8	-0.5
11.07923.....	-1.0	+3.2
11.08756.....	-2.2	+2.6
11.10423.....	-3.5	+1.9
11.31349.....	-0.9	+0.2
11.32923.....	-3.6	+4.3
11.33756.....	-2.3	-0.2
11.35425.....	+1.5	-3.0
11.37090.....	-5.1	+1.3
11.37923.....	+0.2	-2.9
11.39590.....	+1.9	+0.1
11.41256.....	-0.2	+3.1
11.43756.....	-1.2	+0.1
11.45423.....	+0.6	+3.9
11.46256.....	+1.7	-1.5
11.47923.....	+2.3	-1.9
11.49590.....	-0.6	+0.6
11.50423.....	-3.9	-1.4
11.52090.....	+0.6	-0.1
11.53757.....	+3.2	-2.9
11.56347.....	+1.2	+2.3
2005 Mar:		
10.85423.....	(-14.4)	(+10.1)
10.89593.....	-7.1	-2.1
10.91256.....	-0.7	+5.5
10.92090.....	(-7.8)	(-8.6)
10.93756.....	-1.3	-1.4
10.97923.....	+6.0	-3.2
10.99606.....	(-31.2)	(+39.7)
11.00423.....	(-29.6)	(+13.1)
11.02090.....	+2.9	-1.8
11.03756.....	(-40.4)	(+10.0)

^a Including factor $\cos(\text{decl.})$.

so that a total of 31 different types of solution are available. This option proves very beneficial when the convergence is slow or the parameters are highly correlated with one another.

Before applying the upgraded version of this technique to the pair of C/2004 V9 and C/2004 V10, we make two remarks: (1) in nontidally formed configurations of split comets (as defined in Sekanina 1997) it is common that the leading fragment is the most massive one and usually—but not always—the brightest; and (2) our experience with a large number of split comets indicates that plausible fragmentation solutions require low separation velocities, not exceeding a few meters per second.

Now, the fact that the fainter member of the pair, C/2004 V10, preceded the brighter suggests—especially in the absence of activity—that their relative motion was probably dominated by the conditions at splitting rather than by the companion's subsequent differential deceleration. Our early computer runs for this pair convinced us that the available astrometric data, of fairly low accuracy, would at best allow only two-parameter solutions and

that the fragmentation time t_{fig} and the radial component V_R of the separation velocity were the parameters that could not be solved for at all. Accordingly, we assumed $V_R = 0$ and searched for solutions with fixed fragmentation times, which we varied at a constant step from run to run.

We examined two classes of fragmentation scenarios for this pair of comets by solving (1) for the transverse and normal components of the separation velocity (V_T and V_N) and (2) for V_N and the deceleration γ . We were unable to derive a satisfactory solution for a fragmentation time near the 1999 perihelion time. When ignoring four of the nine offsets (Table 12), we were able to come up with a range of solutions, some of which were very satisfactory; six selected solutions are listed in Table 13, and the positional residuals from four of these are presented in Table 12.

The first two solutions in Table 13, which place the splitting at 100 days before the 1999 perihelion, appear to be the most satisfactory ones. They are representative of scenarios whose fragmentation time ranges from two to more than four months before the 1999 perihelion, all offering a nearly identical fit to the five employed offsets in Table 12. Solution 1 shows that V_T is very low, but not well determined, while solution 2 indicates that the same is true about γ . In either case, V_N amounts to less than 3 m per second and the rms residual is equivalent to about 0.3 pixel size of the C2 coronagraph, reaching a broad minimum near 100 days before the 1999 perihelion. Thus, the bulk of the effect was due to the companion's separation velocity in the direction normal to the orbit plane. When the breakup episode was assumed to have taken place closer to the 1999 perihelion, the fit improved only marginally, but the implied value of V_N increased rapidly, making such cases unacceptable, as illustrated by solution 3. All runs with the breakup assumed to have occurred within about a month of perihelion failed to converge. Runs that assumed the fragmentation event to have occurred after the 1999 perihelion led to unacceptable scenarios. The normal component of the separation velocity was much too high, well in excess of 10 m per second until about $t_{\text{fig}} = T + 100$ days. By that time the quality of fit deteriorated markedly (solution 4). The magnitude of V_N reached a minimum of ~ 7 m per second for breakup events ~ 300 days after the 1999 perihelion, after which V_T and V_N were increasing and the fit was steadily deteriorating as the assumed fragmentation time drew closer to the 2004 perihelion. When γ was solved for instead of V_T , the fitting was somewhat better (solution 5), but these scenarios show C/2004 V9 to be decelerated relative to C/2004 V10 and imply, contrary to all indications, that the latter object was the more massive of the two. For fragmentation times greater than about 600 days after the 1999 perihelion, the deceleration began to increase rapidly (solution 6). The fit never became as satisfactory as for the runs with the breakup before the 1999 perihelion, and it further deteriorated as the fragmentation time was approaching the 2004 perihelion.

In summary, we submit that C/1999 J6 broke into C/2004 V9 and C/2004 V10 a few months before the 1999 perihelion, and the event is described fairly well by solutions 1 and 2 in Table 13. Thus, C/1999 J6 was already double when imaged on 1999 May 11. The absence of observed duplicity is explained by the fact that for any breakup time as far back as ~ 130 days before the 1999 perihelion, the fragments were separated by less than $11''$ (a pixel size of the C2 coronagraph's CCD detector array) and therefore unresolved in all the May 11 images of C/1999 J6.

Comets C/2000 C3 and C/2000 C7 made up the only other pair in the Marsden group whose images could be measured in common C2 coronagraph frames. Only two in number, the astrometric offsets (referred to the center of Earth) are listed in Table 14, which shows the separation distances of $\sim 0.6''$, similar

TABLE 10
ORBITAL ELEMENTS FOR MARSDEN COMET C/1996 V2 = C/2002 V5 (EQUINOX J2000.0)

Orbital Element	Apparition 1996	Apparition 2002
Perihelion time T (ET).....	1996 Nov 11.84831 \pm 0.00061	2002 Nov 12.42095
Argument of perihelion ω (deg).....	18.759 \pm 0.064	18.713
Longitude of ascending node Ω (deg).....	86.271 \pm 0.077	86.366
Orbital inclination i (deg).....	34.440 \pm 0.033	34.559
Perihelion distance q (AU).....	0.051706 \pm 0.000089	0.050918
Orbital eccentricity e	0.984347 \pm 0.000027	0.984568
Orbital period P (yr).....	6.00	5.99
Longitude of perihelion L_π (deg).....	101.918	101.953
Latitude of perihelion B_π (deg).....	+10.479	+10.486
Osculation epoch (ET).....	1996 Nov 13.0	2002 Nov 22.0
Observations used:		
Number from C2 images.....	17	
Number from C3 images.....	3	
Period of time covered.....	1996 Nov 12–2002 Nov 12	
Time interval (days).....	2191	
Weighted rms residual (arcsec).....	± 3.17	

to the separation distances of the 2004 pair. The fragments of this pair arrived at perihelion also 0.11 day of each other (Table 4), just as the fragments of the 2004 pair. Another similarity is in their order of arrival: the brighter fragment, C/2000 C3, followed the fainter.

We accepted Marsden's set of parabolic orbital elements for C/2000 C3 but replaced the eccentricity of unity with 0.98435, which, with the perihelion distance of 0.0487 AU, is equivalent to forcing an osculating value of 5.49 yr—the same as C/2004 V9—for the orbital period. With the perihelion of C/2000 C3 on 2000 Feb 4.59 ET, the orbit integration yielded the previous perihelion on 1994 August 15, long before the *SOHO*'s launch. Our experience with the 2004 pair suggests that the order in which the fragments of the 2000 pair arrived rules out a major effect of the deceleration on their relative motion, and we assumed it always to be zero. The time of fragmentation was, not surprisingly, indeterminate, and we used the same procedure as in the case of the 2004 pair in an effort to constrain it. We found that this time the normal component V_N of the separation velocity always came out to be very close to zero, so there was no need to solve for it. The only unknown parameters that we were left with were V_R and V_T . All solutions based on the assumption of the fragmentation event preceding the presumed 1994 perihelion of the parent of the 2000 pair failed, so that the fragments appear to have been less than one revolution old when they arrived in 2000. Table 15 lists selected solutions on various assumptions for a fragmentation time between 1994 and 1999, all of which fit the offsets in Table 14 with an rms residual of $\pm 4''$ or 0.4 the pixel size of the C2 coronagraph's detector.

The best solutions in Table 15—the ones with a low separation velocity near 1.7 m s^{-1} —imply a fragmentation event occurring between 400 and 800 days after the presumed 1994 perihelion (solutions 4 and 5). Assumptions of an earlier breakup, especially at a time of less than 100 days after the 1994 perihelion, result in inferior solutions because of the high values implied for V_T (solutions 1 and 2). Assumptions of a more recent breakup, less than some 700 days before the 2000 perihelion, also lead to unsatisfactory results, as the values required for V_R were unacceptably high (solution 7).

Judging from these results, it appears that pairs of the Marsden group with fragments less than $\sim 1^\circ$ apart near perihelion, can be explained by low separation velocities, not exceeding 3 m per second. The age of the two examined pairs is found to be very short,

on the order of one revolution about the Sun. We strongly suspect that this is the same fragmentation process that has been shown to proceed on a massive scale in the Kreutz system, accounting for the large numbers of pairs and clusters among the sungrazers (e.g., Sekanina 2002a, 2002b). Since the two examined pairs of the Marsden-group comets are some of the closest on record (Table 4), it is desirable to investigate—to the extent possible—whether the above conclusions also apply to other pairs and clusters of the Marsden and Kracht groups. While we cannot extend the application of our fragmentation model to any additional cases, we can use a version of the same computer code to set constraints to known orbital parameters of these objects.

4.3. Clustering and Age of Fragments

From the results for the two comet pairs of the Marsden group in § 4.2, one may be tempted to conclude that the near-perihelion zone tends to be avoided by recent fragmentation events. This is not the case (§ 4.4). We are confronted by a selection effect, which stems from our requirement that both members of the pair appear in the coronagraph's field of view at the same time and that they therefore arrive at perihelion nearly simultaneously, within a few hours of each other. Inspection of Tables 4 and 5 indicates that a median value of the differences between the perihelion times of two consecutive comets in pairs and clusters is near 0.8 day for the Marsden group and near 0.9 day for the Kracht group, if a pair/cluster is defined conservatively by an upper limit of 10 days between any two consecutive entries. The average values for the perihelion-time differences, which are much more sensitive to the choice of the upper limit than the median values, are higher by a factor of ~ 3 .

To investigate these perihelion time differences, we assume that a Marsden- or Kracht-group comet splits at or near perihelion one revolution earlier. We examine the magnitude of the maximum difference ΔT between the perihelion times of the two fragments at the next return caused by their separation velocity V_{sep} of less than 3 m per second (proposed in § 4.2 as an upper limit). For fragmentation events that occur close to perihelion, the difference ΔT (in days) can satisfactorily be approximated by a change in the orbital period between the two fragments derived from the virial theorem:

$$V_{\text{sep}}^* = 27.18 \Delta T r_{\text{fig}}^{-1/2} P^{-4/3} \left(2P^{2/3} - r_{\text{fig}} \right)^{-1/2}, \quad (1)$$

TABLE 11
POSITIONAL RESIDUALS FROM ORBITAL SOLUTION LINKING C/1996 V2
WITH C/2002 V5 (EQUINOX J2000.0)

TIME OF OBSERVATION (UT)	CORONAGRAPH Used	RESIDUALS: OBSERVED MINUS COMPUTED	
		R.A. ^a (arcsec)	Decl. (arcsec)
1996 Nov:			
11.98617.....	C3	(−5.6)	(+41.2)
12.00701.....	C3	(−22.9)	(+13.2)
12.02784.....	C3	(+20.3)	(+7.9)
12.05217.....	C3	−3.8	+1.4
12.10492.....	C3	+1.1	−1.8
12.14937.....	C3	0.0	−0.3
12.18756.....	C3	(−16.4)	(+16.3)
12.22576.....	C3	(−8.1)	(+21.4)
12.26048.....	C3	(−12.0)	(+7.8)
12.29869.....	C3	(+49.9)	(−33.3)
12.34034.....	C3	(+20.0)	(+47.9)
2002 Nov:			
11.85423.....	C2	(+3.9)	(+37.6)
11.89590.....	C2	−3.7	+1.2
11.91256.....	C2	+0.8	−0.2
11.92090.....	C2	−4.4	+1.0
11.93756.....	C2	+3.8	−4.9
11.96257.....	C2	+2.3	+4.1
11.97923.....	C2	(+2.5)	(+13.0)
11.99590.....	C2	+5.3	−5.1
12.00423.....	C2	+0.3	+1.2
12.02090.....	C2	+1.7	+4.2
12.08757.....	C2	−3.1	+2.3
12.10423.....	C2	−3.3	−3.0
12.12090.....	C2	+0.9	−1.4
12.12923.....	C2	−0.3	−1.9
12.14590.....	C2	−3.3	+4.1
12.16258.....	C2	−2.3	+0.4
12.17090.....	C2	+1.2	−5.4
12.18757.....	C2	−2.8	+1.1
12.20423.....	C2	+6.9	+2.5
12.21256.....	C2	(−1.1)	(+9.6)
12.59590.....	C3	(−18.1)	(−42.1)
12.61256.....	C3	(−10.6)	(−23.6)
12.63756.....	C3	(+12.0)	(−18.8)
12.65423.....	C3	(+0.7)	(−46.4)
12.72090.....	C3	(+46.9)	(−26.1)
12.73757.....	C3	(+27.7)	(−52.9)
12.76256.....	C3	(+23.6)	(−46.1)
12.77923.....	C3	(+26.9)	(−31.4)

^a Including factor $\cos(\text{decl.})$.

where V_{sep}^* is the minimum separation velocity (along the orbital-velocity vector; in m s^{-1}) that can cause the effect of ΔT , $r_{\text{frag}} = r(t_{\text{frag}})$ is the comet's heliocentric distance at fragmentation (in AU), and P is the orbital period (in years).

In the virial-theorem approximation, the solution is symmetrical relative to perihelion for both the fragmentation times t_{frag} and the differences ΔT , which are taken in equation (1) to be always positive regardless of whether a fragment precedes or follows a reference fragment in the same cluster or pair. The separation velocities for a hypothetical fragment of C/1999 J6 ($q = 0.0491$ AU, $P = 5.49$ yr; see Marsden's [2004b] elliptical orbit) that are lower than 3 m per second are presented in Table 16, from which one can see that a ΔT effect of up to 10 days is fully accounted for. We point out that in reality there is some minor asymmetry that arises from the planetary perturbations. There

are also systematic deviations from the symmetry that grow with increasing temporal separation of a fragmentation event from perihelion, as the virial-theorem approximation becomes less satisfactory. We randomly checked these effects by rigorously integrating the motions of several hypothetical fragments of C/1999 J6. For this purpose we employed our orbit-integration code, described in § 4.2, but this time linked with another iterative least-squares differential-correction procedure that examines effects of the separation velocity (as well as the deceleration) on the individual orbital elements rather than on astrometric offsets. This version of the computing technique was elaborated upon in Sekanina & Chodas (2002).

We found that the approximation by equation (1) was entirely satisfactory for fragmentation times of up to several tens of days from perihelion. The asymmetry effects in ΔT from events assumed to have occurred 200 days before and after perihelion amounted to several centimeters per second. At 500 days from perihelion the virial-theorem approximation was essentially useless.

An important conclusion from this simple exercise (Table 16) is that the differences in the perihelion times of consecutive entries in Tables 4 and 5 of up to ~ 10 days, typical for the pairs and clusters in the Marsden and Kracht groups, can readily be explained by a single breakup of the parent comet about one revolution earlier. Such fragmentation events require separation velocities of less than 3 m per second and are likely to occur along the perihelion arc of the orbit (within 1 day or so of the perihelion passage). In a large majority of cases, the fragments of a pair or cluster are not in the field of the *SOHO* coronagraphs at the same time, so that the model applied in Tables 12 and 14 cannot now be used. The hierarchy of the Marsden and Kracht groups is consistent with the age of many, if not most, of their members being less than two revolutions about the Sun, equivalent to less than ~ 10 yr. In particular, the fainter comets whose observed arcs did not exceed ~ 10 hr are likely to belong to this class of exceedingly young objects.

This conclusion is corroborated by the failure of the three Marsden-group comets from early 1998—C/1998 A2, C/1998 A3, and C/1998 A4—to reappear in 2003 or early 2004 (§ 4.1). Making up a cluster in 1998, the three objects were each seen for only 2–3 hr in the C2 coronagraph, just like C/2004 V10 (2.8 hr) and C/2000 C7 (2.6 hr). We suggest that they were products of a fragmentation episode (or episodes) that had taken place one revolution earlier, probably in 1992, years before the launch of the *SOHO* spacecraft. Unless the 1998 comets are found during a future *SOHO* archive search in the coronagraphic frames from 2003 or early 2004 (a possibility that a priori is unlikely), their appearance as separate objects nearly 8 yr ago may have been the first as well as the last one. This conclusion applies equally to faint Kracht-group comets, even though their temporal distribution is less favorable for conducting this kind of analysis.

4.4. Evidence of Cascading Fragmentation

The proposed sequence of events offers possible evidence for a process of cascading fragmentation, whereby an initial parent object broke up into two or more first-generation fragments, at least some of which further broke up into two or more second-generation fragments, etc. Strong evidence that this process has been going on for the Kreutz system of sungrazing comets is based on two facts: (1) the disintegration of all *SOHO* sungrazers before perihelion requires that their existence as separate objects cannot predate the previous return to the Sun and (2) the large scatter in the angular orbital elements and in the perihelion distance of these sungrazers indicates that fragmentation proceeded mostly at very

TABLE 12
ASTROMETRIC OFFSETS AND RESIDUALS OF C/2004 V10 RELATIVE TO C/2004 V9 (EQUINOX J2000.0)

TIME OF OBSERVATION 2004 NOV (UT)	RESIDUALS: OBSERVED MINUS MODELED ^a									
	OFFSETS		Solution 1		Solution 2		Solution 3		Solution 6	
	R.A. (arcsec)	Decl. (arcsec)	R.A. (arcsec)	Decl. (arcsec)	R.A. (arcsec)	Decl. (arcsec)	R.A. (arcsec)	Decl. (arcsec)	R.A. (arcsec)	Decl. (arcsec)
8.12924.....	-1443.9	+1689.0	(-10.7)	(+18.1)	(-10.8)	(+18.1)	(-10.7)	(+18.1)	(-10.6)	(+18.5)
8.14590.....	-1402.8	+1673.9	(+13.9)	(+3.1)	(+13.8)	(+3.1)	(+13.9)	(+3.1)	(+14.0)	(+3.4)
8.16257.....	-1399.1	+1668.9	0.0	-0.9	-0.1	-0.9	0.0	-0.9	0.0	-0.8
8.17090.....	-1389.3	+1671.9	+0.6	+2.9	+0.5	+2.9	+0.6	+2.9	+0.5	+3.0
8.18757.....	-1371.2	+1672.8	-0.7	+6.2	-0.8	+6.1	-0.7	+6.2	-0.9	+6.0
8.20423.....	-1350.1	+1660.8	-0.2	-2.5	-0.3	-2.6	-0.2	-2.5	-0.5	-2.8
8.21256.....	-1349.0	+1677.8	(-9.9)	(+16.5)	(-10.0)	(+16.3)	(-9.9)	(+16.5)	(-10.3)	(+16.1)
8.22923.....	-1326.6	+1657.8	(-10.0)	(+1.3)	(-10.1)	(+1.1)	(-9.9)	(+1.3)	(-10.4)	(+0.8)
8.24591.....	-1292.6	+1644.8	+0.3	-5.8	+0.2	-6.0	+0.4	-5.8	-0.2	-6.5

^a Residuals for offsets not used in the solution are in parentheses.

large heliocentric distances, where a separation velocity is not a negligibly small fraction of the orbital velocity.

The most compelling argument for cascading fragmentation of Marsden-group comets is presented by the fact, briefly remarked on in § 4.1, that Marsden (2005a, 2005b) successfully linked C/1999 N5 with both C/2005 E4 and C/2005 G2. The likelihood of the two 2005 comets being fragments of C/1999 N5 led Marsden to a suggestion that C/1999 N5 and C/1999 J6 were themselves fragments that had separated from their common parent one revolution earlier, in 1993 (see also Green 2005a, 2005b). Marsden supported this conclusion by comparing the orbits of the two 1999 comets in late November of 1993: linking C/1999 J6 with C/2004 V9, Marsden (2005a) found that the calculated perihelion time differed by only 1.7 days (within the errors of observation) from the perihelion time calculated by linking C/1999 N5 with C/2005 E4, the brighter (B. G. Marsden 2005, private communication) of the two 2005 fragments. Thus, in this Marsden scenario, the parent of C/1999 J6 and C/1999 N5, the pair itself, and its four fragments—C/2004 V9, C/2004 V10, C/2005 E4, and C/2005 G2—represent three consecutive generations of a branch of the Marsden group. The number of known members would have grown even further, if C/1999 U2 or its fragments returned around 2005 October 8, as predicted (Marsden 2005a). Although this object and the three 1999 August Marsden-group comets, C/1999 P6, C/1999 P8, and

C/1999 P9, could not be linked with C/2005 G2 (Marsden 2005d), they were expected to reappear during 2005 if they survived (Marsden 2005b; Green 2005b). None of the three August comets, whose returns were due between April 28 and May 18, was observed, nor were any remnants of the brighter object C/1999 U2 in early October of 2005.

There are two significant differences between the pairs C/2004 V9–V10 and C/2000 C3–C7 on the one hand and the pairs C/1999 J6–N5 and C/2005 E4–G2 on the other. The members of the first two pairs arrived at perihelion within a few hours of each other, the fainter always preceding the brighter. The members of the latter two pairs arrived at perihelion 1–2 months apart, the fainter always following the brighter. These separations are too large to be explained by low enough separation velocities (unless the fragmentation events occurred, most improbably, many revolutions ago); also, either of the two latter pairs fails to satisfy the criterion for clustering as defined in § 4.3.

These seemingly major discrepancies have a simple explanation. The separations between fragments in each of the latter pairs were so large because they were brought about by a differential nongravitational deceleration, not by a separation velocity. We undertook to investigate this problem in detail, using a version of the iterative least-squares differential-correction code for the fragmentation model, which, described by Sekanina & Chodas (2002) and already employed in § 4.3, fully accounts for the differential

TABLE 13
SELECTED FRAGMENTATION SOLUTIONS FITTING OFFSETS OF C/2004 V10 RELATIVE TO C/2004 V9

Fragmentation Parameter	Solution 1	Solution 2	Solution 3	Solution 4	Solution 5	Solution 6
Assumed time of fragmentation:						
Days from 1999 perihelion, ^a $t_{\text{fig}} - T$	-100	-100	-40	+100	+100	+600
Date 1999/2000 (ET) ^b	Jan 31.6	Jan 31.6	Apr 1.6	Aug 19.6	Aug 19.6	*Dec 31.6
Heliocentric distance (AU).....	2.14	2.14	1.19	2.14	2.14	5.54
Distance from ecliptic (AU).....	-0.57	-0.57	-0.36	-0.13	-0.13	-0.80
Separation velocity ^c (m s ⁻¹):						
Transverse component, V_T	+0.31 ± 0.27	(0)	+0.34 ± 0.32	-1.30 ± 0.01	(0)	(0)
Normal component, V_N	-2.61 ± 0.85	-2.84 ± 0.94	-4.49 ± 1.83	-9.04 ± 2.42	-5.89 ± 2.23	-1.62 ± 0.53
Differential deceleration (units) ^d	(0)	1.05 ± 0.80	(0)	(0)	-1.73 ± 0.01	-10.01 ± 0.01
rms offset residual (arcsec).....	±3.34	±3.36	±3.33	±3.92	±3.62	±3.50

^a C/2004 V9 was at perihelion on 1999 May 11.6 ET. Fragmentation occurred before perihelion for negative $t_{\text{fig}} - T$ and vice versa.

^b The 2000 date, for solution 6, is marked by an asterisk.

^c No solution possible for radial component V_R , which was always assumed to be zero.

^d These are units of 10^{-5} solar attraction; negative deceleration requires that C/2004 V10 be a primary (more massive) fragment.

TABLE 14
ASTROMETRIC OFFSETS AND RESIDUALS OF C/2000 C7 RELATIVE
TO C/2000 C3 (EQUINOX J2000.0)

TIME OF OBSERVATION 2000 FEB (UT)	OFFSETS		RESIDUALS: OBSERVED MINUS MODELED	
	R.A. (arcsec)	Decl. (arcsec)	R.A. (arcsec)	Decl. (arcsec)
4.57923.....	-2138.8	+291.3	+4.5	0.0
4.58756.....	-2157.7	+284.4	-4.5	0.0

planetary perturbations of individual fragments and uses their orbital elements as proxy “observations” to determine the separation parameters.

We began with the pair of C/2005 E4 and C/2005 G2. Table 17 lists the differences between Marsden’s (2005a, 2005b) orbital elements for C/2005 E4 and C/2005 G2 (from his solutions linking them with C/1999 N5) reduced to a common osculation epoch. The errors are from our run in Table 8. It is apparent that only the differences in the perihelion time and the eccentricity and, to a degree, in the perihelion distance are significant. Only marginally significant is the difference in the argument of perihelion.

The results of our calculations are four fragmentation solutions listed in Table 18. Solution 1 is based on an assumption that the comet pair separated with no relative velocity at the 1999 perihelion and moved under a differential nongravitational force. Except for the argument of perihelion, the residuals in the orbital elements are smaller than the errors in Table 17. Relaxing the constraint on the time of separation, we find in solution 2 some tendency for the fragmentation event to have occurred about a day or so before perihelion, with the deceleration nearly doubled. Solving, in addition, for the normal component of the separation velocity yields an indeterminate result (solution 3), which however suggests that C/2005 G2 may have been released slightly to the south of the orbital plane. Forcing a lower separation velocity (conforming to our conclusions in §§ 4.2–4.3) yields solution 4, which in terms of the rms residual is entirely acceptable and the best among the four. It shows a more distinct preference for a preperihelion fragmentation event than solution 2. No satisfactory solutions involving the radial and/or transverse component(s) of the separation velocity were found. Contrary to the pairs C/2004 V9–V10 and C/2000 C3–C7, the breakup of C/1999 N5 into C/2005 E4 and C/2005 G2 shows that fragmentation of Marsden-group comets can occur in the immediate proximity of perihelion and that the motions of fragments can be dominated by a differential deceleration.

Next we examined the relationship between C/1999 J6 and C/1999 N5. Some of our preliminary results have been reported by Green (2005b). Of major interest was the meaning of the orbital similarity in 1993, as published by Marsden (2005a). Using our code, we integrated his 1999 orbits for the two objects back in time to 1993 and were able to reproduce his result. The orbital difference is presented in the first line of Table 19. We then integrated our orbits for the two comets (listed, respectively, in Tables 6 and 8) back in time to the same osculation epoch and computed the differences between these elements. The numbers are in the second line of Table 19. Since there is no compelling reason for a priori preferring either of the two orbital pairs over the other, we have two sets of orbital differences whose comparison provides information on the degree of uncertainty involved in the orbital extrapolation from 1999 to 1993. The discrepancies between the two sets of differences in the six orbital elements is presented in the third line of Table 19 and compared with the combined formal rms errors (from Tables 6 and 8) in the last line.

Table 19 raises serious doubts about the identity of C/1999 J6 with C/1999 N5 before 1993. The large deviations from a common orbit (zero difference) derived from both Marsden’s and our results for three elements, Ω and especially i and e , amounting on the average to, respectively, some 5σ , 19σ , and 20σ , are most disturbing, because the discrepancy is always smaller than 3σ . The discrepancy in ω is smaller than the rms error, which means that the deviation from a common orbit in this element is about 3σ and is only marginally acceptable. Although the discrepancy in T is, not surprisingly, more than 3 orders of magnitude greater than the 1999 rms error, the averaged deviation from a coincident perihelion passage is only about 2σ and therefore still acceptable. The perihelion distance is the element that is most consistent with the notion of the two comets having been identical before 1993. While it is possible that C/1999 J6 and C/1999 N5 separated from a common parent in 1993, they do not appear to be its only two fragments.

Doubts about direct separation of C/1999 J6 and C/1999 N5 from each other are further strengthened by an independent examination of their 1999 orbits, using the technique applied to the pair C/2005 E4 and C/2005 G2. The 1999 orbital differences in the ascending node and inclination require an absurdly high separation velocity of more than 800 m s^{-1} (!) in the direction normal to the orbit plane, if the breakup occurred at perihelion. If it took place far from perihelion, it is the nongravitational deceleration that attains an unacceptably large value. We thus find compelling evidence that even if C/1999 J6 and C/1999 N5 should be fragments of a common precursor, its fragmentation was much more complex than a simple breakup into the two pieces; the process is likely to have involved a number of events and fragments. It

TABLE 15
SELECTED FRAGMENTATION SOLUTIONS FITTING OFFSETS OF C/2000 C7 RELATIVE TO C/2000 C3

Fragmentation Parameter	Solution 1	Solution 2	Solution 3	Solution 4	Solution 5	Solution 6	Solution 7
Assumed time of fragmentation:							
Days from perihelion ^a	+50	+100	+200	+400	+800	-800*	-400*
Year and fraction.....	1994.76	1994.89	1995.17	1995.72	1996.80	1997.76	1999.00
Heliocentric distance (AU).....	1.37	2.13	3.23	4.66	6.02	6.02	4.66
Distance from ecliptic (AU).....	-0.02	-0.12	-0.30	-0.58	-0.94	-1.08	-0.96
Separation velocity ^b (m s ⁻¹):							
Radial component, V_R	-1.31 ± 0.15	-0.85 ± 0.17	-0.68 ± 0.15	-0.72 ± 0.12	-1.15 ± 0.11	-2.24 ± 0.14	-6.34 ± 0.26
Transverse component, V_T	+5.06 ± 0.67	+3.30 ± 0.86	+2.20 ± 0.85	+1.54 ± 0.71	+1.20 ± 0.59	+1.21 ± 0.60	+1.55 ± 0.77

^a For solutions 1–5, the time is reckoned from 1994 Aug 15, for solutions 5 and 6 from 2000 Feb 4.

^b Normal component V_N of separation velocity was very small and assumed to be zero. Deceleration was also assumed to be zero.

TABLE 16
MINIMUM SEPARATION VELOCITY NOT EXCEEDING 3 m s^{-1} THAT PRODUCES DIFFERENCE ΔT BETWEEN TIMES OF NEXT PERIHELION PASSAGE FOR HYPOTHETICAL FRAGMENTS IN ORBIT OF C/1999 J6

DIFFERENCE IN PERIHELION TIMES ΔT (days)	MINIMUM SEPARATION VELOCITY (m s^{-1}) FOR FRAGMENTATION EVENT TEMPORALLY SEPARATED FROM PREVIOUS PERIHELION PASSAGE BY (days)									
	0	0.5	1	2	5	10	20	50	100	200
0.5.....	0.13	0.14	0.17	0.21	0.30	0.40	0.52	0.75	1.01	1.46
1.....	0.25	0.28	0.33	0.43	0.61	0.79	1.03	1.49	2.03	2.92
2.....	0.50	0.56	0.67	0.85	1.21	1.58	2.07	2.98
5.....	1.25	1.41	1.67	2.13	3.0
10.....	2.50	2.81

is premature at this time to speculate on the identity (and survival) of any additional fragments, even though C/1999 U2 comes to mind as one possible candidate. A resolution of this puzzle is clearly a subject for future investigations.

4.5. Erosion Light Curve and Fragment Survival

Whether or not the Marsden and Kracht comets display any activity has been a matter of some debate. Meyer (2003) describes their physical appearance as almost stellar. The lack of a differential deceleration in the motions of some fragments (§ 4.2), but its presence in the motions of others (§ 4.4) provide us with no clear answer about the role of dynamical effects from directed, jetlike outgassing.

With regard to C/1999 J6, Meyer mentions that the comet might have been of magnitude 11 during a close approach to Earth about a month after its perihelion passage. Since Marsden's (2004b) new elliptical orbit suggests that the approach was much closer, to 0.0087 instead of 0.024 AU, the comet would have been of magnitude 9 and unlikely to escape attention of observers.

Comet C/1999 J6 is the only object among the Marsden- and Kracht-group comets for which the light curve is known reasonably well. Listing a crude proxy parameter for the comets' brightness in Tables 4 and 5 is the result of our effort to rectify this unfavorable situation to at least some extent. By contrast, light curves are available for a total of 141 SOHO Kreutz sungrazers, published by Biesecker et al. (2002) and in tabular form by Biesecker & Green (2002). These papers are also sources of information on the magnitude ranges of the C2 and C3 coronagraphs. Generally, fainter comets are detected only in the C2 coronagraph.

Visual magnitudes of C/1999 J6 were measured by Biesecker (2000) from seven images along its track across the field of view of the C2 coronagraph. Although the comet was imaged with the C3 coronagraph until 0.8 day after perihelion, the brightness data cover only the preperihelion arc of the orbit (fortunately the most important part), starting some 0.84 day before perihelion.

TABLE 17
ORBITAL ELEMENT DIFFERENCES BETWEEN C/2005 E4 AND C/2005 G2 AT OSCULATION EPOCH 2005 APRIL 20.0 ET (EQUINOX J2000.0)

Orbital Element	Difference C/2005 G2 minus C/2005 E4
Perihelion time T (days).....	+34.70669 \pm 0.00036
Argument of perihelion ω (deg).....	-0.044 \pm 0.046
Longitude of ascending node Ω (deg).....	+0.004 \pm 0.018
Orbital inclination i (deg).....	-0.001 \pm 0.010
Perihelion distance q (AU).....	+0.000031 \pm 0.000014
Orbital eccentricity e	+0.000162 \pm 0.000004

Figure 1 presents the seven measured magnitudes, normalized by an inverse-square power law to 1 AU from the SOHO spacecraft, H_{Δ} , plotted against the time from perihelion as well as the heliocentric distance. To examine the presence of a possible phase effect, the magnitudes, normalized in addition by an inverse-square power law to 1 AU from the Sun, H_0 , are plotted in the figure against the phase angle.

Two conclusions that can be readily drawn are (1) the brightness variations do not follow an inverse-square law or any other power law, and (2) no phase effect can account for the two brightest data points. Although the first five observations can approximately be fitted, both the slope of the phase law, $0.142 \text{ mag deg}^{-1}$, and the normalized magnitude at zero phase, $H_0 = 9.6$, are meaningless.

On the other hand, the light curve of C/1999 J6 in Figure 1 is very similar to the light curves of the SOHO sungrazers, presented by Uzzo et al. (2001) and by Biesecker et al. (2002), except that the branch of decreasing brightness with decreasing heliocentric distance below $\sim 11 R_{\odot}$ is missing (q of C/1999 J6 is $10.6 R_{\odot}$; Table 4). A less apparent, but still significant difference is in the rate of brightness increase between 20 and $15 R_{\odot}$, which can crudely be approximated by an $\sim r^{-8}$ law, making the slope clearly steeper than for the Kreutz sungrazers.

The light curves of 27 well-observed SOHO sungrazers were fitted most satisfactorily by Sekanina (2003), who employed his model for an erosion process consisting of progressive bulk fragmentation and sublimation of these minicomets on their approach to the Sun. The visual light was shown to be dominated by profuse sublimation of sodium from the continuously fragmenting body, while the loss of mass was found to be primarily due to fragmentation itself. The gradual brightening of a SOHO sungrazer during the first phase of its approach to the Sun followed by the fading is diagnostic of an object subjected to a progressively increasing radius-loss rate: the effect of solar heating prevails farther than about $11-12 R_{\odot}$ from the Sun, while the loss effect dominates at smaller distances. The light curve depends on a number of physical quantities, of which the most important are (1) the latent energy of erosion, which determines the comet's rate of erosion just as the latent heat of sublimation determines the sublimation rate of a volatile substance, and (2) the initial diameter of the approaching comet's nucleus, before the erosion process becomes significant. Among the SOHO sungrazers, the erosion energy distribution is bimodal, with sharp peaks near $35,000$ and $40,000 \text{ cal mol}^{-1}$, except that subfragments that survive down to $\sim 3 R_{\odot}$ have an erosion energy of $60,000$ to nearly $90,000 \text{ cal mol}^{-1}$. The initial diameters of the studied SOHO sungrazers, normalized to a density of 0.5 g cm^{-3} , range from 16 to 130 m , none surviving the perihelion passage. The model also allows one to estimate that for this density the total eroded layer of a sungrazer's nucleus during its perihelion passage amounts to nearly 0.5 km .

TABLE 18
MODEL SOLUTIONS FOR C/1999 N5 SPLITTING INTO C/2005 E4 AND C/2005 G2 (EQUINOX J2000.0)

Fragmentation Parameter	Solution 1	Solution 2	Solution 3	Solution 4
Fragmentation time and location:				
Date (ET)	(1999 Jul 11.2)	1999 Jul 10.3	1999 Jul 9.8	1999 Jul 9.9
Days from perihelion time of C/1999 N5.....	(0)	-0.9 ± 1.1	-1.4 ± 1.1	-1.3 ± 0.9
Heliocentric distance (AU).....	(0.049)	0.084	0.107	0.101
Distance from ecliptic ^a (AU)	(+0.008)	-0.032	-0.046	-0.043
Normal component of separation velocity (m s ⁻¹).....	(0)	(0)	-7 ± 9	(-3)
Differential nongravitational deceleration (units) ^b	8.57 ± 0.01	15 ± 10	19 ± 10	18 ± 9
Sum of squares of normalized residuals	1.9472	1.6202	1.3155	1.4370
rms normalized residual.....	±0.624	±0.636	±0.662	±0.599
Residuals ^c <i>O</i> - <i>C</i> in orbital elements:				
Perihelion time (days).....	0.00000	0.00000	0.00000	0.00000
Argument of perihelion (deg).....	-0.048	-0.040	-0.028	-0.034
Longitude of ascending node (deg).....	+0.010	+0.010	0.000	+0.006
Orbital inclination (deg)	+0.007	+0.007	+0.008	+0.007
Perihelion distance (AU).....	+0.000002	-0.000001	-0.000003	-0.000002
Orbital eccentricity.....	0.000000	+0.000001	+0.000002	+0.000002

NOTE.—Forced values of fragmentation parameters are in parentheses.

^a Minus sign indicates that fragmentation occurred south of the ecliptic.

^b Units of 10⁻⁵ the solar gravitational acceleration.

^c Residuals between Marsden's (2005b) elements for C/2005 G2 and the elements obtained from each model solution.

Thus, only sungrazers more than ~1 km in diameter survive one return to the Sun.

It is important to distinguish this erosion process, which is strongly heliocentric-distance dependent and plays a major role only near the Sun, from the episodically continuing process of spontaneous or nearly spontaneous disruption, which proceeds nearly at random throughout the orbit as part of *cascading fragmentation*; the Kreutz system sungrazers provide ample evidence for both of these mass-loss processes (e.g., Sekanina 2002a; Sekanina & Chodas 2004; Marsden 2005e). In the general proximity of the Sun, erosion, cascading fragmentation, as well as the sungrazers' tidally triggered splitting, may in fact overlap.

We tested the erosion model on the light curve of C/1999 J6. The result in Figure 1 shows an excellent match, given that the data points are accurate probably to ±0.1 mag near the bright end of their range and to ±0.4 mag near the faint end (see Fig. 4 of Sekanina 2003). The parameters of the solution indicate that the derived erosion energy, 47,000 cal mol⁻¹, is markedly higher than for the main components of the *SOHO* sungrazers, perhaps explaining the sunskirters' nearly stellar appearance, noted by Meyer (2003). At an assumed mean molecular weight of 200 g mol⁻¹ (close to the numbers for silicates) and a density of 0.5 g cm⁻³, the initial diameter of C/1999 J6 (including the unknown contribution from C/2004 V10) was found to be 48 m. The loss of diameter by the time the comet reached its 1999 perihelion was 6.3 m. The model suggests that one revolution later, when the object was approaching the Sun as C/2004 V9, it was

35–36 m across. After the 2004 return, the diameter shrank to ~23 m, unless the fragment split again in the meantime.

At least two implications of these findings are clearly worth noticing. If C/1999 J6 and C/2004 V9 are the same object, as is almost certain, it should reappear in up to two more of its returns to the Sun, first in 2010 and as a faint object perhaps again in 2015, which should be its last passage through perihelion before its complete disintegration. Of course, possible intervening fragmentation episodes may further shorten its lifetime. Regarding the comet's brightness at the time of closest approach to Earth in 1999 June, we obtain an estimated apparent visual magnitude 16, corresponding to a diameter of 35.4 m (Table 20) at an assumed geometric albedo of 0.04 and zero phase; at the actual phase angle of nearly 90°, the magnitude should have been between 19 and 21, which for all practical purposes rules out its accidental detection at the time.

Turning now to fragment C/2004 V10, we find in Table 4 that it was observed from 0.32 day to 0.20 day before perihelion. Although no magnitude data are available, it is known that the object was not seen with the C3 coronagraph and was probably fainter than apparent magnitude 8. Table 20 lists three possible erosion solutions, of which cases A and B satisfy a condition that the light curve peaked midway between the first and last observations, but in case A the comet is calculated to have been more than 1 mag brighter than in case B. Since the last observation was made as the comet was leaving the field of view of the C2 coronagraph, its light curve may have peaked a little later than

TABLE 19
COMPARISON OF EXTRAPOLATED 1993 ORBITAL ELEMENTS FOR C/1999 J6 AND C/1999 N5 AT OSCULATION EPOCH 1993 NOVEMBER 29.0 ET (EQUINOX J2000.0)

Quantity	<i>T</i> (days)	ω (deg)	Ω (deg)	<i>i</i> (deg)	<i>q</i> (AU)	<i>e</i>
Difference C/1999 N5 minus C/1999 J6:						
From extrapolated orbits by Marsden (2005a).....	-1.6846	+0.163	-0.265	-0.241	-0.000015	+0.000343
From our independent runs (Tables 6 and 8).....	-2.7730	+0.172	-0.196	-0.261	-0.000145	+0.000390
Discrepancy in absolute value.....	1.0884	0.009	0.069	0.020	0.000130	0.000047
rms error from both comets' 1999 elements.....	±0.0007	±0.056	±0.044	±0.013	±0.000059	±0.000018

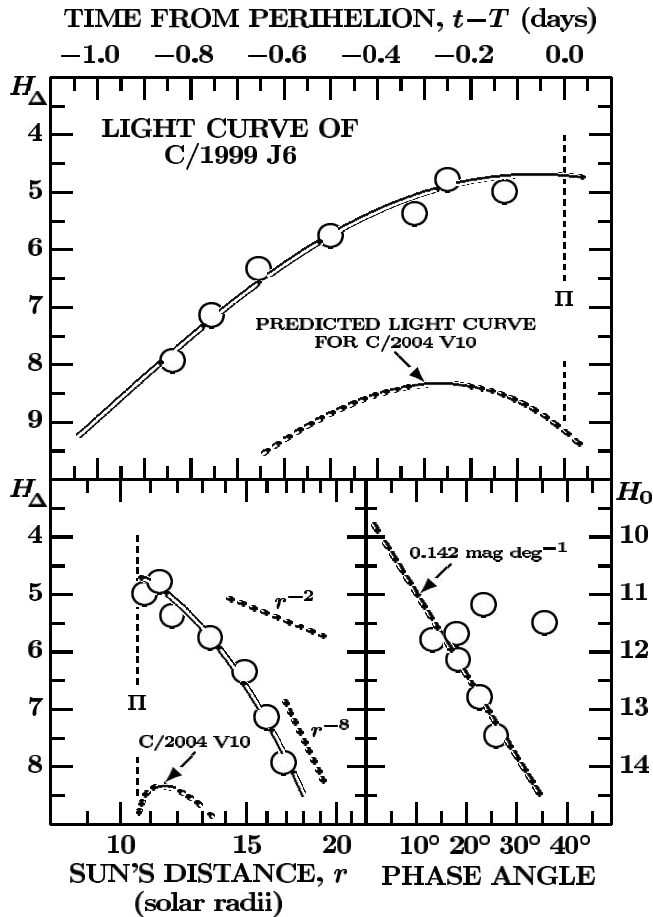


FIG. 1.—Light curve of C/1999 J6. The circles are the V magnitudes measured by Biesecker (2000), normalized to 1 AU from the *SOHO* spacecraft in the upper and lower left panels (H_{Δ}) and to 1 AU from both *SOHO* and the Sun in the lower right panel (H_0). The solid curves fitted through the data points represent the erosion model, whose parameters are listed in Table 20. Also plotted is a predicted light curve for C/2004 V10 (case A), the observed arc being marked by the solid curve. A vertical line Π indicates perihelion. Brightness variations fitting an inverse square and inverse eighth power of heliocentric distance are shown in the lower left panel by dotted curves. The lower right panel implies that no realistic phase law fits the brightness variations.

assumed in cases A and B. Case C is based on the assumption that, instead, the brightness peak was reached at the time of the last observation.

We do not know to what extent each of the three models for C/2004 V10 is representative of the fragment's true behavior. However, in the least they provide us with insight into possible solutions. It is noted that in cases A and B the fragment would disintegrate entirely before completing its 2004 return, while in case C a small boulder might still survive. Perhaps more important is the extrapolation of the three models back to 1999. When splitting from C/1999 J6, the companion would be nearly 25 m across in case A, but only 17 m in cases B and C. Since the companion's brightness contributes to the integrated brightness of C/1999 J6 in Table 20, the latter's corrected initial (pre-1999 approach) diameter would be only 41 m in case A and 45 m in cases B and C, with the preapproach diameter of C/2004 V9 to be scaled down accordingly. The erosion rate of C/1999 J6 may also be slightly affected.

Summarizing the results of §§ 4.1–4.5, we find that the orbital period of the Marsden-group comets (and probably the Kracht-group comets as well) is likely to range at least from 5.5 to 6 yr, thus exceeding the orbital period of 96P but comparable to the

orbital periods of the other contributors to the Machholz complex. Because of this short orbital period, the typical lifespan of the Marsden- and Kracht-group comets is considerably shorter than that of the Kreutz system sungrazers, even though the difference in the perihelion distance may moderate the effect to some extent. The observed Marsden- and Kracht-group comets appear to be products of cascading fragmentation and terminal erosion, just as the *SOHO* sungrazers. Faint members of the Marsden and Kracht groups are likely to be nearly inert objects, surviving for less than two revolutions about the Sun. On the other hand, the brightest members may still be retaining some limited activity and have lifetimes of several revolutions. Both groups must be replenished from the reservoir of a smaller population of more massive parent bodies (direct precursors) in orbits of somewhat higher inclination and greater perihelion distance, of whose existence we currently have at best only indirect evidence—from the clustering in the two groups and from orbit evolution models (§ 7.4). The clusters (Tables 4 and 5) suggest that the number of these objects, which several revolutions earlier may have contained much more mass than all the known members of the two groups today, was very limited. These direct precursors must have had their own parents—still less numerous but more massive objects, all making up a complex population hierarchy of either group.

With one minor exception (long-term changes in the orbital period; § 7.3), this concludes our examination of the terminal phase of evolution of sunskirting comets. Our next subject of interest is the source of this Machholz interplanetary complex.

5. FIRST PRECURSORS OF MACHHOLZ COMPLEX

This investigation of the long-term evolution of the Machholz complex in general and the Marsden and Kracht groups in particular is based on the assumption that comet 96P and the massive, parent bodies of the two groups and other related objects share a common *progenitor*, from which they separated. Because of diverse orbital evolutions of the various contributors to the Machholz complex, we believe that the number of original parent bodies (i.e., the progenitor comet's first-generation fragments), which we call *first precursors*, may have been fairly high. Of greatest interest are the first precursors that split off most recently, because their sizable fragmentation products are the most likely to have survived until the present time.

5.1. Objectives and Approach

Our prime objectives are threefold. Efforts will be made (1) to determine or constrain the times and locations of fragmentation events that the progenitor must have experienced in the process of giving birth to the first precursors and the conditions under which the formation of these offspring objects occurred; (2) to explore the long-term evolution of the first precursors injected into low-inclination orbits that differ substantially from the orbit of comet 96P; and (3) to test the proposed model of the orbital evolution of the Machholz complex on the available data. The origin and evolution of the second precursors (i.e., the first-generation fragments of the first precursors) and higher generations of fragments are not directly addressed in this paper.

To begin with, we focus on the origin and properties of the first precursors. Given the short-lived nature and faintness of the Marsden- and Kracht-group comets (§ 4), we consider it practically certain that there is no first precursor present among their members in Tables 4 and 5. This means that the results for the precursors that we obtain below cannot be compared directly with information on *individual* Marsden- and Kracht-group comets or on meteoroids in the presumably associated streams. However,

TABLE 20
EROSION MODEL PARAMETERS FOR C/1999 J6 AND PREDICTION FOR C/2004 V10

PARAMETER	C/1999 J6	PREDICTION FOR C/2004 V10 ^a		
		Case A ^b	Case B ^b	Case C ^c
Assumed bulk density (g cm ⁻³).....	0.5	0.5	0.5	0.5
Assumed mean molecular weight (g mol ⁻¹).....	200	200	200	200
Latent energy of erosion (cal mol ⁻¹).....	47,000	47,000 ^d	49,000 ^d	50,000 ^d
Initial diameter (m) during approach to Sun ^e	48	12	8	9.4
At time of peak brightness ^e :				
Time from perihelion (days).....	-0.07	-0.26	-0.26	-0.20
Heliocentric distance (R_{\odot}).....	10.63	11.40	11.40	11.07
Visual magnitude (mag).....	4.68	8.36	9.56	9.13
Uneroded diameter (m).....	42.5	9.1	6.1	7.3
At time of perihelion passage ^e :				
Visual magnitude (mag).....	4.69	9.01	10.39	9.48
Uneroded diameter (m).....	41.7	5.7	3.4	5.5
After completing one revolution about Sun ^e :				
Thickness of eroded layer (m).....	6.3	6.3	4.6	3.9
Uneroded diameter (m).....	35.4	0	0	1.6

^a Orbit assumed to be identical with that of C/1999 J6.

^b Predicted from condition that peak brightness occur at middle of observed arc.

^c Predicted from condition that peak brightness occur at end of observed arc.

^d Adopted value.

^e In 1999 for C/1999 J6, in 2004 for C/2004 V10.

one would expect that statistically there is a degree of similarity in the properties of different generations of fragments, and this is the subject of our major effort.

In § 4 we commented on limited evidence for the fainter present-day Marsden- and Kracht-group comets to be nearly inert objects, as we did not find it necessary to solve for differential decelerations between fragments in a comet pair (§ 4.2). On the other hand, we remarked that the bright members of the groups appear to be a little active (§ 4.4). Certainly comet 96P is an active object, even though the nongravitational forces affecting its orbital motion are rather small. To make sure that no relevant orbital solutions are missed, we consider it necessary to include potential effects of differential decelerations on the motions of the first precursors. Thus, in our search for orbits of these objects, we employ the full-scale, five-parameter fragmentation model, introducing both the separation velocity components in the cardinal directions and a differential nongravitational deceleration. However, since the first precursors must be massive objects, persisting for a fairly large number of revolutions about the Sun, experience with split comets (e.g., Sekanina 1982) suggests that such objects should be subjected to only low decelerations, not exceeding 10 units of 10^{-5} solar gravitational attraction, or $\sim 0.6 \mu\text{m s}^{-2}$ at 1 AU from the Sun. The separation velocities must not exceed a few meters per second (§ 4.2).

5.2. Computing Technique

To make the case for a relationship between comet 96P and the precursors of offspring populations compelling, the general orbital characteristics of each such population have to be reproduced by orbital solutions searched for by integrating the motion of 96P back to the time of a fragmentation event, by applying a small orbital momentum change at that time, and then by integrating the adjusted motion forward to the present time. The orbital momentum increment at fragmentation is, as before, expressed in terms of a separation velocity (§ 5.1). Our orbit-integration code (§§ 4.2 and 4.3) was employed in a version not linked to the least-squares differential-correction procedure. Instead, for each integration run the code provided times and minimum encounter

distances (smaller than a prescribed upper limit) of both fragments with each of the planets.

Such a search is in practice a gigantic task, whose exhaustive solution is beyond the capability of a computer with a ~ 1 GHz microprocessor that we had available. Constraints (§ 6) were introduced to make the task tractable.

The starting point of our calculations was the set of osculating orbital elements for comet 96P, derived by M. S. W. Keesey² from 144 astrometric observations made during the object's four apparitions 1986, 1991, 1996, and 2002. For the standard, 40-day osculation epochs nearest the perihelion times, the elements are presented in Table 2, together with a set of nongravitational parameters that satisfy the observations and with additional information on the orbital solution. Not used in our investigation were two three-apparition solutions, 1986–1991–1996 and 1991–1996–2002, which did not require the introduction of nongravitational terms into the equations of motion (M. S. W. Keesey 2003, private communication).

6. SEARCH FOR LOW-INCLINATION SOLUTIONS

The differences between the present-day orbits of 96P and the Marsden-group comets amount to more than 30° in the inclination, more than $\sim 10^\circ$ in the longitude of the ascending node, and more than a factor of 2 in the perihelion distance. The discrepancies between 96P and the Kracht-group comets are even greater in the inclination and the node. And the Southern δ Aquarid swarm ascends the ecliptic on the same side of the Sun on which 96P descends. To address the challenges that these enormous differences present, a search for the first precursors was conducted in a systematic priority-oriented manner.

6.1. Initial Selection of Fragmentation Scenarios

Our top priority, which motivated the line of attack described below, was a search for first precursors of the lowest possible age nowadays moving about the Sun in orbits of low inclination.

² See http://ssd.jpl.nasa.gov/cgi-bin/da_shm?sstr=96P and M. S. W. Keesey 2003, private communication.

This requirement implies a trade-off, because, intuitively, the magnitude of an effect in the orbital inclination increases with the age of first precursors. We began this search by introducing a very large set of hypothetical fragmentation scenarios, which can be described in a matrix form as follows:

$$\Psi = \Psi_0(V_R, V_T, V_N; \gamma) \otimes \Psi_1(\tau_{\text{frg}}) \otimes \Psi_2(\mathfrak{R}_{\text{frg}}), \quad (2)$$

where Ψ_0 involves the combinations of the separation velocity, whose radial, transverse, and normal components are, respectively, V_R , V_T , and V_N (§ 4.2), and the deceleration γ ; Ψ_1 are the scenarios defined by the fragmentation times reckoned from perihelion at a given return to the Sun, $\tau_{\text{frg}} = t_{\text{frg}} - T(\mathfrak{R}_{\text{frg}})$; and Ψ_2 are the scenarios described by the returns $\mathfrak{R}_{\text{frg}}$ during which the assumed fragmentation episodes occur. Symbols \otimes indicate that the summary scenarios, Ψ , are all possible combinations of Ψ_0 , Ψ_1 , and Ψ_2 . If \mathcal{N}_0 , \mathcal{N}_1 , and \mathcal{N}_2 are, respectively, the numbers of scenarios Ψ_0 , Ψ_1 , and Ψ_2 , then the number of scenarios Ψ , or the number of required orbit integration runs, is

$$\mathcal{N} = \mathcal{N}_0 \mathcal{N}_1 \mathcal{N}_2. \quad (3)$$

The combinations of the separation velocity and deceleration that we used are of two types, restricted and expanded. They both assumed that $|V_R| = |V_T| = |V_N|$. Writing X for R , T , and N , the restricted combinations are

$$\Psi_0^*(V_R, V_T, V_N; \gamma) \equiv \Psi_0^*(V_X, \gamma), \quad (4)$$

where

$$\Psi_0^*(V_X, \gamma) = \begin{bmatrix} +V_R, & +V_T, & +V_N, & \gamma \\ +V_R, & +V_T, & -V_N, & \gamma \\ +V_R, & -V_T, & +V_N, & \gamma \\ +V_R, & -V_T, & -V_N, & \gamma \\ -V_R, & +V_T, & +V_N, & \gamma \\ -V_R, & +V_T, & -V_N, & \gamma \\ -V_R, & -V_T, & +V_N, & \gamma \\ -V_R, & -V_T, & -V_N, & \gamma \end{bmatrix}. \quad (5)$$

The expanded combinations are similarly

$$\Psi_0^{**}(V_X, \gamma) = \begin{bmatrix} +V_R, & +V_T, & +V_N, & \gamma \\ +V_R, & +V_T, & -V_N, & \gamma \\ \cdots & \cdots & \cdots & \cdots \\ -V_R, & -V_T, & -V_N, & \gamma \\ 0, & 0, & 0, & \gamma \\ 0, & 0, & 0, & -\gamma \end{bmatrix}. \quad (6)$$

Thus, $\mathcal{N}_0^* = 8$ for the matrix from equation (5) and $\mathcal{N}_0^{**} = 10$ for the matrix from equation (6). In the early phases of our search, we employed three sets of combinations, whose sum was set Ψ_0 in equation (2):

$$\Psi_0 = \Psi_0^*(2, 10) \oplus \Psi_0^*(2, 0) \oplus \Psi_0^*(2, -10), \quad (7)$$

where again the separation velocity is in m s^{-1} and the decelerations in the same units as in § 5.1. Symbols \oplus indicate that the three sets are added together, making $\mathcal{N}_0 = 26$ in equation (3).

The following set of fragmentation times (in days) relative to perihelion was selected

$$\Psi_1 = \begin{bmatrix} -900 \\ -600 \\ -350 \\ -150 \\ -50 \\ 0 \\ +50 \\ +150 \\ +350 \\ +600 \\ +900 \end{bmatrix}, \quad (8)$$

where a minus sign indicates a preperihelion event and vice versa. With the comet's orbital period of $\sim 5\frac{1}{4}$ yr, the entire orbit was covered. Since the matrix in equation (8) has $\mathcal{N}_1 = 11$, the product $\mathcal{N}_0 \mathcal{N}_1 = 286$ in equation (3).

A set of scenarios $\Psi_2(\mathfrak{R}_{\text{frg}})$ is determined by the perihelion returns of comet 96P. To facilitate their description, we list in Table 21 the dates on which the integration of the 1986–2002 orbital elements, described in § 5.2 and listed in Table 2, showed the comet to have passed through perihelion between 1986 and AD 150. The perihelion times \mathfrak{R}_k of the returns in Table 21 are counted from the discovery apparition of 1986, so that, for example, $k = -16$ for the first return of the 20th century, when the comet's perihelion was found to have occurred on 1902 April 26. A set Ψ_2 , defined by \mathfrak{R}_μ and \mathfrak{R}_ν , the perihelion times of, respectively, the most recent and the earliest returns, has a matrix form:

$$\Psi_2(\mathfrak{R}_\mu, \mathfrak{R}_\nu) = \Psi_2(\mathfrak{R}_{\text{frg}}) \equiv \begin{bmatrix} \mathfrak{R}_\mu \\ \mathfrak{R}_{\mu-1} \\ \mathfrak{R}_{\mu-2} \\ \vdots \\ \mathfrak{R}_{\nu+1} \\ \mathfrak{R}_\nu \end{bmatrix}, \quad (9)$$

where $\mu < 0$, $\nu < 0$, and $\mu > \nu$. The number of perihelion returns involving the assumed fragmentation events is $\mathcal{N}_2 = 1 + \mu - \nu$.

The enormity of required computing is apparent from a few estimates. For example, if we knew that the first precursors were born at some time during the past 300 yr, a careful examination at the proposed level implies $\mathcal{N}_2 \simeq 55$, requiring nearly 16,000 computer runs. If the birth of the first precursors took place during the past 800 yr, $\mathcal{N}_2 \simeq 150$ and the number of required runs would exceed 40,000. It should be emphasized that this was not the *total* amount of calculation needed, as these estimated orbit integration runs supported only an early phase of investigation.

6.2. Time Span of Low-Inclination Solutions

It turned out that the above estimates were still too optimistic. To make the problem computationally tractable, we decided to focus in this first phase of our exercise on detecting patterns—rather than individual changes—that were diagnostic of solutions with orbital inclination dropping from $\sim 70^\circ$ to below 30° . We inspected effects of fragmentation episodes not at every single

TABLE 21

PERIHELION DATES OF COMET 96P/MACHHOLZ BETWEEN 1981 AND 150

Return	Perihelion Date (ET)	Difference ^a (days)
-1	1981 Jan 24	1920
-2	1975 Oct 23	1914
-3	1970 Jul 27	1926
-4	1965 Apr 18	1922
-5	1960 Jan 13	1910
-6	1954 Oct 21	1910
-7	1949 Jul 29	1913
-8	1944 May 03	1915
-9	1939 Feb 04	1913
-10	1933 Nov 09	1920
-11	1928 Aug 07	1915
-12	1923 May 11	1927
-13	1918 Jan 30	1924
-14	1912 Oct 24	1917
-15	1907 Jul 26	1917
-16	1902 Apr 26	1919
-17	1897 Jan 22	1924
-18	1891 Oct 17	1919
-19	1886 Jul 16	1928
-20	1881 Apr 05	1922
-21	1875 Dec 31	1937
-22	1870 Sep 11	1933
-23	1865 May 27	1926
-24	1860 Feb 17	1927
-25	1854 Nov 08	1929
-26	1849 Jul 28	1932
-27	1844 Apr 13	1931
-28	1838 Dec 30	1937
-29	1833 Sep 10	1932
-30	1828 May 27	1946
-31	1823 Jan 28	1944
-32	1817 Oct 02	1932
-33	1812 Jun 18	1932
-34	1807 Mar 05	1934
-35	1801 Nov 17	1937
-36	1796 Jul 28	1936
-37	1791 Apr 10	1943
-38	1785 Dec 14	1937
-39	1780 Aug 25	1949
-40	1775 Apr 25	1947
-41	1769 Dec 25	1926
-42	1764 Sep 16	1924
-43	1759 Jun 11	1925
-44	1754 Mar 04	1928
-45	1748 Nov 22	1928
-46	1743 Aug 13	1935
-47	1738 Apr 26	1929
-48	1733 Jan 13	1940
-49	1727 Sep 22	1938
-50	1722 Jun 02	1912
-51	1717 Mar 08	1912
-52	1711 Dec 13	1911
-53	1706 Sep 19	1913
-54	1701 Jun 24	1915
-55	1696 Mar 26	1921
-56	1690 Dec 22	1915
-57	1685 Sep 24	1928
-58	1680 Jun 14	1925
-59	1675 Mar 08	1909
-60	1669 Dec 15	1908
-61	1664 Sep 24	1909
-62	1659 Jul 04	1911
-63	1654 Apr 10	1912
-64	1649 Jan 14	1919

TABLE 21—Continued

Return	Perihelion Date (ET)	Difference ^a (days)
-65	1643 Oct 14	1914
-66	1638 Jul 18	1931
-67	1633 Apr 04	1928
-68	1627 Dec 24	1918
-69	1622 Sep 23	1919
-70	1617 Jun 22	1919
-71	1612 Mar 21	1923
-72	1606 Dec 15	1922
-73	1601 Sep 10	1929
-74	1596 May 30	1926
-75	1591 Feb 20	1945
-76	1585 Oct 24	1942
-77	1580 Jun 20	1932
-78	1575 Mar 07	1931
-79	1569 Nov 22	1932
-80	1564 Aug 08	1935
-81	1559 Apr 22	1936
-82	1554 Jan 02	1942
-83	1548 Sep 08	1938
-84	1543 May 20	1953
-85	1538 Jan 13	1949
-86	1532 Sep 12	1930
-87	1527 Jun 01	1929
-88	1522 Feb 18	1928
-89	1516 Nov 08	1931
-90	1511 Jul 27	1932
-91	1506 Apr 12	1938
-92	1500 Dec 21	1934
-93	1495 Sep 05	1946
-94	1490 May 08	1944
-95	1485 Jan 10	1912
-96	1479 Oct 17	1910
-97	1474 Jul 25	1910
-98	1469 May 02	1912
-99	1464 Feb 06	1914
-100	1458 Nov 10	1919
-101	1453 Aug 09	1915
-102	1448 May 12	1930
-103	1443 Jan 29	1925
-104	1437 Oct 22	1908
-105	1432 Aug 01	1908
-106	1427 May 12	1907
-107	1422 Feb 20	1910
-108	1416 Nov 28	1912
-109	1411 Sep 04	1918
-110	1406 Jun 04	1916
-111	1401 Mar 06	1935
-112	1395 Nov 18	1932
-113	1390 Aug 04	1922
-114	1385 Apr 30	1921
-115	1380 Jan 26	1922
-116	1374 Oct 22	1925
-117	1369 Jul 15	1926
-118	1364 Apr 06	1932
-119	1358 Dec 22	1931
-120	1353 Sep 08	1951
-121	1348 May 06	1947
-122	1343 Jan 06	1934
-123	1337 Sep 20	1934
-124	1332 Jun 04	1933
-125	1327 Feb 18	1936
-126	1321 Oct 31	1937
-127	1316 Jul 12	1944
-128	1311 Mar 17	1941
-129	1305 Nov 22	1955

TABLE 21—Continued

Return	Perihelion Date (ET)	Difference ^a (days)
-130	1300 Jul 16	1950
-131	1295 Mar 15	1924
-132	1289 Dec 07	1922
-133	1284 Sep 02	1921
-134	1279 May 31	1923
-135	1274 Feb 23	1924
-136	1268 Nov 17	1930
-137	1263 Aug 06	1929
-138	1258 Apr 25	1940
-139	1253 Jan 01	1936
-140	1247 Sep 14	1908
-141	1242 Jun 24	1907
-142	1237 Apr 04	1905
-143	1232 Jan 16	1908
-144	1226 Oct 26	1910
-145	1221 Aug 03	1916
-146	1216 May 05	1915
-147	1211 Feb 06	1930
-148	1205 Oct 25	1927
-149	1200 Jul 16	1912
-150	1195 Apr 22	1912
-151	1190 Jan 26	1912
-152	1184 Nov 01	1915
-153	1179 Aug 05	1917
-154	1174 May 06	1922
-155	1169 Jan 30	1925
-156	1163 Oct 24	1946
-157	1158 Jun 26	1942
-158	1153 Mar 02	1931
-159	1147 Nov 18	1931
-160	1142 Aug 05	1930
-161	1137 Apr 23	1933
-162	1132 Jan 07	1935
-163	1126 Sep 20	1941
-164	1121 May 28	1941
-165	1116 Feb 03	1957
-166	1110 Sep 25	1951
-167	1105 May 23	1931
-168	1100 Feb 08	1930
-169	1094 Oct 27	1929
-170	1089 Jul 16	1931
-171	1084 Apr 02	1932
-172	1078 Dec 18	1938
-173	1073 Aug 28	1938
-174	1068 May 08	1950
-175	1063 Jan 05	1943
-176	1057 Sep 10	1911
-177	1052 Jun 17	1909
-178	1047 Mar 27	1906
-179	1042 Jan 06	1909
-180	1036 Oct 15	1910
-181	1031 Jul 24	1915
-182	1026 Apr 26	1916
-183	1021 Jan 26	1930
-184	1015 Oct 15	1924
-185	1010 Jul 09	1908
-186	1005 Apr 18	1908
-187	1000 Jan 27	1907
-188	994 Nov 07	1909
-189	989 Aug 16	1912
-190	984 May 22	1918
-191	979 Feb 20	1923
-192	973 Nov 15	1946
-193	968 Jul 18	1940
-194	963 Mar 27	1930

TABLE 21—Continued

Return	Perihelion Date (ET)	Difference ^a (days)
-195	957 Dec 13	1929
-196	952 Sep 01	1928
-197	947 May 23	1931
-198	942 Feb 07	1933
-199	936 Oct 23	1938
-200	931 Jul 04	1943
-201	926 Mar 09	1957
-202	920 Oct 29	1951
-203	915 Jun 27	1935
-204	910 Mar 10	1933
-205	904 Nov 23	1931
-206	899 Aug 11	1933
-207	894 Apr 26	1935
-208	889 Jan 07	1940
-209	883 Sep 16	1943
-210	878 May 22	1953
-211	873 Jan 15	1945
-212	867 Sep 19	1912
-213	862 Jun 25	1910
-214	857 Apr 02	1907
-215	852 Jan 12	1909
-216	846 Oct 21	1911
-217	841 Jul 28	1915
-218	836 Apr 30	1919
-219	831 Jan 28	1931
-220	825 Oct 15	1925
-221	820 Jul 08	1908
-222	815 Apr 18	1907
-223	810 Jan 27	1905
-224	804 Nov 09	1907
-225	799 Aug 21	1910
-226	794 May 29	1914
-227	789 Mar 02	1924
-228	783 Nov 25	1944
-229	778 Jul 30	1938
-230	773 Apr 09	1928
-231	767 Dec 29	1927
-232	762 Sep 19	1925
-233	757 Jun 12	1928
-234	752 Mar 02	1931
-235	746 Nov 18	1935
-236	741 Aug 01	1943
-237	736 Apr 06	1958
-238	730 Nov 26	1951
-239	725 Jul 24	1936
-240	720 Apr 05	1934
-241	714 Dec 19	1932
-242	709 Sep 04	1934
-243	704 May 19	1935
-244	699 Jan 31	1940
-245	693 Oct 09	1945
-246	688 Jun 12	1954
-247	683 Feb 05	1944
-248	677 Oct 10	1915
-249	672 Jul 13	1912
-250	667 Apr 19	1911
-251	662 Jan 24	1911
-252	656 Oct 31	1913
-253	651 Aug 06	1917
-254	646 May 07	1924
-255	641 Jan 29	1933
-256	635 Oct 15	1926
-257	630 Jul 07	1909
-258	625 Apr 15	1907
-259	620 Jan 25	1906

TABLE 21—Continued

Return	Perihelion Date (ET)	Difference ^a (days)
-260	614 Nov 06	1907
-261	609 Aug 17	1910
-262	604 May 25	1914
-263	599 Feb 27	1926
-264	593 Nov 19	1941
-265	588 Jul 27	1935
-266	583 Apr 10	1924
-267	578 Jan 02	1923
-268	572 Sep 27	1921
-269	567 Jun 25	1923
-270	562 Mar 20	1926
-271	556 Dec 10	1931
-272	551 Aug 28	1942
-273	546 May 04	1957
-274	540 Dec 24	1947
-275	535 Aug 26	1936
-276	530 May 08	1933
-277	525 Jan 21	1932
-278	519 Oct 08	1933
-279	514 Jun 23	1934
-280	509 Mar 07	1939
-281	503 Nov 15	1946
-282	498 Jul 18	1956
-283	493 Mar 10	1943
-284	487 Nov 14	1922
-285	482 Aug 10	1918
-286	477 May 10	1916
-287	472 Feb 10	1916
-288	466 Nov 12	1918
-289	461 Aug 12	1922
-290	456 May 08	1930
-291	451 Jan 25	1939
-292	445 Oct 04	1927
-293	440 Jun 25	1911
-294	435 Apr 02	1907
-295	430 Jan 11	1906
-296	424 Oct 23	1907
-297	419 Aug 04	1909
-298	414 May 13	1913
-299	409 Feb 15	1927
-300	403 Nov 07	1938
-301	398 Jul 18	1930
-302	393 Apr 05	1920
-303	388 Jan 02	1917
-304	382 Oct 03	1916
-305	377 Jul 05	1918
-306	372 Apr 04	1920
-307	367 Jan 01	1925
-308	361 Sep 24	1941
-309	356 Jun 01	1955
-310	351 Jan 24	1945
-311	345 Sep 27	1936
-312	340 Jun 09	1932
-313	335 Feb 24	1932
-314	329 Nov 10	1932
-315	324 Jul 27	1934
-316	319 Apr 11	1938
-317	313 Dec 20	1949
-318	308 Aug 19	1957
-319	303 Apr 11	1943
-320	297 Dec 15	1927
-321	292 Sep 05	1923
-322	287 Jun 01	1920
-323	282 Feb 27	1922
-324	276 Nov 23	1923

TABLE 21—Continued

Return	Perihelion Date (ET)	Difference ^a (days)
-325	271 Aug 19	1926
-326	266 May 11	1936
-327	261 Jan 21	1943
-328	255 Sep 27	1929
-329	250 Jun 16	1912
-330	245 Mar 22	1910
-331	239 Dec 29	1907
-332	234 Oct 09	1908
-333	229 Jul 19	1909
-334	224 Apr 27	1914
-335	219 Jan 30	1928
-336	213 Oct 20	1936
-337	208 Jul 02	1926
-338	203 Mar 25	1917
-339	197 Dec 24	1914
-340	192 Sep 27	1912
-341	187 Jul 04	1913
-342	182 Apr 08	1916
-343	177 Jan 08	1919
-344	171 Oct 08	1942
-345	166 Jun 14	1952
-346	161 Feb 08	1942
-347	155 Oct 16	1934
-348	150 Jun 30	

^a Difference listed for return N is the time interval between the perihelion dates at returns N and $N - 1$, where N is an integer between -1 and -347 .

return, but only at about 40 essentially randomly selected returns during the past millennium. Still, more than 10,000 orbit integration runs were needed to complete successfully this scaled-down task.

We soon realized that the investigated major orbital transformation was much more probably a sum of relatively minor, uneven orbital changes accumulating over a period of time rather than an effect of a single, extremely close approach to Jupiter. Periods of time that contained lower inclination solutions alternated with periods of only high-inclination solutions, requiring constant readjustments in the search procedure.

The most significant result of this first phase of our search was the finding that orbital solutions with a present-day inclination lower than $\sim 30^\circ$ and a perihelion distance of ~ 0.05 AU or less became suddenly more frequent (although by no means common) for fragmentation events assumed to have occurred around or before the year AD 1000. Our experimentation further showed that low-inclination solutions correlated with the location of fragmentation events in the orbit, indicating that episodes occurring within about 100 days of perihelion were favored. The effects were approximately symmetrical relative to perihelion, suggesting that as far as the orbital transformation was concerned, the transverse component of the separation velocity played a greater role than the other two components.

We next proceeded to a second phase of our exercise. It is well known that the nongravitational parameters of comets cannot be approximated by constant values of A_1 and A_2 over long intervals of time. Since the only set of nongravitational parameters for comet 96P was determined by Keesey from the comet's four linked apparitions 1986–2002 (§ 5.2 and Table 2), we tested the sensitivity of our fragmentation scenarios to the nongravitational effects by applying a reasonable, but arbitrary, correction. We changed the value of A_2 , the more critical of the two parameters, from -0.0001×10^{-8} AU day⁻² to -0.0011×10^{-8} AU day⁻², a

TABLE 22
CURRENT MINIMUM ORBITAL INCLINATION OF FIRST PRECURSOR FOR TWO CLASSES OF SOLUTIONS CORRESPONDING
TO FRAGMENTATION SCENARIOS $\Psi_0 = [+2, +2, +2; +10]$ AND $\Psi_0 = [-2, -2, -2; -10]$ (EQUINOX J2000.0)

PARENT'S RETURN TO SUN ^a	MINIMUM ORBITAL INCLINATION ^b (deg)	TIME DIFFERENCE ^c		AVERAGE ORBITAL PERIOD ^d (yr)
		Years	Rev.	
Class 1 Solutions (96P = Primary Fragment)				
1960.03.....	59.96	184.72	35	5.278
1775.31.....	54.47	231.93	44	5.271
1543.38.....	55.39	221.55	42	5.275
1321.83.....	56.82	216.40	41	5.278
1105.43.....	56.96	168.62	32	5.269
936.81.....	19.31			
Class 2 Solutions (96P = Secondary Fragment)				
1881.26.....	58.90	206.08	39	5.284
1675.18.....	52.80	242.60	46	5.274
1432.58.....	55.04	195.32	37	5.279
1237.26.....	55.75	237.19	45	5.271
1000.07.....	27.03			

^a Time of perihelion passage at the return at which the fragmentation event occurred.

^b Calculated for an osculation epoch of 1999 May 12.0 ET.

^c Difference listed for each return is the time interval and the number of revolutions between this entry and the one on the next line.

^d Suggesting probable influence of a 9 : 4 resonance with Jupiter, for which the orbital period is 5.274 yr.

modest effect, considering that the nongravitational parameters of some periodic comets undergo variations more than an order of magnitude greater over periods of time that amount to only a dozen or so revolutions about the Sun (e.g., Sekanina 1993a, 1993b; Marsden & Williams 2003). The postulated change in A_2 of 96P resulted in changes of several days in the perihelion time when the comet's motion was integrated back for several centuries. These changes were sufficient to eliminate virtually all our low-inclination solutions based on the assumption of a separation velocity effect alone ($\gamma = 0$), while confirming most solutions that assumed the precursor's motion to be affected by a deceleration. We concluded that fragmentation scenarios involving no deceleration were hypersensitive to the nongravitational forces affecting the motion of the parent comet and thereby to the location of a fragmentation event in the heliocentric orbit. Such scenarios become essentially unpredictable, and their investigation could not provide the basis for a meaningful hypothesis of the origin, history, and evolution of a population in low-inclination orbits.

In a third phase of our search for low-inclination solutions, we began to map systematically the long-term dependence of a precursor's orbit inclination on the fragmentation time. We considered only events occurring at perihelion and involving nonzero decelerations. Using two sets of fragmentation parameters,

$$\Psi_0 = \begin{bmatrix} +2, +2, +2, +10 \\ -2, -2, -2, -10 \end{bmatrix}, \quad (10)$$

we looked for trends in a minimum orbit inclination. The two scenarios led to two classes of solutions: either the first precursor was the less massive (secondary) component of the progenitor comet ($\gamma = 10$ units), in which case comet 96P was the more massive (primary) fragment (Class 1 solutions); or the other way around ($\gamma = -10$ units), with 96P being the secondary fragment (Class 2 solutions).

We established that the set of scenarios with the first precursor's inclination calculated for an osculation epoch on 1999

May 12 varied fairly systematically as the fragmentation time was pushed further into the past, with each new minimum inclination being reached over periods of 32–46 revolutions about the Sun (Table 22). The times of minimum inclination for the Class 1 and Class 2 solutions alternated in a quasi-periodic fashion, so that when a new minimum inclination was attained among fragmentation events for the Class 1 solutions, inclinations for the Class 2 solutions remained high, and vice versa. Consistent with the results from the first phase of this experiment, no fragmentation events more recent than about AD 1000 could send a precursor off en route to a sequence of close encounters with Jupiter, which are shown in § 7.3 to be responsible for the present-day low-inclination orbits (Table 22). The Class 1 solutions provide a minimum inclination as low as $\sim 19^\circ$ at the return of 936, the Class 2 solutions a minimum inclination of $\sim 27^\circ$ only 12 revolutions later. Although the orbital period of 96P varies from return to return by as much as 53 days (between 5.22 and 5.36 yr), the times between consecutive inclination minima in Table 22 are always multiples of an orbital period that is within 4 days equal to that of the 9 : 4 resonance with Jupiter, which may be interpreted as a confirmation of the planet's dominant gravitational influence. Of the two types, we strongly prefer the Class 1 solutions, with the first precursor being the less massive fragment, because comet 96P could not survive as a single, large object for more than a millennium if it was not the most massive fragment of the progenitor comet.

7. SEARCH FOR FIRST PRECURSORS

Based on our experience with modeling split comets (e.g., Sekanina 1982, 1997) and on information about low-inclination orbital solutions (§ 6), a search was initiated for first precursors of the Machholz complex populations. We confined this search to separation velocities of less than 2 m s^{-1} and to decelerations not exceeding 6×10^{-5} of the solar gravitational attraction. Only a small subset of Class 2 scenarios (with negative decelerations) was incorporated. The fragmentation times were selected so as to

be distributed symmetrically relative to perihelion, and, in most cases, they were restricted to 100 days from perihelion. No progenitor returns to the Sun after AD 1000 were included, and the span of the investigated period was limited by computer-time constraints to 850 yr, so that the starting year was AD 150. The perihelion dates for the returns are listed in Table 21.

7.1. Selection of Fragmentation Scenarios

We adopt the following sets of fragmentation parameters:

1. Altogether five types of combinations of the separation velocity and the deceleration (from eqs. [5] and [6] in § 6.1): $\Psi_0^{**}(1, 5)$, $\Psi_0^*(\frac{1}{2}, 5)$, $\Psi_0^{**}(\frac{1}{2}, 5)$, $\Psi_0^{**}(\frac{1}{2}, 4)$, and $\Psi_0^{**}(\frac{1}{2}, 6)$. Unweighted by sets Ψ_1 and Ψ_2 , the ratio of Class 1 scenarios to Class 2 scenarios is 21 : 1. We remark that $V_X = 1$ implies V_{sep} of 1.73 m s^{-1} , whereas $V_X = \frac{1}{2}$ indicates V_{sep} of 0.87 m s^{-1} .

2. Three symmetrical sets of fragmentation times relative to perihelion (in days), of which the most extensively applied one is

$$\Psi_1^* = \begin{bmatrix} -100 \\ -50 \\ -25 \\ 0 \\ +25 \\ +50 \\ +100 \end{bmatrix}, \quad \mathcal{N}_1^* = 7; \quad (11)$$

a small fraction of sets include

$$\Psi_1^{**} = \begin{bmatrix} -400 \\ -300 \\ -200 \\ -150 \\ +150 \\ +200 \\ +300 \\ +400 \end{bmatrix}, \quad \mathcal{N}_1^{**} = 8; \quad (12)$$

whereas a very minor fraction of them contains the least employed one,

$$\Psi_1^{***} = \begin{bmatrix} -900 \\ -800 \\ -700 \\ -600 \\ -500 \\ +500 \\ +600 \\ +700 \\ +800 \\ +900 \end{bmatrix}, \quad \mathcal{N}_1^{***} = 10. \quad (13)$$

3. Five combinations of sets Ψ_0 and Ψ_1 are used at all returns between AD 1000 and 150, $\Psi_2(-187, -348)$, with $\mathcal{N}_2 = 162$.

Two additional combinations are used at the returns 493–451, $\Psi_2(-283, -291)$, with $\mathcal{N}_2 = 9$.

The list of all sets of fragmentation scenarios used in our exercise is described by

$$\Psi = \left\{ \left[\Psi_0^{**}(1, 5) \oplus \Psi_0^*\left(\frac{1}{2}, 5\right) \oplus \Psi_0^{**}\left(\frac{1}{2}, 4\right) \oplus \Psi_0^{**}\left(\frac{1}{2}, 6\right) \right] \otimes \Psi_1^* \oplus \Psi_0^{**}(1, 5) \otimes \Psi_1^{**} \right\} \\ \otimes \Psi_2(-187, -348) \\ \oplus \left[\Psi_0^*\left(\frac{1}{2}, 5\right) \otimes \Psi_1^{**} \oplus \Psi_0^{**}\left(\frac{1}{2}, 5\right) \otimes \Psi_1^{***} \right] \\ \otimes \Psi_2(-283, -291). \quad (14)$$

The total number of orbit-integration runs required by this set of fragmentation scenarios is

$$\mathcal{N} = \{(10 + 8 + 2 \times 10) \times 7 + 10 \times 8\} \times 162 \\ + (8 \times 8 + 10 \times 10) \times 9 = 57,528. \quad (15)$$

Of these, only 4788, or 8.3%, are Class 2 scenarios ($\gamma < 0$). Altogether 28,512 (49.6%) have a separation velocity 0.87 m s^{-1} , 19,440 (33.8%) have a velocity of 1.73 m s^{-1} , while 9576 (16.6%) have a zero velocity. On the other hand, 43,092 (74.9%) have the fragmentation time within 100 days of perihelion, 13,536 (23.5%) have it 150–400 days from perihelion, and 900 (1.6%) have it 500 or more days from perihelion. All returns are equally represented, 346 scenarios per return, except for the nine between 451 and 493, for which there are 510 scenarios per return (47.4% more).

The back-and-forth orbit integration code, described in § 5.2, was run for each of the 57,528 scenarios, providing us with a massive sample of osculating orbits for the epoch of 1999 May 12, from which our systematic search for first precursors of the various populations of the Machholz complex subsequently began. Because the observed objects are all believed to be higher generation fragments (§ 5.1), our task was not to look for one-to-one relationships between the observed orbits and the sample orbits. Rather, the selection of a population of first precursors was based on the required compatibility of their orbital elements with the orbital boundaries of the observed population, which we established from the orbits of the population's known members. Defining these boundaries by the intervals $\langle \omega_{\min}, \omega_{\max} \rangle$, $\langle \Omega_{\min}, \Omega_{\max} \rangle$, $\langle i_{\min}, i_{\max} \rangle$, $\langle q_{\min}, q_{\max} \rangle$, and $\langle e_{\min}, e_{\max} \rangle$, we say that a scenario yields a *potential first precursor* of the population when its set of orbital elements $\{\omega_{\text{fp}}, \Omega_{\text{fp}}, i_{\text{fp}}, q_{\text{fp}}, e_{\text{fp}}\}$ satisfies each of the conditions $\omega_{\min} < \omega_{\text{fp}} < \omega_{\max}$, \dots , $e_{\min} < e_{\text{fp}} < e_{\max}$. In practice, no firm conditions could be provided by the populations' orbital data for e_{fp} . Because of the constraint imposed by the orientation of the line of apsides, it was not necessary to restrict all three angular elements. Actually, we found it quite adequate to specify population boundaries only in the longitude of the ascending node, inclination, and perihelion distance.

7.2. General Results of the Search

Most populations of the Machholz complex whose potential first precursors we searched for are shown in Figure 2 in a plot of

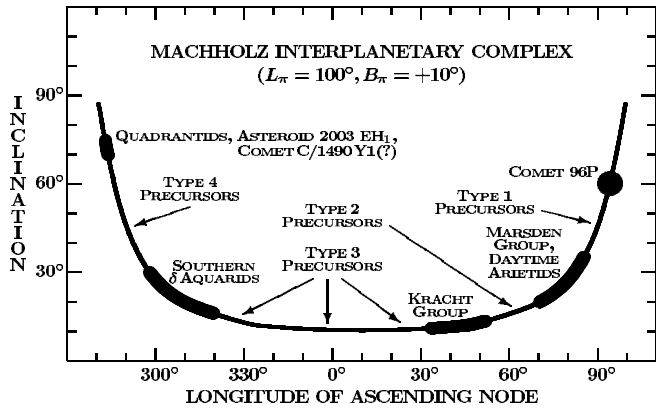


FIG. 2.—Schematic representation of the Machholz interplanetary complex in a plot of the longitude of the ascending node against the inclination for an invariable orientation of the line of apsides defined by the longitude of perihelion L_π and the latitude of perihelion B_π . An integrated effect of Jovian perturbations during close encounters increases systematically from comet 96P to the left. The orientation of the line of apsides does not remain even approximately constant over very long periods of time. Here the reference time frame is the second half of the 20th century, with the exception of C/1490 Y1.

the longitude of the ascending node against the orbital inclination, using the approximation of a fixed line-of-apsides orientation. We found no Quadrantid-like orbits in the sample (§ 7.5), nor orbits similar to those of the other suspected high-inclination meteor streams (Table 3), the Ursids, the Carinids, and the κ Velids. Likewise, the sample contains no *low-inclination* orbits that would resemble those of the Northern δ Aquarids or the α Cetics.

For the Marsden and Kracht groups and for the Southern δ Aquarid and Daytime Arietid streams, the search constants and findings are summarized in Table 23. The most astonishing result is that almost 8% of the entire sample, nearly 4500 orbital sets, fit the specified boundaries of the Marsden group. Although the range in the longitude of the ascending node that we searched through was 44° , all potential first precursors detected by the computer code for this population had this orbital element confined to a narrow interval of about 11° ($74^\circ < \Omega < 85^\circ$). The statistics of these data is discussed in § 7.6. We found no orbits similar to the orbits of the two possible Marsden-group comets of 2003 (Table 4), which in all probability had arrived from a different source.

Potential first precursors in the Kracht-group orbits were found to be rare, totaling only 32 or less than 0.1% of the sample.

Considering that the Kracht group is more populous than the Marsden group (Table 1), this result is rather unexpected, although the clustering (§ 4) may account for it. Besides, it is the existence, not the number, of first precursors that counts.

The Southern δ Aquarid stream is represented in the sample by nearly 100 potential first precursors. On the other hand, there is only one Daytime Arietid-like orbit, unless the lower limit for perihelion distance is allowed to drop below $14 R_\odot$; when this constraint is relaxed, the number of orbits balloons to more than 400, with the perihelion distance confined to a range from about 8 to $14 R_\odot$. The observed perihelion distances of the Daytime Arietids, mostly near $18\text{--}20 R_\odot$, must be due to long-term effects of the planetary perturbations and/or other interplanetary forces on fragments of first precursors. The observed Southern δ Aquarids and Daytime Arietids cannot contain meteoroids whose perihelion distances are smaller than a certain limit, because such meteoroids fail to intersect the Earth's orbit. For example, for an assumed orbital period of 5.2 yr, this limit is $\sim 7.5 R_\odot$ for the Southern δ Aquarids (at $\Omega_{2000} \simeq 297^\circ$, the stream's approximate boundary), but more than $10 R_\odot$ for the Daytime Arietids, so that the meteor radar techniques may map only fringe regions of this stream.

Figure 3 is a histogram of the highly nonrandom fragmentation time distribution of the potential first precursors for the four populations of the Machholz complex. Very few of them are found to result from fragmentation events after about AD 750. Before then, the highly correlated Marsden group and Daytime Arietid distributions show a clear periodicity, with major peaks in the early 8th, 6th, and 4th centuries. Terminated at AD 150, the distribution would have apparently peaked again in the early 2nd century. Interspersed approximately midway between the major peaks are minor peaks centered on the early to middle 7th, 5th, and 3rd centuries. This pattern, with a period of ~ 200 yr or ~ 38 revolutions of 96P about the Sun, is undoubtedly related to the pattern of minimum inclination presented in Table 22 (§ 6.2). Since the great majority of the orbital solutions in the sample is Class 1 (§ 7.1), the peaks in Figure 3 should timewise represent an extension to the numbers in the first column of the upper part of Table 22, which they do. The minor peaks in Figure 3 refer to Class 2.

The distribution of potential first precursors for the Southern δ Aquarids also appears to display similar behavior to both the Marsden-group and the Daytime Arietid distributions, with a few fluctuations that may be due to the fact that the sample is smaller. The Kracht-group distribution is so underpopulated that it is impossible to distinguish between random and systematic variations.

TABLE 23
SUMMARY STATISTICS OF POTENTIAL FIRST PRECURSORS FOR MARSDEN AND KRACHT GROUPS, SOUTHERN δ AQUARIDS,
AND DAYTIME ARIETIDS (57,528 SCENARIOS; EQUINOX J2000.0)

QUANTITY	MARSDEN GROUP	KRACHT GROUP	SOUTHERN δ AQUARID STREAM	DAYTIME ARIETID STREAM	
				Set I	Set II
Orbital constraints:					
Boundaries of Ω (deg).....	43.0–87.0 ^a	32.0–54.0	297.0–321.0	76.0–79.0	76.0–79.0
Boundaries of i (deg).....	22.0–34.5	11.5–15.0	18.0–34.0	20.0–29.0	20.0–29.0
Boundaries of q (R_\odot).....	6.7–11.4	6.7–11.8	8.6–26.0	14.0–21.0	all ^b
Detected precursors:					
Total number.....	4,459	32	91	1 ^c	422
Percent of sample.....	7.75	0.056	0.16	0.002	0.73

^a Interval is so wide because it includes two questionable entries from Table 3; no potential first precursors were found to have Ω between 43° and 73° .

^b All detected potential first precursors had q between ~ 8 and $\sim 14 R_\odot$.

^c The only candidate had q at the lower limit.

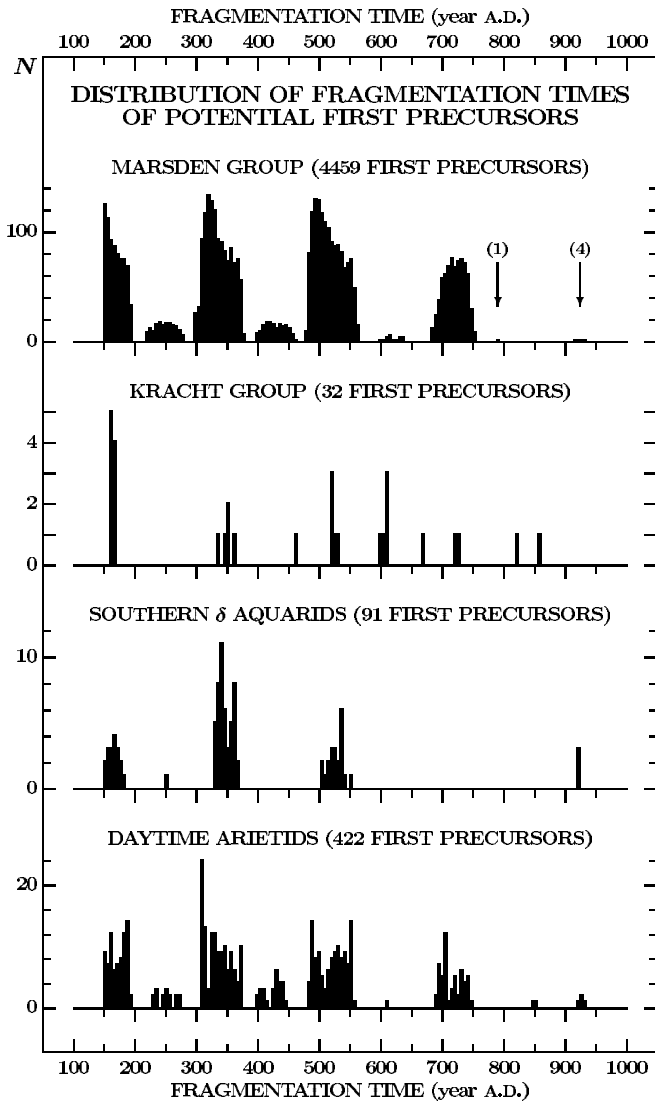


FIG. 3.—Histograms of the distribution of fragmentation times of potential first precursors for the Marsden and Kracht groups and for the Southern δ Aquarid and Daytime Arietid swarms. The numbers in parentheses in the histogram of the Marsden group are the numbers of potential first precursors in the two tiny peaks in the years 789 and 915–931 (Table 29).

However, since nearly 30% of the sample comes from the returns before AD 200, the population of these first precursors may be somewhat older than for the Marsden group.

A puzzling aspect of Figure 2 is the existence of wide gaps between any two contributors to the Machholz complex in the longitude of the ascending node. We searched the sample of fragmentation scenarios and found fairly large numbers of potential first precursors in each of the gaps: thousands (the exact number depending on the choice of orbital boundaries) between comet 96P and the Marsden group, which we call the type 1 precursors; more than 300 between the Marsden group and the Kracht group—the type 2 precursors; and more than 200 between the Kracht group and the Southern δ Aquarids—the type 3 precursors. We even found about 50 of them at smaller nodal longitudes, in the direction of the Quadrantids, at Ω as small as 287° , i as high as 55° , and q of up to ~ 0.1 AU—type 4 precursors. It therefore appears that the seemingly discrete components of the Machholz complex derive from the same, *essentially continuous population* of first precursors. It is not clear at this time why the gaps exist, especially the one between the Marsden group

and the Kracht group, and why the detected members of the Kracht group are confined to such a narrow interval in the longitude of the ascending node. In Table 24 we list a few representative sets of orbital elements for these possible members of the Machholz complex. The elements refer to the first precursors and apply only approximately to their debris. We have not investigated the geometry for these orbits in the *SOHO* coronagraphic fields. The existence of most of these predicted groups cannot be tested by meteor techniques, as their orbits do not approach Earth's orbit.

7.3. Close Encounters with Jupiter

As already suggested in § 6.2, the enormous diversity of the orbital behavior among the various components of the Machholz complex in general and the current prevalence of low-inclination orbits in particular are believed to be a result of strong perturbations that parent objects of the Marsden and Kracht groups and the associated meteor streams were subjected to during their close encounters with Jupiter. Comet 96P is remarkable in that, at least for two millennia, it has been very successful in avoiding the planet, apparently because of the resonance (§ 3). Our integration of the comet's motion back to AD 150 shows that it has never approached Jupiter to less than 0.5 AU, the closest encounters having occurred on five occasions between the years 679 and 1059, when the minimum distance from the planet was between 0.504 and 0.538 AU.

The history of 96P contrasts with the history of all potential first precursors of the low-inclination population. Table 25 compares five Marsden precursors, M1–M5, with one type 3 precursor, T₃1. They represent essentially a random sample, except for M1 and T₃1, which were chosen to illustrate the orbital diversity for objects with nearly identical birth conditions (see below for details).

Table 26 compares two Kracht precursors, K1 and K2, with four precursors, A1–A4, in orbits of the Southern δ Aquarid type that have a wide range of inclinations, longitudes of the ascending node, and perihelion distances. The orbital elements in Tables 25 and 26 are listed for the epoch of perihelion. The perihelion passage chosen is between 1999 and 2003 for the Marsden, Kracht, and type 3 precursors, but in the early 1950s for precursors A1–A4, because the best photographically determined orbits of the Southern δ Aquarids date from the years 1952–1953 (Jacchia & Whipple 1961).

The encounter data in Tables 25 and 26 illustrate Jupiter's considerable gravitational influence exercised on the Machholz complex objects that ended up in low-inclination orbits. The numbers are interesting from several standpoints. Unlike for comet 96P, there were, in each scenario, at least six approaches within 0.5 AU and at least one approach within 0.3 AU, all occurring when the precursors were on their way to aphelion. The Kracht precursors and those with orbits resembling the orbits of the Southern δ Aquarids had at least four encounters within 0.3 AU, the latter also at least two encounters within 0.2 AU.

A pivotal role among the encounters is played by the year 1059, when a close approach occurred in 10 out of the 12 cases. This explains why low-inclination objects could not arise from fragmentation events occurring after AD ~ 1000 . Interestingly, when there was a close encounter in 1059, there was a high probability of additional close encounters (especially for the Marsden first precursors) in 1249, 1438, 1545, and 1593, or 16, 32, 41, and 45 Jovian years after 1059, corresponding, respectively, to 36, 72, ~ 92 , and ~ 101 average orbital periods of 96P. The first two periods are obviously equal to quadruples of the 9:4 resonance (§ 3), whereas the latter two are likely to reflect a slight systematic increase in the orbital periods of the precursors. This

TABLE 24
PREDICTED REPRESENTATIVE SETS OF ORBITAL ELEMENTS FOR TYPE 1, TYPE 2, AND TYPE 3 PRECURSORS (EQUINOX J2000.0)

Orbital Element	Type 1 Precursors	Type 2 Precursors	Type 3 Precursors (I)	Type 3 Precursors (II)	Type 3 Precursors (III)
Argument of perihelion ω (deg).....	15	36	75	105	134
Longitude of ascending node Ω (deg).....	90	65	25	355	325
Orbital inclination i (deg).....	50	17	10	10	14
Perihelion distance q (AU).....	0.08	0.04	0.04	0.04	0.04
Orbital eccentricity e	0.974	0.987	0.987	0.987	0.987
Orbital period P (yr).....	5.3	5.3	5.5	5.4	5.4

is the effect of a differential nongravitational deceleration apparently affecting the motion of these potential first precursors, illustrating rather dramatically the way in which a fragment acquires an orbital period that is somewhat longer than the comet's (§ 4.5).

A close approach in 1059 was always followed by at least five more close approaches. For first precursors arising from earlier fragmentation events, there seems to be, in addition, a correlation between encounters in 1059, 869, and even 679, again a repetitive pattern with a period of 16 Jovian yr. In the two scenarios in Table 26 with no close approach in 1059 (A2 and A3), the pat-

terns involve encounters in 679, 786, 869, 928, and 1011, with the intervals of, respectively, 9, 7, 5, and 7 Jovian yr, after which the two sequences became very different. Also, there appear to be mutually exclusive close-approach patterns: in not a single of the 12 scenarios did close encounters occur in both 928 and 1059 (which are 11 Jovian yr apart) or in both 1011 and 1059 (4 Jovian yr apart).

The complex nature of the orbit transformation process is illustrated by comparing the orbital evolutions of the potential first precursors M1 and T₃1 in Table 25. In these scenarios, the

TABLE 25
ORBITS FOR SIX POTENTIAL FIRST PRECURSORS OF MARSDEN GROUP AND TYPE 3 (EQUINOX J2000.0; EPOCH OF PERIHELION PASSAGE)

PROPERTY	FRAGMENTATION EVENT DURING PROGENITOR COMET'S PERIHELION RETURN TO SUN					
	AD 931	AD 931	AD 693	AD 546	AD 514	AD 155
First-precursor identification:	M1	T ₃ 1	M2	M3	M4	M5
Type of orbit:	Marsden	Type 3 precursor	Marsden	Marsden	Marsden	Marsden
Orbital elements:						
Time of perihelion passage T (ET).....	1999 Dec 24	2002 Jan 30	2000 Nov 8	2002 Jul 1	2002 Sep 3	1999 Mar 6
Argument of perihelion ω (deg).....	25.62	85.73	22.16	22.82	23.55	23.24
Longitude of ascending node Ω (deg).....	78.09	16.20	81.71	81.32	80.44	80.27
Orbital inclination i (deg).....	24.65	10.30	27.02	27.45	26.68	26.24
Perihelion distance q (R_{\odot}).....	9.69	9.67	9.41	10.38	10.12	9.18
Perihelion distance q (AU).....	0.0451	0.0450	0.0438	0.0483	0.0471	0.0427
Orbital eccentricity e	0.9850	0.9852	0.9855	0.9841	0.9845	0.9859
Orbital period P (yr).....	5.23	5.31	5.24	5.30	5.29	5.24
Longitude of perihelion (deg).....	101.64	101.86	101.65	101.80	101.72	101.34
Latitude of perihelion (deg).....	+10.39	+10.27	+9.87	+10.30	+10.33	+10.05
Fragmentation parameters:						
Time of breakup, $t_s - T$ (days).....	+150	+100	+25	-25	+100	+50
Separation velocity ($m s^{-1}$):						
Radial component V_R	-1.0	-1.0	+0.5	-0.5	+0.5	0.0
Transverse component V_T	-1.0	-1.0	+0.5	-0.5	+0.5	0.0
Normal component V_N	+1.0	+1.0	-0.5	-0.5	-0.5	0.0
Differential deceleration γ (units ^a).....	5.0	5.0	6.0	6.0	6.0	5.0
Jovian close encounters ^b						
(yr and minimum distance in AU if <0.5 AU).....	1059.3 0.18	1059.3 0.17	869.6 0.46	869.6 0.47	679.8 0.48	679.8 0.49
	1118.6 0.26	1118.6 0.43	1059.4 0.40	1059.4 0.41	869.6 0.44	869.6 0.45
	1249.2 0.45	1166.0 0.36	1166.0 0.45	1166.0 0.42	1059.3 0.37	976.2 0.49
	1308.4 0.38	1249.1 0.20	1249.1 0.32	1249.1 0.31	1118.6 0.47	1059.4 0.38
	1438.9 0.32	1332.1 0.30	1308.3 0.48	1355.8 0.40	1249.1 0.31	1166.0 0.46
	1545.6 0.45	1379.6 0.38	1355.8 0.41	1438.9 0.27	1308.4 0.34	1249.1 0.29
	1593.0 0.41	1438.8 0.37	1438.9 0.27	1545.6 0.36	1355.8 0.49	1308.4 0.36
		1486.3 0.34	1545.6 0.36	1593.0 0.37	1438.9 0.28	1355.8 0.47
		1593.0 0.43	1593.0 0.37	1723.5 0.45	1545.6 0.38	1438.9 0.27
			1723.5 0.45	1771.0 0.48	1593.0 0.45	1545.6 0.36
			1771.0 0.48		1676.1 0.48	1593.0 0.35
					1723.5 0.45	1723.5 0.46
					1771.0 0.49	

^a Units of 10^{-5} solar gravitational acceleration, which is 0.593 cm s^{-2} at 1 AU from Sun.

^b Always along the preaphelion leg of the comet's orbit.

TABLE 26
ORBITS FOR SIX POTENTIAL FIRST PRECURSORS OF KRACHT AND SOUTHERN δ AQUARID TYPES (EQUINOX J2000.0; EPOCH OF PERIHELION PASSAGE)

PROPERTY	FRAGMENTATION EVENT DURING PROGENITOR COMET'S PERIHELION RETURN TO SUN					
	AD 920	AD 725	AD 599	AD 535	AD 361	AD 171
First-precursor identification:	A1	K1	K2	A2	A3	A4
Type of orbit:	Southern δ Aquarid	Kracht	Kracht	Southern δ Aquarid	Southern δ Aquarid	Southern δ Aquarid
Orbital elements:						
Time of perihelion passage T (ET)	1951 Nov 2	2003 Aug 10	2000 Apr 18	1952 Apr 23	1951 Nov 11	1952 Aug 26
Argument of perihelion ω (deg)	148.14	57.64	48.91	158.22	141.67	157.55
Longitude of ascending node Ω (deg)	312.39	44.41	53.61	301.81	318.84	302.56
Orbital inclination i (deg)	18.07	12.07	12.67	25.58	14.99	23.79
Perihelion distance q (R_{\odot})	11.80	10.68	9.50	15.05	15.91	13.09
Perihelion distance q (AU)	0.0549	0.0497	0.0442	0.0700	0.0740	0.0609
Orbital eccentricity e	0.9821	0.9839	0.9855	0.9776	0.9767	0.9803
Orbital period P (yr)	5.35	5.42	5.33	5.52	5.68	5.43
Longitude of perihelion (deg)	101.81	101.47	101.82	101.99	101.47	101.85
Latitude of perihelion (deg)	+9.42	+10.17	+9.52	+9.22	+9.23	+8.86
Fragmentation parameters:						
Time of breakup, $t_s - T$ (days)	+150	+25	-100	+25	0	+25
Separation velocity (m s^{-1})						
Radial component V_R	-1.0	+1.0	+1.0	+1.0	+1.0	-1.0
Transverse component V_T	-1.0	+1.0	-1.0	+1.0	+1.0	+1.0
Normal component V_N	+1.0	-1.0	-1.0	+1.0	+1.0	+1.0
Differential deceleration γ (units ^a)	5.0	5.0	5.0	5.0	5.0	5.0
Jovian close encounters ^b						
(yr and minimum distance in AU if <0.5 AU)	1059.3 0.14	786.4 0.49	1059.3 0.35	679.8 0.44	679.8 0.44	679.8 0.46
	1106.7 0.14	869.6 0.41	1166.0 0.39	786.4 0.48	786.4 0.48	869.6 0.41
	1213.5 0.20	976.2 0.47	1249.1 0.26	869.5 0.33	869.5 0.33	976.2 0.47
	1284.6 0.24	1059.3 0.30	1308.3 0.41	928.8 0.23	928.8 0.24	1059.3 0.29
	1343.9 0.28	1118.6 0.19	1355.8 0.40	1011.8 0.11	1011.8 0.12	1118.6 0.17
	1450.7 0.35	1201.6 0.16	1438.9 0.25	1118.6 0.13	1071.1 0.12	1201.6 0.16
		1249.1 0.40	1486.3 0.27	1225.3 0.20	1130.5 0.27	1249.1 0.17
		1308.4 0.32	1533.7 0.30	1272.8 0.32	1213.5 0.23	1296.5 0.24
		1462.6 0.29	1581.2 0.38	1332.1 0.35	1320.2 0.26	1355.8 0.26
		1593.0 0.38	1687.9 0.45	1403.3 0.33	1438.8 0.32	1427.0 0.29
		1652.4 0.46		1557.4 0.49	1557.4 0.43	1557.5 0.43

^a Units of 10^{-5} solar gravitational acceleration, which is 0.593 cm s^{-2} at 1 AU from Sun.

^b Always along the preaphelion leg of the comet's orbit.

fragmentation occurred during the same return to the Sun (in 931), less than 130 yr before the first close approach to Jupiter, and both the differential decelerations and the separation velocity vectors in the RTN coordinate system were identical; only the fragmentation times were 50 days apart. Yet their present-day orbits, while nearly coinciding in perihelion distance, differ by more than 60° in argument of perihelion and in longitude of the ascending node, by nearly 15° in inclination, by more than 2 yr in perihelion time, and by some 30 days in orbital period. The minimum distance from the planet during the first Jovian close encounter, in 1059, was nearly the same in the two scenarios, as expected. Nevertheless, the minor difference, 0.18 versus 0.17 AU, was sufficient to cause the circumstances during the second encounter, in 1118, to be much more different. The net result of this discrepancy was two independent histories of subsequent encounters. After 1118, the M1 precursor never approached Jupiter closer than to 0.32 AU in 1438, whereas the T_{31} precursor was 0.20 AU from the planet in 1249 and 0.30 AU in 1332. The T_{31} precursor was thus much more strongly perturbed than the M1 precursor and ended up in an orbit whose spatial orientation differs from the orbit of 96P even more substantially than the orbit of the M1 precursor, although both are of low inclination.

No close encounters in Tables 25 and 26 occurred more recently than the second half of the 18th century. In six cases these

episodes terminated before the end of the 16th century and in one case even in the mid-15th century. Similarly, the tables show no close approach to Jupiter before 679, although the ages of two of the precursors were by then more than 500 yr. It is thus possible that Jovian close encounters were confined to a limited period of time, with a bulk of them having occurred between the second half of the 9th century and the end of the 16th century. This is also consistent with our finding that the tabulated scenarios do not show a strong correlation between the fragmentation time and the number of Jovian close approaches.

Besides Jupiter, there were close encounters with other planets, including, for example, grazing approaches to some 300,000 km of Venus. However, we found no major effects from these perturbations on the orbital evolution of any of the investigated potential first precursors.

7.4. Modeling the Orbital Evolution

Although close encounters of Jupiter with the selected first precursors of the Machholz complex ceased between the 15th and 18th centuries, the profound transformation of the orbits did not terminate at that time. In fact, it is continuing even at present.

Long-term variations in, respectively, the inclination, the longitude of the ascending node, and the perihelion distance of comet 96P and three potential first precursors of the Machholz

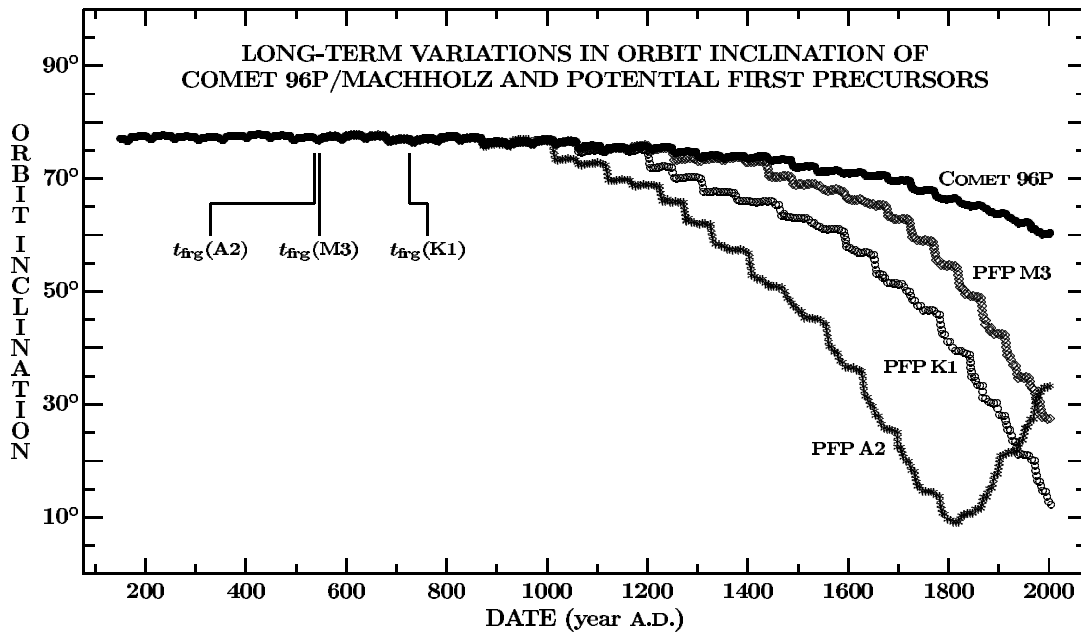


FIG. 4.—Long-term variations in the inclination of comet 96P and three potential first precursors (PFPs): a Marsden-group precursor M3, a Kracht-group precursor K1, and a Southern δ Aquarid precursor A2. Their birth times are marked, respectively, by $t_{fr}(M3)$, $t_{fr}(K1)$, and $t_{fr}(A2)$. For the object identification, fragmentation parameters, and history of Jovian close encounters, see Tables 25 and 26.

complex are presented in Figures 4, 5, and 6. The precursors are M3 from Table 25 and K1 and A2 from Table 26. Figure 4 shows that the inclination of the M3 precursor did not differ markedly from the comet’s until the 15th century, even though the M3’s close approaches to Jupiter dated back to 869. However, the closest one, to 0.27 AU, occurred in 1438, coinciding with the first major “wiggle” on the curve. Similarly, one can see that the inclination curves for the K1 and A2 precursors began to deviate markedly from the comet’s curve at, respectively, the beginning of the 13th century (coinciding with the closest encounter in 1201) and early in the 11th century (coinciding with the closest encounter in 1011).

The longitude of the ascending node (Fig. 5) began to deviate from the comet’s value even more recently, during the 14th and 15th centuries in the case of the A2 precursor, during the 17th century for the K1 precursor, and in the 18th century for the M3 precursor. On the other hand, the perihelion distance (Fig. 6) appears to have had a somewhat shorter response time to the close encounters than the inclination.

The most striking features in the orbit evolution curves are the reversals in the inclination of the A2 precursor in Figure 4 and in its perihelion distance in Figure 6. The passage of the Southern δ Aquarid part of the Machholz complex through the point of minimum perihelion distance in the 19th century implies

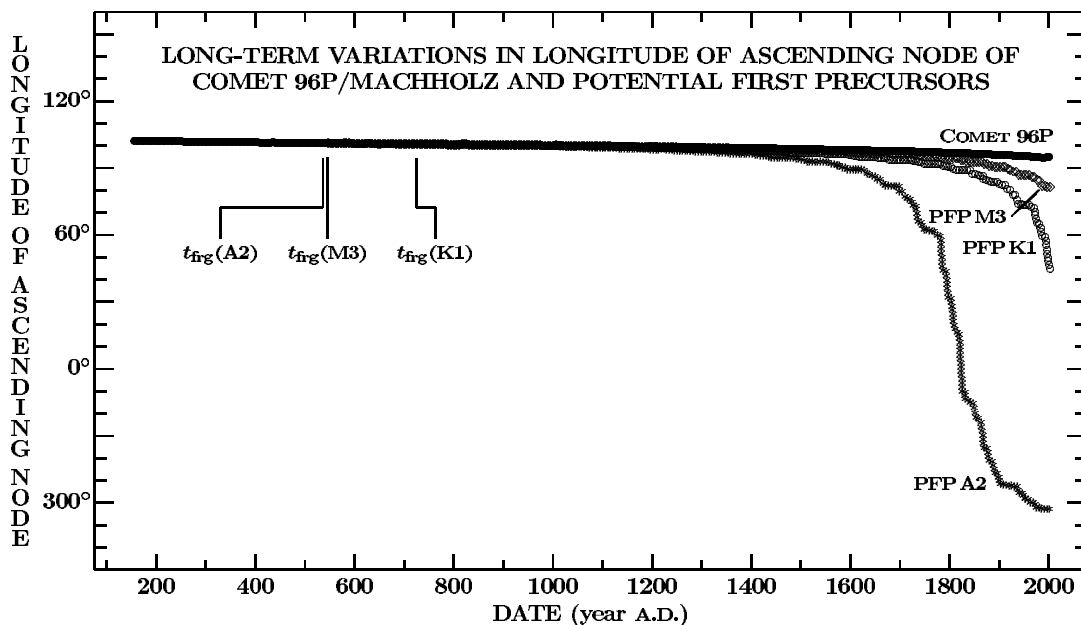


FIG. 5.—Long-term variations in the longitude of the ascending node of comet 96P and three potential first precursors (PFPs). For more information, see the caption to Fig. 4.

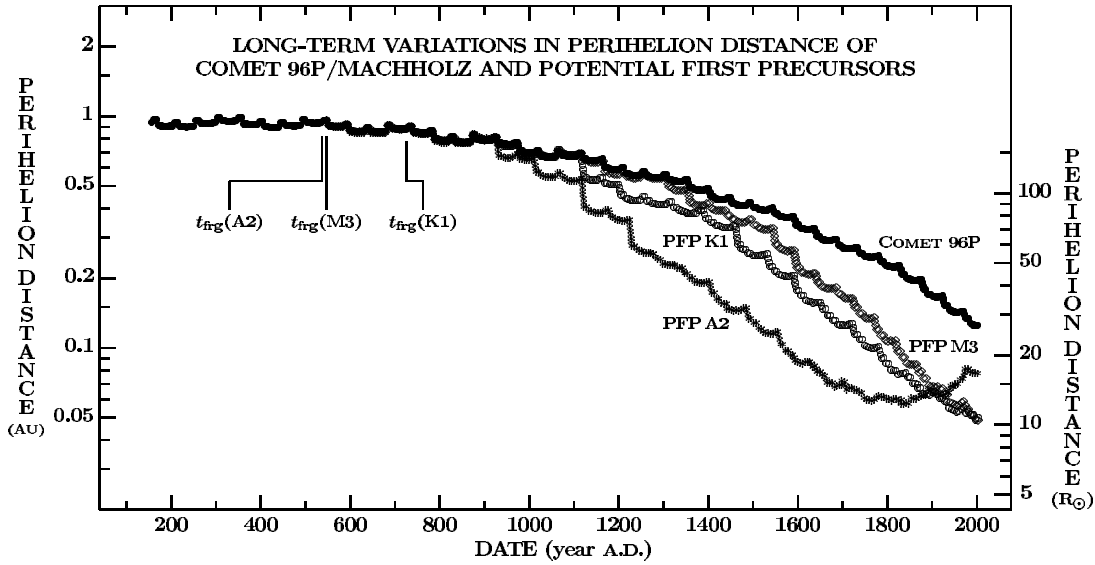


FIG. 6.—Long-term variations in the perihelion distance of comet 96P and three potential first precursors (PFPs). For more information, see the caption to Fig. 4.

that these precursors were subjected to an intense erosion process, so that the chances that sizable objects still exist in these orbits are not very good (cf. § 7.2).

The reversals in the two orbital elements of scenario A2, together with the continuing strong trends in the evolution curves for the other two scenarios plotted in Figures 4–6 long after the termination of the close encounters, indicate that the motions are controlled by the secular planetary (primarily Jovian) perturbations. However, the brief, powerful perturbations exerted by Jupiter during close encounters have *accelerated* the precursors' evolution relative to the comet. As a result, the precursor scenarios refer currently to evolutionary stages that 96P will not reach until several centuries from now. It is noted that the more numerous and closer the encounters are, the stronger are the perturbations and the higher is the rate of orbit-evolution acceleration. Indeed, the Southern δ Aquarid precursors, which were more perturbed than the Kracht and Marsden groups (§ 7.3), have evolved most rapidly.

An obvious quantity to measure the rate of orbit-evolution acceleration is the time of minimum inclination, t_{incl} , although the perihelion distance also varies in phase (Fig. 6). From Figure 4, time t_{incl} is estimated to be AD ~ 1820 for the Southern δ Aquarids, and it is well known that it is ~ 2450 for comet 96P (e.g., McIntosh 1990). Considering that the entire cycle of orbital variations for 96P is nearly 4000 yr (§ 3), the effect on the Southern δ Aquarids is significant, amounting to more than 30% of the half-cycle (from the maximum to the minimum inclination).

Although the integrated perturbation effect of a sequence of close encounters is a complex function of the geometry of the approaching body during each episode, we develop a simple characteristic, called a perturbation factor Π , that we use in the following to measure quantitatively the severity of Jupiter's gravitational influence during close approaches and to correlate it with the rate of orbit-evolution acceleration. The dimensionless factor Π is defined as

$$\Pi = \sqrt{\sum_{(\text{enc})} \left\{ \left[\frac{\Delta_0}{\min(\Delta_J, 0.5\Delta_0)} \right]^2 - 4 \right\}}, \quad (16)$$

where $\Delta_0 = 1$ AU, Δ_J is the minimum encounter distance (in AU), and the expression is summed up over all encounters

between the time of fragmentation and t_{incl} . Contributions to Π from the encounters with $\Delta_J \geq 0.5$ AU are all zero.

We have integrated the motions of comet 96P and the 12 potential first precursors listed in Tables 25 and 26, calculated their osculating elements annually, and determined the minimum inclination i_{min} , its time t_{incl} , the perihelion distance at t_{incl} (which was always very close to its minimum value), and the perturbation factor Π . The results are summarized in Table 27, which shows that the times of minimum inclination span 630 yr, as estimated above. Figure 7 is a plot of the perturbation factor against the time of minimum inclination. It can satisfactorily be fitted by an empirical law,

$$\Pi = \frac{2447 - t_{\text{incl}}}{73} \left(1 + \frac{2447 - t_{\text{incl}}}{1000} \right), \quad (17)$$

where 2447 is the time of minimum inclination for 96P, whose perturbation factor is 0 (Table 27). The wide range of orbit-evolution accelerations relative to the comet notwithstanding, the differences in the minimum inclination and in the perihelion distance among the potential first precursors in Table 27 are relatively small. One can in fact say that, except for the temporal compression effect, the scenarios are nearly equivalent, so that the evolution of the entire population of the Machholz complex is governed by the same rules.

Comparison of the scenarios plotted in Figures 4–6 is presented in Table 28. In each case we searched the lists of osculating orbital elements for a set that coincided with the longitude of the ascending node of a reference scenario. For the Marsden group, for example, this scenario is represented by the potential first precursor M3, highlighted in the table. It is apparent that the Southern δ Aquarid precursor A2 yielded the same nodal longitude in 1699, the Kracht-group precursor K1 in 1913, and that comet 96P will have this nodal longitude in 2304. The orbits are not entirely identical, but the systematic deviations in the inclination, the perihelion distance, and the orbital period are small. Thus, relative to the Marsden group, the orbital evolution of the Southern δ Aquarid swarm is accelerated by 303 yr and the Kracht group by 89 yr, whereas the evolution of the comet is decelerated by 302 yr. We similarly determine the rates of orbital evolution from the data on the Kracht group and the

TABLE 27
ORBIT-EVOLUTION ACCELERATION AND PERTURBATION FACTOR FOR SELECTED LOW-INCLINATION SCENARIOS RELATIVE TO COMET 96P (EQUINOX J2000.0)

OBJECT/SCENARIO	MINIMUM INCLINATION		PERIHELION DISTANCE (R_{\odot}) AT TIME t_{incl}	PERTURBATION FACTOR II	TYPE OF OBJECT/SCENARIO
	t_{incl}	i_{min} (deg)			
M1	2103	10.60	8.0	7.11	Marsden-group precursor
M2	2103	9.78	7.5	5.49	Marsden-group precursor
M3	2125	9.92	8.4	5.49	Marsden-group precursor
M4	2115	10.09	8.2	5.57	Marsden-group precursor
M5	2115	10.11	7.0	5.93	Marsden-group precursor
K1	2044	9.90	10.5	9.45	Kracht-group precursor
K2	2044	9.77	8.9	7.37	Kracht-group precursor
T ₃ 1	2009	10.15	9.8	8.91	Type 3 precursor
A1	1878	9.65	10.7	11.77	Southern δ Aquarid precursor
A2	1817	9.09	12.4	13.91	Southern δ Aquarid precursor
A3	1865	9.65	14.9	13.92	Southern δ Aquarid precursor
A4	1841	8.74	10.9	11.87	Southern δ Aquarid precursor
96P	2447	11.94	6.7	0.00	Comet Machholz

Southern δ Aquarids in Table 28. The numbers are approximately, but not exactly, the same.

The times in Table 28 that indicate the orbital correspondence between the present-day Marsden and Kracht groups and comet 96P in the future compare favorably with the dates derived by Ohtsuka et al. (2003). They determined the year 2319 for the Marsden group and 2408 for the Kracht group, while we found 2304 and 2411, respectively.

Our findings confirm that we deal with a single all-encompassing population of the Machholz complex (§ 7.2) that dynamically evolves in a fairly organized manner. This is remarkable given that the underlying cause—the perturbations exerted by Jupiter during a sequence of close encounters—is in principle a stochastic process.

7.5. The Quadrantids

In the light of the continuing controversy (§ 3), we briefly examined whether the model of the single all-encompassing popu-

lation also applies to the Quadrantids. We succeeded in simulating their orbit by the Southern δ Aquarid scenario A2. As the last entry of Table 28 indicates, the orbit of the A2 precursor matches the mean orbit of the Quadrantid stream (Table 3) remarkably well in about the year 2906. The time span between this epoch and that of minimum inclination for precursor A2 (Table 27) amounts to 1089 yr. A similar exercise conducted for the Kracht-group precursor K1 and the Marsden-group precursor M3 showed, as expected, that they would reach the Quadrantid stage long after the year 3000.

There is thus an indication that the Quadrantids are an integral part of the Machholz complex. To detect the Quadrantids in the 19th and 20th centuries requires first precursors that had a much higher rate of orbit-evolution acceleration than the Southern δ Aquarid precursor A2. While the time of their separation from the progenitor comet is unknown, we estimate that they should have been in orbits perturbed by Jupiter strongly enough during close encounters to have reached a minimum inclination ($\sim 10^\circ$) probably before the 11th century. From equation (17) we find a perturbation factor of at least ~ 50 , which is equivalent to the effect of a single, dynamically dominant approach to 0.02 AU or less. Could 2003 EH₁ be related to 96P by virtue of being a fragment of a Quadrantid first precursor that had shared a common parent with 96P and, after breaking off, experienced a very close encounter with Jupiter? Could this first precursor split at the time into two or more pieces due to the Jovian tidal forces? Could comet C/1490 Y1 be identical with 2003 EH₁? All these fascinating possibilities remain to be explored.

7.6. Orbital Correlations for the Marsden Group

The set of nearly 4500 potential first precursors for the Marsden group detected in our sample of fragmentation scenarios allows us to examine the expected distribution of fragmentation events along the progenitor's orbit and the correlations between the precursors and the observed members of the group. Table 29 shows the complex nature of the fragmentation distribution of the Marsden group. The returns, grouped into sets of five, reveal the periodicity that was already noted in § 7.2, but the purpose of this table is to show variations with the time from perihelion. Given the choice of the fragmentation scenarios (§ 7.1), a uniform distribution along the orbit should result, at the foot of the table, in a constant total number of events at the times within 100 days of

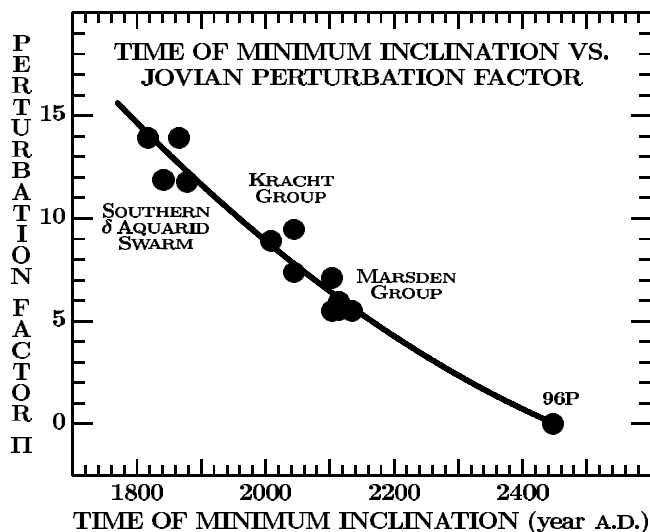


FIG. 7.—Relationship between the acceleration rate of orbital evolution, expressed in terms of the time of minimum inclination, and the integrated perturbation effect during close encounters with Jupiter, represented by the perturbation factor. The regions populated by the Marsden group, the Kracht group, and the Southern δ Aquarid swarm are marked.

TABLE 28
 ORBITAL EVOLUTION OF THREE POTENTIAL FIRST PRECURSORS AND COMET 96P (EQUINOX J2000.0)

OBJECT/SCENARIO	TIME FRAME (yr A.D.)	OSCULATING ORBITAL ELEMENTS				
		ω (deg)	Ω (deg)	i (deg)	q (R_{\odot})	P (yr)
Evolutionary Stage: Marsden Group						
A2.....	1699	23	81	25	14.8	5.5
K1.....	1913	23	81	26	12.7	5.4
M3.....	2002	23	81	27	10.3	5.3
96P.....	2304	23	81	32	9.4	5.3
Evolutionary Stage: Kracht Group						
A2.....	1786	59	44	11	13.1	5.5
K1.....	2003	58	44	12	10.7	5.4
M3.....	2091	58	44	12	8.4	5.3
96P.....	2411	59	44	14	6.8	5.3
Evolutionary Stage: Southern δ Aquarid Swarm						
A2.....	1952	158	302	26	15.0	5.5
K1.....	2174	157	302	27	12.2	5.4
M3.....	2234	157	302	27	10.4	5.3
96P.....	2589	156	302	31	9.4	5.3
Evolutionary Stage: Quadrantid Swarm						
A2.....	2906	170.4	283.1	73.7	0.976 ^a	5.60

^a In AU; equal to 210 R_{\odot} .

TABLE 29
 FRAGMENTATION DISTRIBUTION OF POTENTIAL FIRST PRECURSORS FOR MARSDEN GROUP AT RETURNS AD 150–1000
 (SUMMARIZED OVER SETS OF FIVE CONSECUTIVE RETURNS)

RETURNS	FRAGMENTATION TIME RELATIVE TO PERIHELION (days)															TOTAL	RETURNS
	−400	−300	−200	−150	−100	−50	−25	0	+25	+50	+100	+150	+200	+300	+400		
150–171.....	6	8	9	6	63	70	59	52	49	71	68	6	9	10	8	494	150–171
177–197.....	1	2	4	3	26	41	41	34	35	35	17	4	4	1	...	248	177–197
203–224.....	3	3	5	5	4	20	203–224
229–250.....	6	12	13	9	12	12	7	71	229–250
255–276.....	5	11	11	10	10	9	2	58	255–276
282–303.....	2	2	10	14	13	11	2	2	56	282–303
308–329.....	2	4	9	9	49	83	93	84	81	89	55	10	10	7	3	588	308–329
335–356.....	7	9	10	4	64	59	42	40	36	50	68	3	10	10	10	422	335–356
361–382.....	...	4	4	3	20	29	31	29	30	30	16	4	4	2	...	206	361–382
388–409.....	4	5	7	7	5	2	30	388–409
414–435.....	8	13	12	9	12	15	7	76	414–435
440–461.....	3	9	7	8	7	8	3	45	440–461
466–487.....	2	...	8	27	40	42	35	30	14	5	2	1	...	206	466–487
493–514.....	5	8	10	12	52	92	74	75	79	84	61	12	10	8	2	584	493–514
519–540.....	6	10	10	9	52	69	42	30	38	68	48	7	10	9	2	410	519–540
546–567.....	...	2	4	4	13	31	32	36	37	29	10	4	3	2	...	207	546–567
572–593.....	0	572–593
599–620.....	1	3	4	2	1	11	599–620
625–646.....	1	1	3	1	1	7	625–646
651–672.....	0	651–672
677–699.....	4	16	29	36	28	12	3	128	677–699
704–725.....	8	12	47	69	75	71	44	14	4	344	704–725
730–752.....	4	6	30	48	63	52	30	8	2	243	730–752
757–778.....	0	757–778
783–804.....	1	1	783–804
.....
915–936.....	1	2	1	4	915–936
Total.....	27	47	62	62	394	650	665	666	640	638	407	64	62	50	25	4459	150–1000

TABLE 30
FRAGMENTATION DISTRIBUTION OF POTENTIAL FIRST PRECURSORS FOR MARSDEN GROUP AT RETURNS 292–382 (CLOSE-UP)

RETURN	FRAGMENTATION TIME RELATIVE TO PERIHELION (days)															TOTAL	RETURN
	-400	-300	-200	-150	-100	-50	-25	0	+25	+50	+100	+150	+200	+300	+400		
292.....	0	292
297.....	4	8	6	6	...	1	25	297
303.....	2	2	6	6	7	5	2	1	31	303
308.....	1	2	5	14	16	16	14	14	7	2	2	93	308
313.....	...	1	2	1	9	16	18	21	17	18	7	2	2	2	...	116	313
319.....	2	2	9	18	21	21	18	21	14	2	2	2	1	133	319
324.....	...	1	2	2	13	17	23	15	19	17	12	2	2	2	...	127	324
329.....	2	2	2	2	13	18	15	11	13	19	15	2	2	1	2	119	329
335.....	...	1	2	2	13	15	9	7	7	14	15	2	2	2	2	93	335
340.....	1	2	2	2	14	14	8	10	8	8	15	...	2	2	2	90	340
345.....	2	2	2	...	13	9	8	11	8	8	13	...	2	2	2	82	345
351.....	2	2	2	...	12	10	6	6	4	9	13	1	2	2	2	73	351
356.....	2	2	2	...	12	11	11	6	9	11	12	...	2	2	2	84	356
361.....	...	2	2	...	11	8	7	8	8	11	8	2	2	2	...	71	361
367.....	...	2	2	2	5	11	10	7	12	13	6	2	2	74	367
372.....	1	4	8	12	12	10	6	2	55	372
377.....	2	2	2	6	377
382.....	0	382
Total.....	9	17	23	16	135	173	176	167	160	180	141	19	24	19	13	1272	292–382

perihelion and again in a constant total number, lower by a factor of ~3.2, at the times of ≥150 days from perihelion. The tabulated totals show an approximately constant number of events only within 50 days of perihelion, with a gradual decline farther out from the Sun. The ratio between the numbers at ±100 and ±150 days is twice the expected ratio of 3.2. Thus, our sample shows that fragmentation events within 50 or so days from perihelion are the most likely ones to produce potential first precursors for the Marsden group. A close-up view of the distribution in Table 30 shows that the rate of potential first precursors in some returns holds out to, or even increases at, ±100 days from perihelion, but the drop at larger heliocentric distances persists.

Because of the nature of the relationship between the first precursors and the members of the Marsden group, one cannot expect one-to-one correlations (§ 7.1), but there should be a general orbital affinity between the two kinds of objects. To make the comparison meaningful requires an estimate of uncertainties in the observed elements, caused by the observational errors due to short arcs on which the orbit determination has to rely and, to some extent, due also to a large pixel size of the CCD arrays used (11".4 for the C2 coronagraph, 56" for the C3 coronagraph).

To demonstrate that these uncertainties are not large, we list in Table 31 the differences between Marsden’s (2004b, 2005a, 2005b; Marsden & Williams 2003) preliminary parabolic elements and final, elliptical elements computed for the five Marsden-group comets of two apparitions (§ 4). The length of the covered orbital arc was extended by a factor of more than 1000 by the linkage, increasing the accuracy of the orbit determination accordingly. The differences between the preliminary and the linked osculating orbits are essentially the errors of the parabolic approximations.

It is apparent from Table 31 that these errors amount to up to about 1 hr in the perihelion time, up to about 1° in the angular elements, and up to 0.1 R_⊙ in the perihelion distance. An exception was the argument of perihelion for C/1999 N5, which for unknown reasons was off by 5° in the parabolic approximation; this error of course also shows up in the orientation of the line of apsides, especially in the longitude of perihelion. Also, C/1999 J6 and C/2004 V9, observed over the longest arcs at each return, had parabolic orbits much more accurate than the three fainter comets.

The histograms in Figure 8 compare the predicted distributions of the 4459 potential first precursors with the observed members of the Marsden group in each of the orbital elements, except the

TABLE 31
UNCERTAINTIES IN THE ORBITAL ELEMENTS OF MARSDEN-GROUP COMETS C/1999 J6, C/1999 N5, C/2004 V9, C/2005 E4, AND C/2005 G2 (EQUINOX J2000.0)

ORBITAL ELEMENT	DIFFERENCE: PRELIMINARY ORBIT MINUS FINAL, LINKED ORBIT				
	C/1999 J6	C/1999 N5	C/2004 V9	C/2005 E4	C/2005 G2
Perihelion time <i>T</i> (days).....	+0.01	+0.04	0.00	-0.01	+0.01
Argument of perihelion ω (deg).....	+0.26	+5.03	+0.19	-0.04	+1.30
Longitude of ascending node Ω (deg).....	-0.11	+0.71	-0.17	-1.03	-0.94
Orbital inclination <i>i</i> (deg).....	-0.06	+0.47	-0.06	-0.06	+0.35
Perihelion distance <i>q</i> (R _⊙).....	+0.015	+0.087	+0.030	-0.101	0.000
Orbital eccentricity <i>e</i>	+0.016	+0.015	+0.016	+0.015	+0.015
Longitude of perihelion <i>L</i> _π (deg).....	+0.14	+5.29	+0.02	-1.05	+0.20
Latitude of perihelion <i>B</i> _π (deg).....	+0.09	+2.28	+0.06	-0.03	+0.66

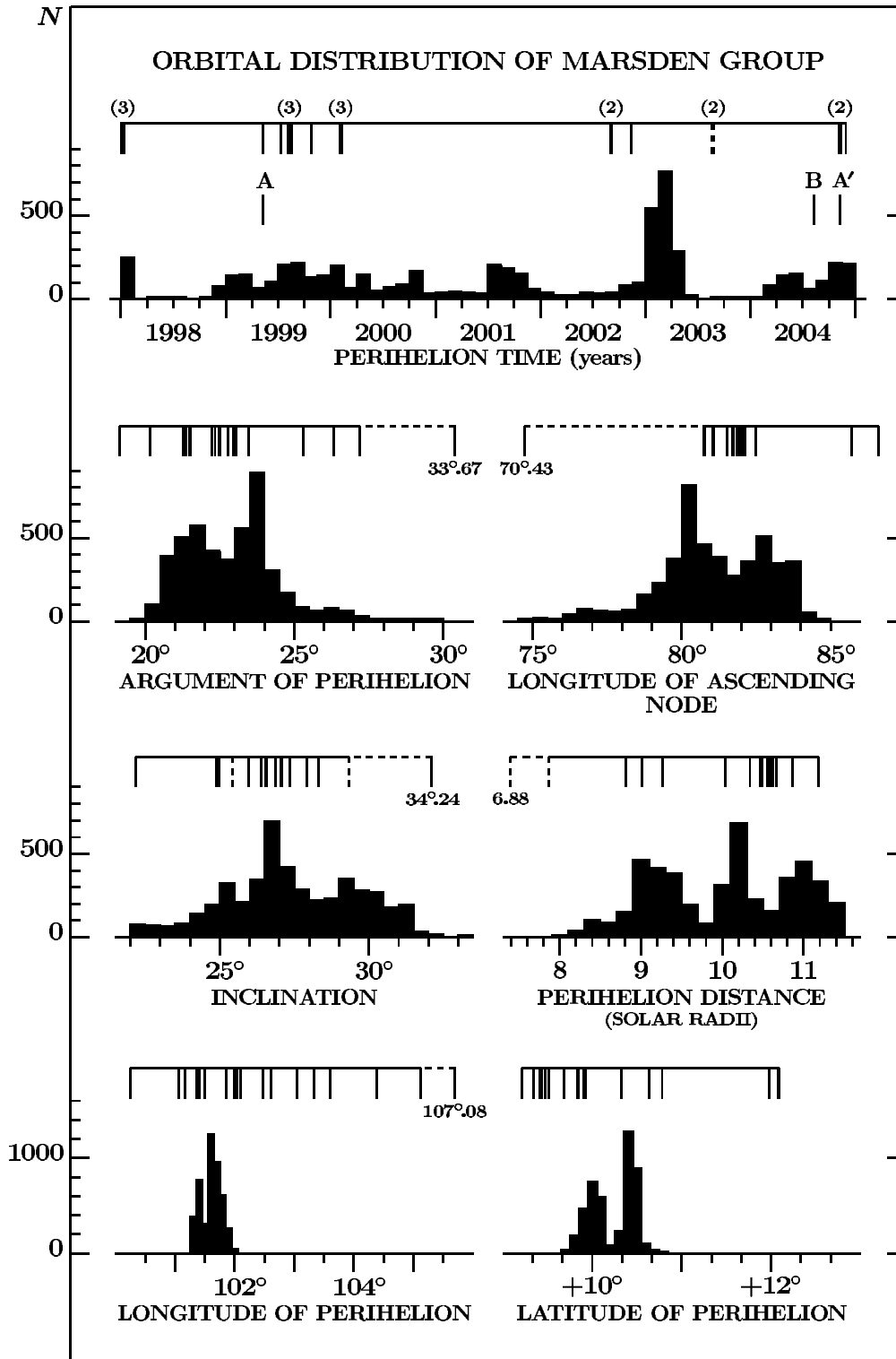


FIG. 8.—Histograms of the orbital distribution for 4459 potential first precursors of the Marsden group. The orbital elements of the group’s observed members are shown by vertical ticks above each histogram. An entry in parentheses indicates the number of comets in a cluster. The dotted ticks refer to the two 2003 comets whose membership is questionable. The perihelion time was chosen between 1998 and 2004. Tick A indicates the perihelion time of C/1999 J6; B is its position one revolution about the Sun later, if its orbital period were equal to that of comet 96P; while A’ is its actual arrival time as C/2004 V9.

eccentricity, which was assumed by Marsden to be unity. There is clearly a general agreement between the two sets, even though peaks of the precursor distribution do not necessarily coincide with high concentrations of the observed members. We explained in § 4 that clustering is a product of recent fragmentation and, accordingly, is not directly related to the first precursors.

Interestingly, the precursor distributions of the argument of perihelion, the longitude of the ascending node, and, especially, the longitude and latitude of perihelion are bimodal, while the distributions of the inclination and the perihelion distance are trimodal. We have made a concerted effort to find the source of this behavior. We inspected various subsets of the whole sample

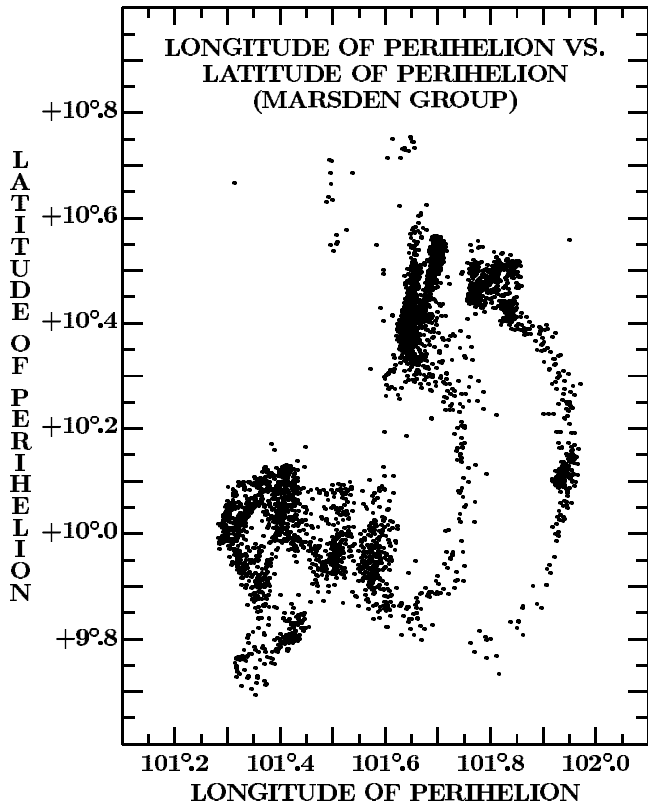


FIG. 9.—Relation between the longitude and latitude of perihelion for the 4459 potential first precursors of the Marsden group.

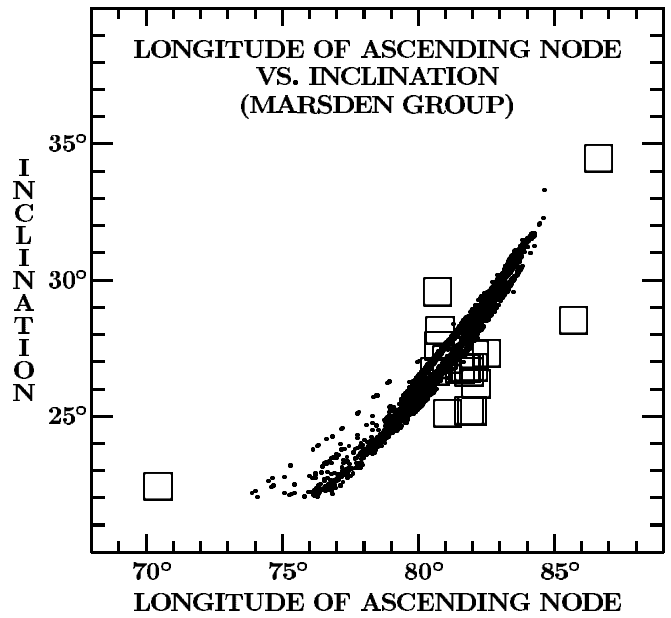


FIG. 11.—Relation between the longitude of the ascending node and the inclination for the Marsden group. See the caption to Fig. 10.

but found that the effect is essentially independent of the fragmentation time in the examined period of 850 yr. It is possible that the effect is a product of different patterns of close encounters, but comparison of the five potential Marsden precursors in Table 25 does not indicate any obvious differences in the encounter sequences.

Figure 9 shows considerable structure in the distributions of the perihelion longitude and latitude. It suggests that, with some exceptions, the cluster peaking in Figure 8 at longitude 101.4 correlates with the low-latitude cluster, and vice versa. Table 25 shows that precursor M2 is apparently one of the exceptions. The range in both axes in Figure 9 is very narrow, comparable to, or smaller than, the estimated observational errors, so that no

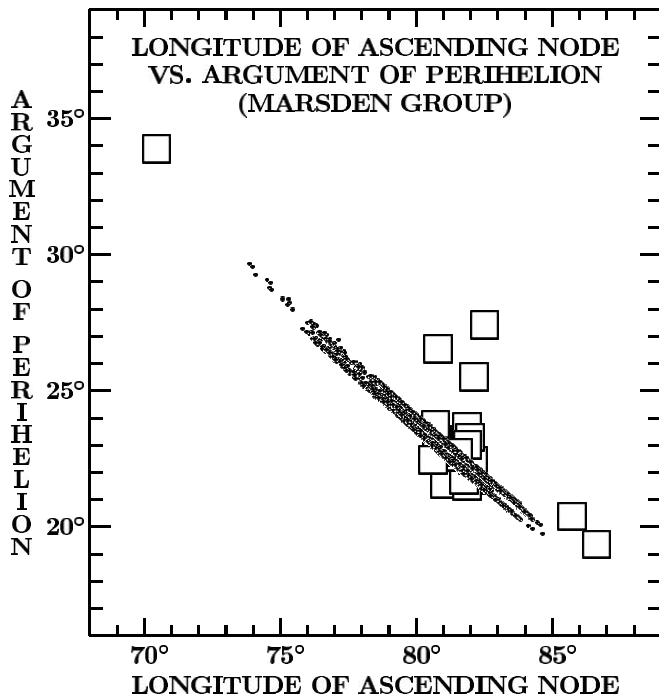


FIG. 10.—Relation between the longitude of the ascending node and the argument of perihelion for the Marsden group. The dots are the 4459 potential first precursors, and the squares are the observed members, most of which fit closely the precursors' predicted distribution.

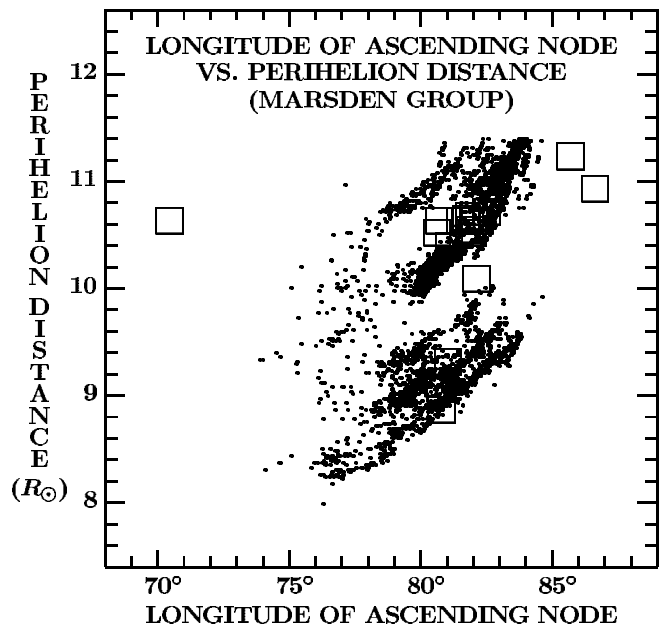


FIG. 12.—Relation between the longitude of the ascending node and the perihelion distance for the Marsden group. See the caption to Fig. 10.

information would be gained by plotting the members of the Marsden group.

Bimodality is also an attribute of the relations between the longitude of the ascending node on the one hand and the argument of perihelion and the inclination on the other hand, as indicated, respectively, by Figures 10 and 11. We found correlations between the bimodal distributions of the latitude and longitude of perihelion and the characteristics of the plots in Figures 10 and 11.

A complex relationship between the longitude of the ascending node and the perihelion distance, consisting of several nearly parallel branches, is presented in Figure 12. We are encouraged by the correspondence, in Figures 10–12, between the orbital distributions of first precursors and the Marsden group's orbits, which indicates that only minor orbital differences remain to be accounted for by the intervening process of cascading fragmentation.

Similar analysis could be presented for the orbital correlations of the Kracht group and the Southern δ Aquarids. However, little would be gained by such a presentation since the numbers of potential first precursors are much smaller (Table 23).

8. CONCLUSIONS AND FUTURE RESEARCH

SOHO detected comets of the Marsden and Kracht groups differ in many respects from comets of the Kreutz sungrazer system. To emphasize this distinction, it is appropriate that, together with the Meyer-group members, they be called the sunskirters. Two of the most important differences are (1) the role of the Sun's tidal forces, which is substantial for the sungrazers but trivial for the sunskirters; and (2) the observed rate of perihelion survival, which is nil for the small (*SOHO*) sungrazers, but more than 50% for each group of sunskirting comets.

Similarities between the sungrazers and sunskirters include their common susceptibility to nontidal cascading fragmentation, documented by the clustering effect, and to progressive erosion. Generation after generation, the recurrent splitting into ever smaller pieces leads ultimately to their complete disappearance. We were impressed by the success of the erosion model, developed for sungrazer applications (Sekanina 2003), in fitting the light curve of C/1999 J6 of the Marsden group. The derived erosion rate of only ~ 6 m per revolution shows that the greater perihelion distance and a generally higher erosion energy relative to the sungrazers help protect C/1999 J6 (and, presumably, other brighter sunskirters) against complete disintegration during a single return to perihelion.

Figure 2 confirms that a common line-of-apsides orientation is a valid rule-of-thumb criterion for detecting a genetic association among objects of the Machholz complex over limited periods of time. The relationship of the Marsden and Kracht groups with comet 96P/Machholz and with the Southern δ Aquarids and the Daytime Arietids is given a new dimension in this study. The notion of separate, mutually related populations, implied by the observed morphology of the Machholz complex, is replaced with a concept of one all-encompassing population indicated by the proposed model. Critical to our investigation is the postulated existence of first precursors, the initial direct ancestors of the Machholz complex, which were the first-generation fragments of the progenitor comet that they originally shared with 96P.

Only objects whose birth dated back to nontidal fragmentation events (at heliocentric distances exceeding 0.6 AU) before AD 950 and which experienced a sequence of encounters with Jupiter within 0.5 AU, starting in AD 1059 or earlier and continuing for centuries, could become first precursors of the low-inclination population. In the process, they must have split repeatedly into smaller pieces in a cascading fashion. In our sample

of nearly 60,000 fragmentation episodes between AD 150 and 950, we found a wide range of scenarios that included not only orbits of the Marsden and Kracht groups and of the Southern δ Aquarid swarm, but essentially a continuous stream of orbits with the nodal line spanning more than 160° .

These scenarios imply very diverse paths of orbital evolution, which are exemplified by the curve of long-term inclination variations. For a fragment with a history of Jovian close approaches, the more frequent the encounters and the more severe the perturbations exerted by the planet, the more rapidly the fragment's inclination drops from an initial value of $>75^\circ$. The inclination reaches a minimum of $\sim 10^\circ$ at a time that measures the perturbation effect during the encounters. Since precursors are found to precede comet 96P (which avoids close approaches) by hundreds of years, the precursors' orbital evolution is significantly accelerated relative to the comet. On a plot of the longitude of the ascending node Ω versus the inclination i in Figure 2, the severity of Jovian perturbations during close encounters increases systematically with decreasing Ω from 96P to the Quadrantids.

All fragments have a nearly equivalent orbital evolution path, but they reach the same stage at very different times. A present-day Marsden-group comet would in the future pass through a Kracht-group stage, then through a Southern δ Aquarid stage, and eventually through a Quadrantid stage of evolution. In reality, the short lifetime interrupts this evolution, so that Marsden-group comets never reach even the Kracht-group stage.

On the other hand, the Jovian-encounter-driven orbital evolution is relatively insensitive to the age of a first precursor, except that there must be enough time for completing the needed Jovian close approaches. While we do not know the temporal rate of fragmentation events of this type (yielding sufficiently massive first precursors), we can conclude with certainty that there is no unique solution to the problem of the origin of the Marsden and Kracht groups and the associated meteoroid swarms of the Machholz complex.

Work on the orbital evolution of the Machholz population is far from complete. Although we made progress in our understanding of an early, first-precursor stage and of the end products, they need to be connected by modeling the process of cascading fragmentation and the properties of successive generations of fragments.

We have no explanation for the "missing" segments of the first-precursor population. Using the terminology of Figure 2, we especially look for evidence on fragments of type 1 and type 2 precursors. Survival chances of most type 3 and all type 4 precursors are not good, because they are already past the stage of peak erosion rate (minimum perihelion distance).

The Quadrantids present a particularly difficult problem. To establish firmly their birth and evolution with the Machholz complex is a major task that remains to be addressed.

Although we have for now ruled out the Northern δ Aquarids, α Cetids, and a few high-inclination streams as members of the Machholz complex investigated in this paper, this issue will have to be reexamined over a longer temporal scale. Except for the κ Velids, a common orbital feature of these streams is a southern latitude of perihelion. An integration of the motion of 96P over 750 revolutions back to 2000 BC predicts that the comet had a southern latitude of perihelion at all times prior to AD 319. Between 684 BC and AD 1543, the line of apsides had changed by nearly 28° , the latitude of perihelion having increased from -14.5 to $+13.2$. The comet's orbit was similar in both its shape and orientation to the orbits of the Northern δ Aquarids shortly after 1500 BC and to the orbits of the α Cetids between 1800 and

1700 BC, and it was not too far from the orbits of the Carinids during the first three centuries AD. Much analysis remains to be done to find out what the orbital evolution implies for the ages of these streams, if they should be associated with the Machholz complex after all.

In spite of the enormity of the nearly 60,000 orbit integration runs, the parametric steps in our fragmentation scheme have remained very crude. So crude in fact that “neighboring” scenarios, M1 and T₃1 in Table 25, led to orbits that differ from each other by many tens of degrees in the angular elements. In at least some cases, it will be necessary to address the issue of orbital-solution sensitivity to fine changes in the fragmentation conditions.

With regard to the Marsden group, there are at least three tasks ahead of us. One puzzle is the fragmentation hierarchy of the parent of C/1999 J6 and C/1999 N5, including the roles of C/1999 U2 and possibly other fragments. The second puzzle is presented by the multimodal distributions of the orbital elements and their correlations (§ 7.6). The third puzzle is the nature of the relationship between the Marsden group and the Daytime Arietids, a broad stream whose activity extends from May 29 to June 19 according to Cook (1973). Since Marsden’s (2004b)

orbital solution for C/1999 J6 showed the comet to have passed only 0.0087 AU from Earth on 1999 June 12, the branch of the stream associated most closely with the Marsden group should have a longitude of the ascending node of 82° (equinox J2000.0). Recent radar observations of the Daytime Arietids may prove most helpful in testing this relationship.

The second part of this investigation will attend to at least some of the outstanding issues. Detections of new members of the Marsden and Kracht groups, observations of known members at their second apparition, and possible searches for the “missing” segments of the Machholz population are all likely to present new challenges.

We thank M. S. W. Keesey for providing information on his orbital determination of comet 96P. B. G. Marsden’s comments on a draft of this paper proved most helpful. This research was carried out at the Jet Propulsion Laboratory, California Institute of Technology, under contract with the National Aeronautics and Space Administration.

REFERENCES

- Babadzhanov, P. B., & Obruchov, Yu. V. 1992, *Celest. Mech. Dyn. Astron.*, 54, 111
- . 1993, in *Meteoroids and Their Parent Bodies*, ed. J. Štohl & I. P. Williams (Bratislava: Slovak Academy of Sciences), 49
- Baggaley, W. J., & Taylor, A. D. 1992, in *Asteroids, Comets, Meteors 1991*, ed. A. W. Harris & E. Bowell (Houston: Lunar and Planetary Inst.), 33
- Baggaley, W. J., Taylor, A. D., & Steel, D. I. 1993, in *Meteoroids and Their Parent Bodies*, ed. J. Štohl & I. P. Williams (Bratislava: Slovak Acad. Sci.), 245
- Bailey, M. E., Chambers, J. E., & Hahn, G. 1992, *A&A*, 257, 315
- Biesecker, D. A. 2000, *IAU Circ.* 7386
- Biesecker, D. A., & Green, D. W. E. 2002, *Int. Comet Quart.*, 24, 95
- Biesecker, D. A., Lamy, P., St. Cyr, O. C., Llebaria, A., & Howard, R. A. 2002, *Icarus*, 157, 323
- Cook, A. F. 1973, in *Evolutionary and Physical Properties of Meteoroids*, ed. A. F. Cook, C. L. Hemenway, & P. M. Millman (Washington: GPO), 183
- Gonczy, R., Rickman, H., & Froeschlé, C. 1992, *MNRAS*, 254, 627
- Green, D. W. E., ed. 2000, *IAU Circ.* 7364
- . 2002, *IAU Circ.* 7832
- . 2005a, *IAU Circ.* 8494
- . 2005b, *IAU Circ.* 8519
- Green, D. W. E., Rickman, H., Porter, A. C., & Meech, K. J. 1990, *Science*, 247, 1063
- Hasegawa, I. 1979, *PASJ*, 31, 257
- Jacchia, L. G., & Whipple, F. L. 1956, *Vistas Astron.*, 2, 982
- . 1961, *Smithsonian Contrib. Astrophys.*, 4, 97
- Jenniskens, P. 2004, *AJ*, 127, 3018
- Jenniskens, P., Betlem, H., de Lignie, M., Langbroeck, M., & Vliet, M. 1997, *A&A*, 327, 1242
- Jones, J., & Jones, W. 1993, *MNRAS*, 261, 605
- Lindblad, B. A., & Steel, D. I. 1994, in *IAU Symp. 160 Asteroids, Comets, Meteors 1993*, ed. A. Milani, M. Di Martino, & A. Cellino (Dordrecht: Kluwer), 497
- Marsden, B. G. 2000a, *Minor Planet Electron. Circ.* 2000-C53
- . 2000b, *Minor Planet Electron. Circ.* 2000-C52
- . 2002a, *Minor Planet Electron. Circ.* 2002-C28
- . 2002b, *Minor Planet Electron. Circ.* 2002-E25
- . 2002c, *Minor Planet Electron. Circ.* 2002-E18
- . 2002d, *Minor Planet Electron. Circ.* 2002-F03
- . 2002e, *Minor Planet Electron. Circ.* 2002-F43
- . 2002f, *Minor Planet Electron. Circ.* 2002-O35
- . 2003, *Minor Planet Electron. Circ.* 2003-C02
- . 2004a, *Minor Planet Electron. Circ.* 2004-N22
- . 2004b, *Minor Planet Electron. Circ.* 2004-X73
- Marsden, B. G. 2005a, *Minor Planet Electron. Circ.* 2005-E87
- . 2005b, *Minor Planet Electron. Circ.* 2005-H24
- . 2005c, *Minor Planet Electron. Circ.* 2005-F31
- . 2005d, *Minor Planet Electron. Circ.* 2005-G94
- . 2005e, *ARA&A*, 43, 75
- Marsden, B. G., Sekanina, Z., & Yeomans, D. K. 1973, *AJ*, 78, 211
- Marsden, B. G., & Williams, G. V. 2003, *Catalogue of Cometary Orbits* (15th ed.; Cambridge: SAO)
- McBride, N., & Hughes, D. W. 1990, in *Asteroids, Comets, and Meteors III*, ed. C.-I. Lagerkvist, H. Rickman, B. A. Lindblad, & M. Lindgren (Uppsala: Uppsala Univ.), 555
- McIntosh, B. A. 1990, *Icarus*, 86, 299
- McKinley, D. W. R. 1961, *Meteor Science and Engineering* (New York: McGraw-Hill)
- Meyer, M. 2003, *Int. Comet Quart.*, 25, 115
- Ohtsuka, K., Nakano, S., & Yoshikawa, M. 2003, *Publ. Astron. Soc. Japan*, 55, 321
- Poole, L. M. G., Hughes, D. W., & Kaiser, T. R. 1972, *MNRAS*, 156, 223
- Rickman, H., & Froeschlé, C. 1988, *Celest. Mech.*, 43, 243
- Sekanina, Z. 1970, *Icarus*, 13, 475
- . 1973, *Icarus*, 18, 253
- . 1976, *Icarus*, 27, 265
- . 1978, *Icarus*, 33, 173
- . 1982, in *Comets*, ed. L. L. Wilkening (Tucson: Univ. Arizona Press), 251
- . 1993a, *AJ*, 105, 702
- . 1993b, *A&A*, 271, 630
- . 1997, *A&A*, 318, L5
- . 2002a, *ApJ*, 566, 577
- . 2002b, *ApJ*, 576, 1085
- . 2003, *ApJ*, 597, 1237
- Sekanina, Z., & Chodas, P. W. 2002, *ApJ*, 581, 760
- . 2004, *ApJ*, 607, 620
- Sekanina, Z., Chodas, P. W., & Yeomans, D. K. 1998, *Planet. Space Sci.*, 46, 21
- Southworth, R. B. 1962, *AJ*, 67, 283
- Uzzo, M., Raymond, J. C., Biesecker, D., Marsden, B., Wood, C., Ko, Y.-K., & Wu, R. 2001, *ApJ*, 558, 403
- Welch, P. G. 2001, *MNRAS*, 328, 101
- Whipple, F. L. 1938, *Proc. Amer. Phil. Soc.*, 79, 499
- . 1955, *PASP*, 67, 367
- Williams, I. P., & Collander-Brown, S. J. 1998, *MNRAS*, 294, 127
- Williams, I. P., Ryabova, G. O., Baturin, A. P., & Chernetsov, A. M. 2004, *MNRAS*, 355, 1171
- Wright, F. W., Jacchia, L. G., & Whipple, F. L. 1954, *AJ*, 59, 400